Low power and stable RRAM device based on α-In_2Se_3 nanosheet / γ-In_2Se_3 nanoparticle homojunction embedded in Organic Polymer (PMMA) for Non Volatile Memory Application

A thesis submitted towards partial

fulfilment of the requirements for the degree of

Master of Technology in

Nano Science and Technology

Submitted by

Gourav Ray

Roll No: 002130701012

Exam Roll No: M4NST23007

Registration No. : 160437 of 2021-2022

Under the guidance of

Prof.(Dr.) Sourav Sarkar

School of Materials Science and Nanotechnology

Jadavpur University

Course affiliated to

Faculty of Interdisciplinary Studies, Law and Management (FISLM)

Jadavpur University

Kolkata-700032

India

2023

Dedicated to my family

CERTIFICATE OF RECOMMENDATION

This is to clarify that the thesis entitled "**Low power and stable RRAM device based on α-In_2Se_3 nanosheet / γ-In_2Se_3 nanoparticle homojunction embedded in Organic Polymer (PMMA) for Non Volatile Memory Application**'' is a bonafide work carried out by GOURAV RAY under our supervision and guidance for partial fulfilment of the requirement of Master of Technology (Nano Science and Technology) in School of Materials Science and NanoTechnology, during the academic session 2021-2023.

THESIS ADVISOR
Dr. Sourav Sarkar
School of Materials Science and Nanotechnology
Jadavpur University, Kolkata-700032

DIRECTOR
Dr. Sourav Sarkar
School of Materials Science and Nanotechnology
Jadavpur University, Kolkata-700032

DEAN
Faculty Council of Interdisciplinary Studies, Law and Management (FISLM)
Jadavpur University, Kolkata-700032

CERTIFICATE OF APPROVAL**

This forgoing thesis is hereby approved as a credible study of an engineering subject carried out and presented in a manner satisfactorily to warranty its acceptance as a prerequisite to the degree for which it has been submitted. It is understood that by this approval the undersigned do not endorse or approve any statement made or opinion expressed or conclusion drawn therein but approve the thesis only for purpose for which it has been submitted.

Committee of final examination for evalution of thesis

.....

.....

.....

.....

** Only in case the thesis is approved.

DECLARATION OF ORGINALITY AND COMPLIANCE OF ACADEMIC ETHICS

I hereby declare that this thesis contains literature survey and original research work by the undersigned candidate, as part of his **Master of Technology** (Nano Science and Technology) studies during academic session 2021-2023.

All information in this document has been obtained and presented in accordance with academic rules and ethical conduct.

I also declare that, as required by this rules and conduct, I have fully cited and referred all material and results that are not original to this work.

Name: **GOURAV RAY**

Roll Number: **002130701012**

Exam Roll number**: M4NST23007**

Registration Number: **160437 of 2021-2022**

Thesis Title: **Low power and stable RRAM device based on α-In_2Se_3 nanosheet / γ-In_2Se_3 nanoparticle homojunction embedded in Organic Polymer (PMMA) for Non Volatile Memory Application.**

SIGNATURE: **DATE:**

ACKNOWLEDGEMENT

I sincerely thank Dr. Sourav Sarkar, my adviser, for his unwavering encouragement, passion and vast expertise during my Master's studies and research. He helped me every step of the way as I wrote my thesis. My entire study project was driven by your insightful comments, and I am appreciative of that. Additionally, I'd like to thank the thin film and Nano Science Lab as well as the Nanoscience and Nanotechnology Lab for creating a welcoming work atmosphere for me.

My appreciation is extended to my mentor, Ms. Nabamita Chakraborty, for her guidance, inspiration, aid with all of my project-related challenges and for collaborating with me to make it what it is today.

I sincerely appreciate the help, encouragement, recommendations, and counsel that Dr. Sourav Sarkar, Dr. Kalyan Kumar Chattopadhyay, Dr. Chandan Kumar Ghosh, Dr. Mahua Ghosh provided. They created a supportive and productive learning environment, and their enthusiasm encouraged me to follow the study project with great passion.

My seniors, Dimitra Das, Sk Najes Riaz, Ankita Chandra, Piyali De, Nabanita Sen, Manas Kumar Thakur, my classmates Arnab, Abhrajit, Sampurna, Aaishiki, Soumyajit, Soudip, Tanbir deserve my deepest appreciation for making my project such a wonderful experience. I sincerely appreciate the help and support that my classmates gave me throughout this course. Without their help, I would not have been able to finish my project. My expressions of thanks to them are insufficient in light of their extraordinary assistance.

Finally, I want to sincerely thank my parents and all of my supporters for their love and support.

Abstract

The Von Neumann Architecture has become more of a problem whose severity increases with every newer generation of the central processing unit. To solve the issue, memristors and other novel electronic heterojunctions are expected to become the most promising candidate. Resistive switching random access memory (RRAM) device is one of those promising candidates for next generation non volatile memory due to its high stacking density, Low power consumption, high scalability, fast fabrication process and multistate behaviors. The resistive switching (RS) behavior has been observed in the wide range of binary/ multinary oxides or chalcogenides and some organics in recent years.

Here in, for the first time novel α-In_2Se_3 nanosheet/ γ-In_2Se_3 nanoparticle homojunction embedded in poly-methyl methacrylate (PMMA) is employed as an active layer of Resistive random access memory device (RRAM) for non volatile memory application. This homojunction is synthesized via simple solvothermal method and dispersed in PMMA solution with different weight concentrations. Several characterizations such as Field emission scanning electron microscopy (FESEM), X-ray diffraction (XRD), UV-Visible spectroscopy (UV-Vis), High-resolution transmission electron microscopy (HRTEM), Raman spectroscopy are performed for analysis and perfect study of the synthesized material. The composite sample is deposited on a FTO coated transparent glass substrate to form Al/ In_2Se_3@PMMA/ FTO device. I-V characterizations of the cell reveal a formation free, bipolar, non volatile and multilevel Resistive-switching (RS) properties for memory application. Variation of In_2Se_3 concentration is performed to get the best performing device. The

best device shows a significantly large resistance ON/OFF ratio of 10^4, low operating voltage (<2V) and long retention time (more than 9000 s) at room temperature. After the analysis of experimental data, the conduction mechanism for our In_2Se_3-PMMA based RRAM device is explained by trap-assisted space-charge limited conduction (SCLC) for high resistive state (HRS) and ohmic conduction for low resistive sate (LRS). The proposed RS active material is a promising candidate for future artificial neural systems for mimicking the characteristics of human memory.

Contents

Chapter 1

INTRODUCTION

1.1 Introduction to Nanotechnology

"Nanotechnology is the idea that we can create devices and machines all the way down to the nanometer scale, which is a billionth of a meter, about half the width of a human DNA molecule" ***---Paul McEuen.***

Nanotechnology has multiple applicability as well as the soil on which the future technology is growing on is well maintained by Physics, Chemistry, Material science, Bio-Science, Electronics engineering, Bio-medical engineering etc. In Nanotechnology an atom can modify the basic idea of science. Basically Nanoscience is the investigation of mechanical, electrical, optical, and magnetic properties of nano structures in the range of 1-100 mm [1 nm=10^{-9} m]. Molecules are a few tenths of a nanometer in diameter and molecules are typically a few nanometers in size. Reduced materials to nano scale can show very different properties compared to what they exhibit on bulk scale, which enable technologists to use the unique properties of Nano-materials for developing their respective technological fields.[1]

The U.S. National Nanotechnology Initiative (NNI) provides the following definition: Nanotechnology is the understanding and control of matter at dimensions between approximately 1 and 100 nanometres, where unique phenomena enable novel applications. Encompassing Nanoscale science, engineering, and technology, nanotechnology involves imaging, measuring, modelling, and manipulating matter at this length scale.[2]

The origin of the term 'nano' derives from the Greek word "dwarf", but in scientific terminology nano means one billionth of a meter. Basically one nanometer (1 nm) is 1/1,000,000,000 of a

meter or 10^{-9} m. To indicate the smallness of any object we often compare it with a human hair. To get a better sense of nanoscale, the average diameter of a human hair is about 50,000 nanometers. In comparison, the smallest features that one commonly etched on a commercial microchip is now less than 15 nm. The smallest thing the unaided human eye can resolve is 10,000 nm across. Physics is the mother of natural sciences. In principle, physics can be used to explain everything that goes on at the nanoscale. There is active physics research going on in nanomechanics, quantum computation, quantum teleportation, artificial atoms etc. At nanometer scale physics is completely different. Properties that are irrelevant or not seen on a macroscopic scale become very prominent at nanoscale level- such as quantum mechanical and thermodynamic properties. By understanding and controlling individual atomic and molecular properties, they can be put together in very well-defined and organized ways to produce new materials with completely new and different characteristics. In 1974 Norio Taniguchi, a researcher at the University of Tokyo, Japan used the term 'nanotechnology' for the first time to refer to the ability to engineer materials precisely at the nanometer scale. The primary driving force for miniaturization at that time came from the electronics industry, which aimed at developing tools to create smaller (and therefore faster and more complex) electronic devices on silicon chips. Inspired by Feynman's ideas, K. Eric Drexler used the term "nanotechnology" in his 1986 book Engines of Creation: The Coming Era of Nanotechnology, which proposed the idea of a nanoscale "assembler" which would be able to build a copy of itself and of other items of arbitrary complexity with atomic control. According to Drexler -Nanotechnology is at the molecular level. It entrails the ability to build molecular systems with atom-by-atom precision, yielding a variety of nano machines. Binnig and Rohrer expanded on Drexler's theories in a practical way, they were the first to see atoms in 1981 and hence make nanotechnology a possibility. Scientists were soon able to pick up and move atoms to build structures. Originally the term nanotechnology was

restricted to these original experiments only, which held no immediate practical use. However, as soon as the significance of these discoveries was appreciated, interest and enthusiasm increased, and the term has been more broadly used at nano-meter level.

1.2 History of Nanotechnology

Although nanotechnology is a relatively recent development in scientific research, the development of its central concepts happened over a longer period of time. Researchers have supported the development of new instruments that allow the investigation of nanomaterial properties with an atomic level resolution and the timeline of these inventions are listed below.

- In the year 1969 American Physical Society arranged a meeting on December 29, in that meeting famous physicist Richard Feynman had given a lecture named “There's Plenty of Room at the Bottom”: invention of nanotechnology.
- In the year 1974 Nanotechnology term was first introduced by Taniguchi.
- Field Emission Scanning Electron Microscope was invented by Albert in 1972 with the help of Hitachi.
- The first Transmission Election Microscope was built by Max Knoll and Ernst Ruska in 1931, with this group developing the first TEM with resolution greater than that of light in 1933 and the first commercial TEM in 1939. In 1986, Ruska was awarded the Nobel Prize in physics for the development of transmission electron microscopy.
- In 1981 Gerd Binnig and Heinrich Rohrer developed an instrument for imaging the surfaces of the materials at the atomic level (Scanning Probe Microscope) and were awarded the Nobel Prize in 1986. Which adds some speed for analysis of Nanomaterials.
- In 1985 Harold Kroto, James R. Heath. Sean O'Brien, Robert Curl, and Richard Smalley at Rice University synthesised Fullerene. Kroto, Curl and Smalley were awarded the 1996 Nobel

Prize in Chemistry for their roles in the discovery of buckminsterfullerene and the related class of molecules, the fullerenes.

- In 1986 Binnig, Calvin Quate and Christoph Gerber invented the first atomic force microscope and the atomic force microscope was commercially introduced in 1989.[3]
- In 1991 Carbon Nano Tube was first synthesised by Morinobu Endo and visualised by Sumio Iijima, there are two types CNTs, Multi walled and Single walled CNT, both have different properties.
- Graphene was discovered, isolated and characterized in 2004 by Andre Geim and Konstantin Novoselov at the University of Manchester. They used scotch tape for mechanical exfoliation of graphite to gate single layered Sp2 carbon atom sheets. For which they were awarded the Nobel prize in Physics in 2010.

1.3 Synthesis of Nanomaterials

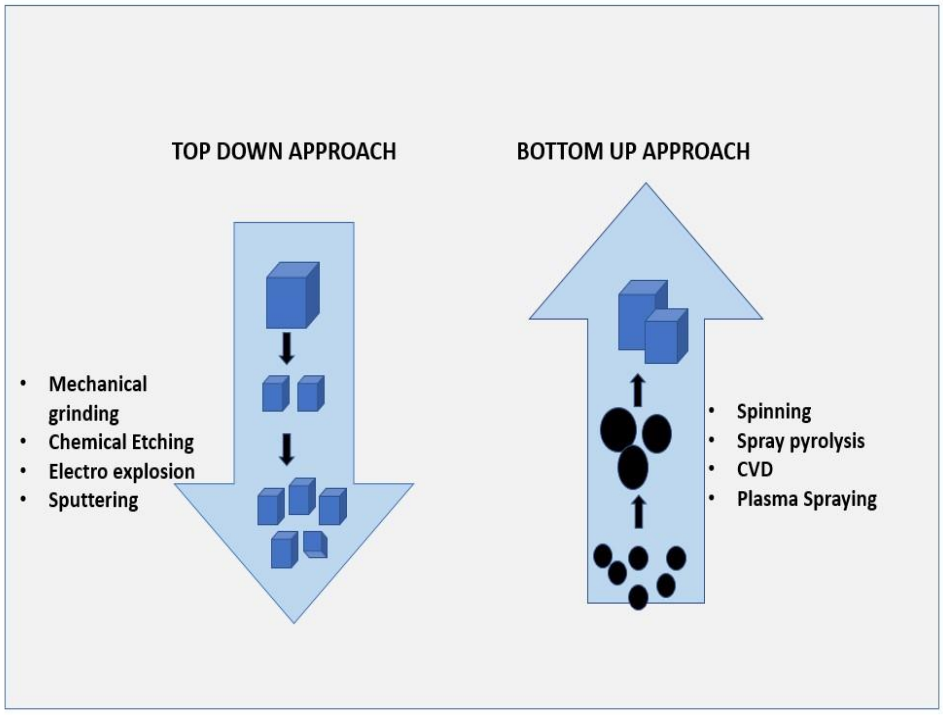

Fig. 1.1 Top down and Bottom up approach

The goal of any synthetic method for nanomaterials is to yield a material that exhibits properties that are a result of their characteristic length scale being in the nanometer range (1 - 100 nm). Accordingly, the synthetic method should exhibit control of size in this range so that one property or another can be attained. Often the methods are divided into two main types, “bottom up” and “top down”. Bottom up methods involve the assembly of atoms or molecules into nanostructured arrays. In these methods the raw material sources can be in the form of gases, liquids or solids. The latter require some sort of disassembly prior to their incorporation onto a nanostructure. Bottom up methods generally fall into two categories: chaotic and controlled. Chaotic processes involve elevating the constituent atoms or molecules to a chaotic state and then suddenly changing the conditions so as to make that state unstable. Through the clever manipulation of any number of parameters, products form largely as a result of the insuring kinetics. The collapse from the chaotic state can be difficult or impossible to control and so ensemble statistics often govern the resulting size distribution and average size. Accordingly, nanoparticle formation is controlled through manipulation of the end state of the products. Examples of chaotic processes are laser ablation, exploding wire, arc, flame pyrolysis, combustion, and precipitation synthesis techniques. Controlled processes involve the controlled delivery of the constituent atoms or molecules to the site(s) of nanoparticle formation such that the nanoparticle can grow to a prescribed size in a controlled manner. Generally the state of the constituent atoms or molecules are never far from that needed for nanoparticle formation. Accordingly, nanoparticle formation is controlled through the control of the state of the reactants. Examples of controlled processes are self-limiting growth solution, self-limited chemical vapor deposition, shaped pulse femtosecond laser techniques, and molecular beam epitaxy.[4] Top down methods adopt some ‘force’ (e. g. mechanical force, laser) to break bulk materials into

nanoparticles. A popular method involving mechanical break apart bulk materials into nanomaterials is ‘ball milling’. Besides, nanoparticles can also be made by laser ablation which apply short pulse lasers (e.g. femtosecond laser) to ablate a target (solid).

1.4 Type of Nanostructures

Nanomaterials are mostly classified based on five factors: nanoparticle geometry, morphology, composition, uniformity, and agglomeration. Based on nanoparticle geometry, nanomaterials are classified as OD, 1D, 2D, or 3D.

- A 0D structure is the simplest block which is used for the design of nanomaterials. In this case, the three dimensions are in the nanometer regime and have a diameter less than 100 nm. Quantum dots, Nanoparticles, nanocrystals, and nanoclusters correspond to this group.

- The 1D structures have a variable length, conserving two dimensions (height and width) in the nanometer regime. The 1D nanostructures correspond to the nanowires and nanotubes.

- The 2D nanomaterials are basically nanomaterials formed by very thin layers; thin nanolayers with areas of undefined size and a thickness between 1 and 100 nm. The nanosheets/nanofilms (only thickness below 100 nm), etc. are 2D nanostructures.[5]

- 3D nanomaterials are materials that are not confined to the nanoscale in any dimension. This class can contain bulk powders, dispersions of nanoparticles, bundles of nanowires, and nanotubes as well as multi-nanolayers.

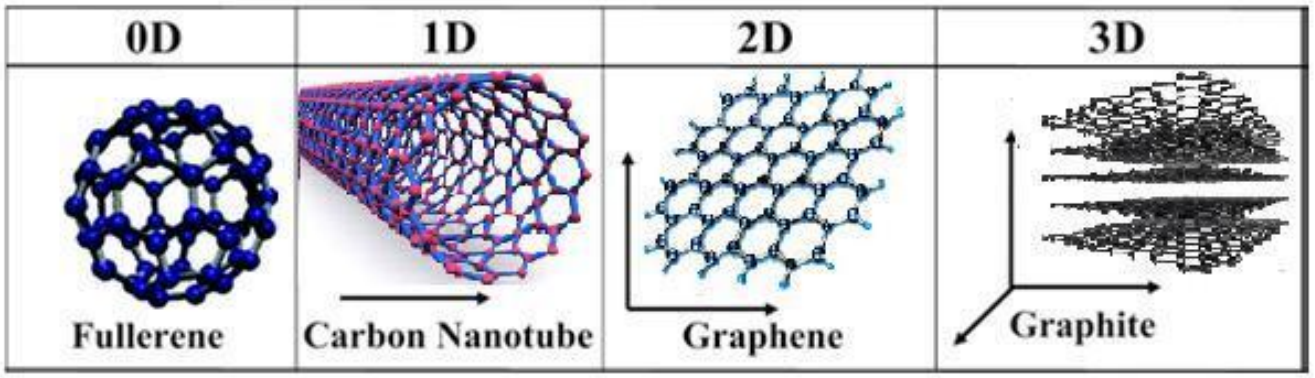

Fig. 1.2 Classification of Nanomaterials 0D, 1D, 2D, 3D Nanomaterials

The size dependent effect for novel properties of nanomaterials is the quantum size effect. This effect changes the density of states or band structure in the nanomaterial transforming insulators to semiconductors, or nonmetals to metals or even nonmagnetic systems to magnetic. Quantum size effect can be understood as physical confinement of electrons in nanoparticles due to their small size which causes the energy states to become discrete. One can imagine this confinement similar to the "particle in a box" problem in quantum mechanics. Thus, both the position of energy states and distribution of electrons in the energy states changes leading to effects such as increased band gap in semiconductors, ferromagnetic behavior and surface plasmons in metals. Properties influenced by quantum size effects show a discontinuous behavior due to the discontinuous nature of filling of electrons in energy levels. The overall behaviour of bulk crystalline materials changes when the dimensions are reduced to the nanoscale. For 0D nanomaterials, where all the dimensions are at the nanoscale, an electron is confined in 3D space. No electron

delocalization (freedom to move) occurs. For 1D nanommaterials, electron confinement occurs in 2D space. Where delocalization takes place along the long axis of the nanowire/rod/tube. For 2D nanomaterials, the conduction electrons will be confined across the thickness but delocalization occurs in the plane of the sheet. Therefore, the electrons are fully confined in case of 0D nanomaterials. Also, the electrons are fully delocalized in case of 3D nanomaterials. The electron confinement and delocalization coexist for 1D and 2D cases. The effect of confinement can be treated as particles in the box. An electron is considered to exist inside of an infinitely deep potential well from which it cannot escape and is confined by the dimensions of the nanostructure.

Density of states in 3D momentum space (k- space) can be written as,

$$g(k) = (\ell/2\pi)^3\, 4\pi k^2\, dk\ ;$$

Further we know that,

$$\hbar^2 k^2 = 2mE$$

$$2k\hbar^2\, dk = 2mE\, dE$$

$$dk = (\sqrt{2mE}/\hbar)E^{-1/2}\, dE$$

Therefore,

$$g(E)\, dE = (\ell/2\pi)^3 \times 4\pi \times (\sqrt[3]{2m}/\hbar) \times E^{1/2}\, dE$$

$$g(E) \propto E^{1/2}$$

For 1D momentum space, density of states takes the form as,

$$g(E) \propto E^{-1/2}$$

In general the density of states by reducing dimensions depends on Energy value E as,

$$\boldsymbol{g(E) \propto E^{d/2-1}}$$

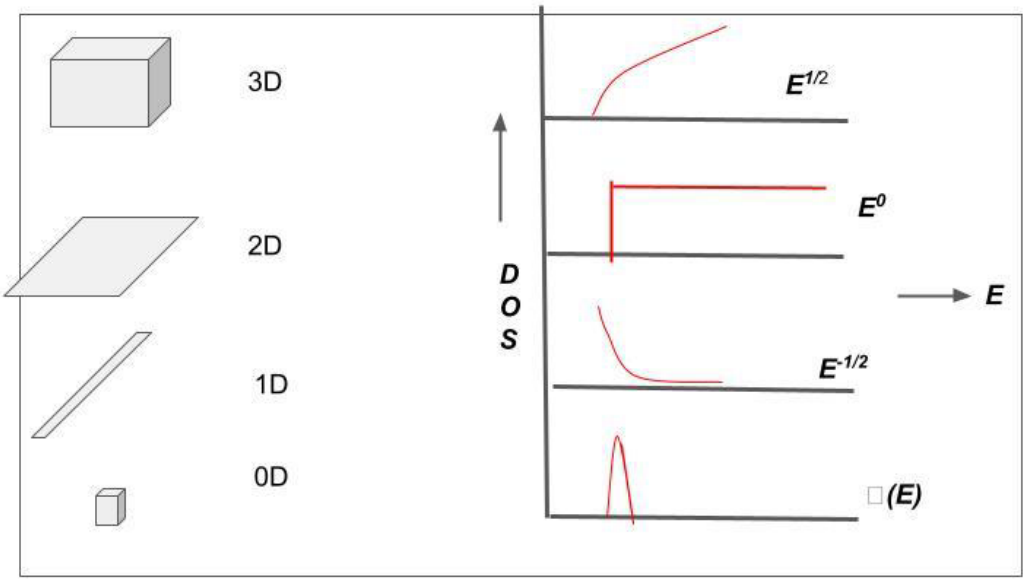

Fig. 1.3 Density of States of Nanomaterials

1.5 Application of Nanotechnology

Today's nanotechnology harnesses current progress in chemistry, physics, materials science, and biotechnology to create novel materials that have unique properties because their structures are determined on the nanometer scale. Some of these materials have already found their ways into consumer products, such as sun screens and stain resistant pants. Others are being intensively researched for solutions to humanity's greatest problems - diseases, clean energy, clean water, etc. Other work is aimed at developing a roadmap for productive nanosystems, in which a path is sought from today's nanotechnology capabilities to advanced future systems in which molecular tools will build useful materials, devices, and complex systems to atomic precision. The products of advanced nanotechnology that will become available in the coming decades promise

even more revolutionary applications than the products of recent and future generation nano-technology. Following are the few Nanotechnology Challenges in which current and near term nanotechnology is providing hope for solving critical challenges facing humanity.

1.5.1 Providing Renewable Clean Energy

Balancing humankind's need for energy with the environmental cost to our planet is a major challenge. Demand for energy is forecasted as increasing 50% by the year 2025 with most of these being fossil fuels. Currently over 1.6 billion humans have no access to electricity and 2.4 billion rely on plant material, vegetation, or agricultural waste as an energy and heating source. Our fossil fuel consumption is escalating and could double. Meanwhile, Earth's glaciers are re-ceding. the CO_2, concentrations in the atmosphere have nearly doubled, and world temperatures, recorded since 1861, were the hottest in three of the past five years. 1998 was the warmest on record, 2001 came in the second warmest and 2004 was the fourth warmest. Nanotechnology will help fill our need for energy solutions through more efficient lighting, fuel cells, hydrogen storage, solar cells, and locally distributed power sources.

1.5.2 Improving Health and Longevity

Humans are living longer lives. At the turn of the century, men and women were expected to live to 48 and 51 years respectively. That life expectancy is now 74 and 80 years and could be significantly longer with anti-aging advancements currently being researched. At the same time, 30 new highly infectious diseases have been discovered in the last 20 years. These diseases account for 30% of the deaths worldwide and include HIV/AIDS, Ebola and the Avian Flu. HIV/AIDS, the most critical threat, has killed 22 million and infected 42 million. In 2003 roughly 5 million people became infected worldwide. AIDS according to a United Nations study is increasingly becoming global as it spreads rapidly to Eastern Europe and Asia. Cancer kills

over 500,000 people and 1.5 million are diagnosed annually in the United States. According to the World Cancer Report, there could be a 50% increase to 15 million new cases in the year 2020 primarily attributed to an aging population worldwide.[6]

1.5.3 Healing and Preserving the Environment

There is an ever increasing demand for natural resources and living space for humans, while toxics continue to build up in our water and soil. Biodiversity is being destroyed world-wide with 7 million hectares of forest being lost annually. Half of our world's forests and a quarter of our coral reefs are gone. Biodiversity decreases each year, with increasing threats especially to the oceans. Damage to the atmosphere's ozone layer has slowed but a hole still remains. Many believe that man made greenhouse gases are disturbing the earth's climate. This effect is popularly called global warming. Proposals to correct this are expensive and unlikely to be followed by developing nations who see economic advance as more urgent. Nanotechnology will provide solutions through precision pollution monitoring using nanosensors, lower energy needs due to lightweight strong materials, and reducing the use of harsh cleansers through the applications of nanocoatings to surfaces. A more advanced nanotechnology solution will be building our products with molecular level precision through the use of productive nanosystems, resulting in virtually no chemical waste.

1.5.4 Making Information Technology Available to All

In 2005 an estimated 13.9% of the world's population had Internet access with the greatest saturation in North America and the least in Africa. The tsunami disaster in the recent past has elucidated how rapidly the world can be informed about and how crises can be handled. A "planetary nervous system" would enable humanity to work collectively to make a better world for all of us. There are currently many who lack widespread access to communications, information,

services and resources. This lack of access creates insurmountable barriers to education, democratization, and economic growth. Electronics is an area where nanotechnology is making great gains. The use of nanotechnology applications will drastically reduce the cost and increase the performance of memory, displays, processors, solar powered components, and embedded intelligence systems. It will also enable networks to be self-configuring. These improvements would create a pervasive computing environment that would promote greater global communication, cross-cultural understanding and cooperation.

1.5.5 Enabling Space Development

The earthly challenges facing humanity are the result of our heavy demand on resources and raw materials. Many of these materials can be found in space but the expense to extract them is a major barrier. In addition to cost, other obstacles to developing space are safety, reliability, and performance. According to the National Space Society there are four reasons why we need to pursue space exploration and colonization. These reasons- survival, growth, prosperity and curiosity all point to the fact that we, as species, want more room. Space exploration will give us a means to monitor the health of our planet, a source of resources and an outlet for our imagination. Nanotechnology will create the ability for humans to operate in space more safely. Applications where nanotechnology will impact space exploration are propulsion fuels, coatings, structural materials, smart uniforms, field of electronics and life support environments. These will be more efficient, stronger, self-healing and lighter than what is currently available.

1.5.6 Electronics Application

Nanoelectronics holds some answers for how we might increase the capabilities of electronics devices while we reduce their weight and power consumption. Some of the nanoelectronics areas under development, which can be explored in more detail by following the sections. Improving display screens on electronics devices. This involves reducing power consumption while decreasing the weight and thickness of the screens. Increasing the density of memory chips. Researchers are developing a type of memory chip with a projected density of one terabyte of memory per square inch or greater. Reducing the size of transistors used in integrated circuits.

1.5.7 Computer Memory

Solid-state drives store information on a type of transistor called flash. Currently, flash memory manufacturers use nanolithography techniques to build memory chips with minimum feature sizes as small as 20 nm. Researchers have demonstrated vertical flash transistors. The idea is that by making the transistors vertically memory cells could be stacked on top of each other, with the potential for increasing the memory density. Researchers suggest that the memory cell density could be 8 to 16 times higher than for planar transistors. Hewett Packard is developing a memory device that uses nanowires coated with titanium dioxide. One group of these nanowires is deposited parallel to another group. When a perpendicular nanowire is laid over a group of parallel wires, at each intersection a device called a memristor is formed. A memristor can be used as a single-component memory cell in an integrated circuit. By reducing the diameter of the nanowires, researchers believe memristor memory chips can achieve higher memory density than flash memory chips. HP is working with Hynix Semiconductor to develop memory components based upon memristors, called Resistive Random Access Memory (RRAM). Magnetic nanowires made of an alloy of iron and nickel are being used to create dense memory devices. Researchers at IBM have developed a method to magnetize sections of these nanowires. By applying a current they can move the magnetized sections along the length of the wire. As

the magnetized sections move along the wire, the data is read by a stationary sensor. This method is called race track memory because the data races by the stationary sensor. The plan is to grow hundreds of millions of U-shaped race track nanowires on a silicon substrate to create low-cost, high-density, and highly reliable memory chips. Another method of using nanowires is being investigated at Rice University. Researchers at Rice have found that they can use silicon dioxide nanowires to create memory devices. The nanowire is sandwiched between two electrodes. By applying a voltage, you change the resistance of the nanowire at that location. Each location where the nanowire sits between two electrodes becomes a memory cell. The key to this approach is that researchers have found that they can repeatedly change the state of each memory cell between conductive and nonconductive without damaging the material's characteristics. These researchers believe that they can achieve high memory densities by using nanowires with a diameter of about 5 nm and by stacking multiple layers of arrays of these nanowires like a triple-decker club sandwich. An alternative method being developed to increase the density of memory devices is to store information on magnetic nanoparticles. Researchers at North Carolina State University are growing arrays of magnetic nanoparticles, called nanodots, which are about 6 nm in diameter. Each dot would contain information determined by whether or not they are magnetized. Using billions of these 6-nm diameter dots in a memory device could increase memory density.

1.5.8 Nanosensors

An analyte, sensor, transducer and detector are the components of a sensor system, with feedback from the detector to the sensor. Sensitivity, specificity and ease of execution are the main goals in designing a sensor. Nanosensors typically work by monitoring electrical changes in the

sensor materials. For example, carbon nanotube-based sensors work in this way. When a molecule of nitrogen dioxide (NO_2) is present, it will strip an electron from the nanotube, which in turn causes the nanotube to be less conductive. Nanosensors include

- Carbon Nanotube Based Fluorescent Nanosensors
- Quantum Dot Based Fluorescent Nanosensors
- DNA-Based Fluorescent Nanosensors
- Peptide-Based Fluorescent Nanosensors
- Plasmon Coupling-Based Nanosensors
- Plasmonic Enhancing /Quenching- Based Nanosensors
- Magnetic Resonance Imaging-Based Nanosensors
- Photoacoustic-Based Nanosensors
- Multimodal Nanosensors (synergistic nanosensors with multiple modalities to overcome individual challenges)[7]

1.5.9 Quantum Computers

Quantum computing is the use of quantum-mechanical phenomena such as superposition and entanglement to perform computation. It is a new approach in the computer industry. Quantum computing is modeled by quantum circuits. It has quantum bit memory which is called qubit which is similar to bit in conventional computing for several computations at the same time. It improves the facility of the older system. Quantum computing will start to provide solutions to complex problems that are difficult or impossible to solve by conventional computing systems.

1.5.10 Drug Delivery

Nanotechnology drug delivery applications occur through the use of designed nanomaterials as well as forming delivery systems from nanoscale molecules such as liposomes. The application of nanotechnology for drug delivery[8] provides the potential for enhanced treatments with targeted delivery and fewer side effects

1. Improve the ability to deliver drugs that are poorly water soluble.

2. Provide site-specific targeting to reduce drug accumulation within healthy tissue.

3. Help retain the drug in the body long enough for effective treatment.

4. The extension of drug bioactivity through protection from the biological environment.

5. Allow for the transportation of drugs across epithelial and endothelial barriers.

6. Combine therapeutic and diagnostic modalities into one agent.

1.6 Introduction to Memory Device

Computer memory is any physical device, used to store data, information or instruction temporarily or permanently. It is the collection of storage units that stores binary information in the form of bits. The memory block is split into a small number of components, called cells. Each cell has a unique address to store the data in memory, ranging from zero to memory size minus one. Examples are Floppy disk, Compact disc, Magnetic memory, RAM, ROM etc.

1.7 Classification of Memory Device

Computer memory can be basically classified into two types:

- **Primary Memory**

Primary memory is the main memory of the computer which can be directly accessed by the central processing unit. It is a memory which is used to store frequently used programs which can be directly accessed by the processing unit for further processing. The examples of primary memory are Random Access Memory (RAM) and Read Only Memory (ROM). RAM is a volatile memory where data is temporarily stored for faster access by the processor. Different forms of RAM are Static RAM (SRAM) and Dynamic RAM (DRAM). ROM is a non-volatile memory and stores crucial information essential to operate the system, like the program essential to boot the computer. Different forms of ROM are Programmable (PROM), Electrically programmable ROM (EPROM), Electrically erasable programmable (EEPROM).

- **Secondary Memory**

Secondary memory is the external memory of the computer which can be used to store data and information on a long-term basis. It is a non-volatile memory. Data cannot be directly processed by the processing unit in secondary memory, in fact, it is first transferred into the main memory and then it's transferred back to the processing unit. It's generally slower than primary memory but can store a substantial amount of data. Secondary memory refers to all external storage devices that are capable of storing high volumes of data such as hard drives, floppy disks, magnetic tapes, USB flash drives, CDs, DVDs. etc.

Secondary Memory device can be further:

- **Volatile Memory**

It is a type of computer storage which requires a continuous power supply to maintain its saved data.This memory only keeps the stored data till the system is powered. When there is no electric power in the system, the data automatically erases from the computers. In desktop and laptop computers, 'Random Access Memory (RAM)' is a volatile memory. The read and write operations on RAM are faster than the hard disk and solid-state drive. That's why the computers, tablets, mobiles, and other electronic systems used RAM for high-speed data access. When we are working on a document in our computer systems, the document is kept in RAM, and when the computer is turned off, the random access memory automatically loses its documents. If we want to save our documents from erasing, then we should save our files and documents in non-volatile memory, such as hard disks, optical disks, and removal disk.

Volatile memory is categorized into two different types of RAM:

1. SRAM (Static RAM)
2. DRAM (Dynamic RAM)

- **Nonvolatile memory**

It is a type of memory device which retains data even if the power source is removed. It is also referred to as permanent memory. These types of memory devices generally are slower in operation. All such information that needs to be stored for an extended amount of time is stored in non-volatile memory. Examples of non-volatile memory include read-only memory (ROM), flash memory, most types of magnetic computer storage devices (e.g. hard disks, floppy discs and magnetic tape) and optical discs (e.g. compact disc. blu-ray disc and digital versatile disc).[9]

Other type of memory devices includes :

- **Magnetic Storage**

One of the most widely used types of digital data storage is magnetic storage refers to any type of data storage using a magnetized medium. Digital data consists of binary information, which is data in the form of zero and ones. There are two types of magnetic polarities, each one used to represent either zero or one. Magnetic storage is a form of non-volatile storage. This means that the data is retained even when the storage device is not powered. Magnetic storage is widely used because it is relatively cheap in comparison with other storage technologies. Magnetic storage is read-write, which makes it possible to re-use the storage capacity over and over again by deleting older data. The storage capacity is also very large, making it attractive for storing very large amounts of data. The major limitation of magnetic storage is that accessing the data can be quite slow. Examples of magnetic storage devices are magnetic tape, cassettes, floppy disks and hard disk drives.

- **Optical Storage**

Optical storage is any storage type in which data is written and read with a laser. Typically, data is written to optical media, such as compact discs (CDs) and DVDs. Optical media is more durable than tape, HDDs and flash drives and less vulnerable to environmental conditions such as wear and tear like most non-volatile memory, such as flash; and much more physically sturdy than magnetic tape, which is the leading archival storage medium. Optical discs are not vulnerable to data loss due to power failure like volatile memory. Another advantage of optical discs is that the storage medium is inexpensive to manufacture. The materials are mainly aluminum foil and plastic. However, it tends to be slower than typical HDD speeds and offers lower storage capacities.

- **Solid State Storage Device**

Solid-state storage (SSS) is a new generation method of data storage accomplished by using integrated circuit devices to store data rather than moving magnetic or optical media. SSS is typically non-volatile and speeds up computers significantly due to their low read-access times and fast throughputs. It takes various forms, such as a solid state drive, solid-state card, solid state module or flash-based memory. In addition, SSS includes PATA (legacy), SATA, SAS, Fibre Channel or PCIe interface options.

1.8 Resistive Random Access Memory Device (RRAM)

RRAM or memristor is a non-linear two-terminal electrical component that limits or regulates the flow of electrical current in a circuit and remembers the amount of charge that has previously flowed through it. Memristors are important because they are non-volatile, meaning that they retain memory without power. It was described and named in 1971 by Leon Chua, completing a theoretical quartet of fundamental electrical components which also comprises the resistor, capacitor and inductor. Since then, the definition of memristor has been broadened to include any form of non-volatile memory that is based on resistance switching, which increases the flow of current in one direction and decreases the flow of cent in the opposite direction. Chua in his 1971 paper identified a theoretical symmetry between the non-linear resistor (voltage vs. current), non-linear capacitor (voltage vs. charge), and non-linear inductor (magnetic flux linkage vs. cwrent). From this symmetry he inferred the characteristics of a forth fundamental nonlinear circuit element, linking magnetic flux and charge, which he called the memristor. [10]In contrast to a linear (or nonlinear) resistor the memristor has a dynamic relationship between current and voltage including a memory of past voltages or currents. Memristors, which are considered to

be a sub-category of Resistive RAM, are one of several storage technologies that have been potential to replace flash memory. Scientists at HP Labs built the first working memristor in 2008 and since that time, researchers in many large IT companies have explored how memristors can be used to create smaller, low-power, faster computers that do not require data to be transferred between volatile and non-volatile memory.

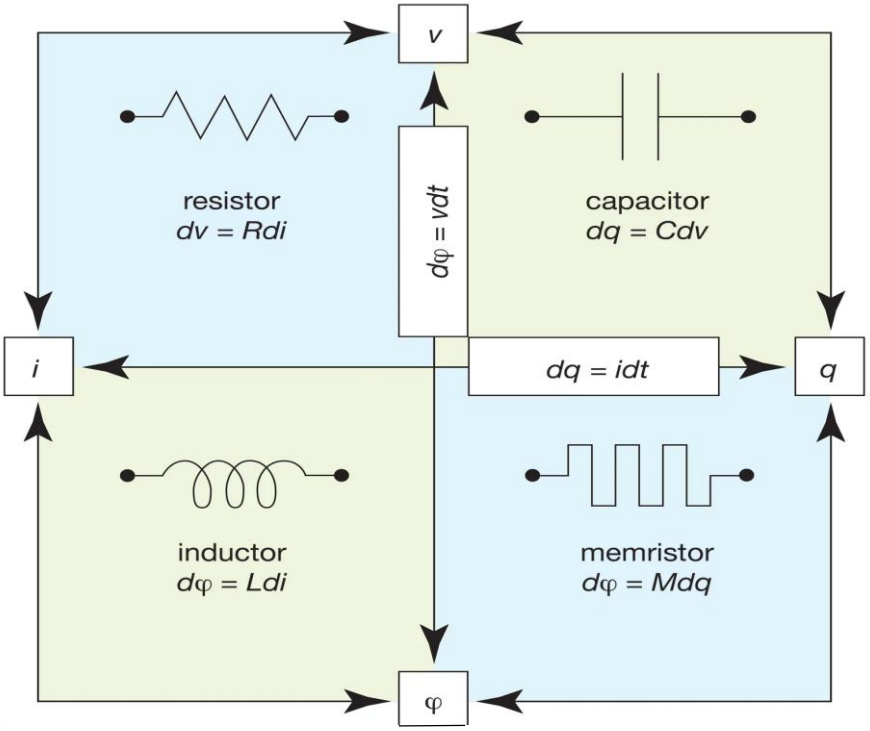

Fig 1.4 Symmetrical picturization of four fundamental circuit elements.

1.9 Working of Resistive Switching

So far, a few mechanisms have been proposed to explain the RS phenomena, each of which accounts for the RS behavior of a series of materials, as can be found from literature reviews. Resistive switching can be classified into few groups based on their scale such as carrier trap-

ping/detrapping (electronic scale), migration of point defect (atomic scale), metal-insulator transition (apparent change of the atomic structure), thermochemical reaction (apparent change of the microstructure and complex mechanism. The changes of the resistance due to various mechanisms are actually caused by the evolution of these defected structures triggered by the electric/thermal effects.

- **Carrier trapping/detrapping**

The charge carrier can be trapped by the defects inside the insulator layer or by the electrode/insulator interface, which will build an internal electric field and impact the injection or transport of the carrier that eventually leads to the RS behavior. Space-charge-limited conduction (SCLC) takes place when the charge is trapped by the point defects such as the vacancies inside the insulator layer. This effect brings the bipolar switching where the trapping and detrapping corresponds to applied voltage with opposite polarity. When a Schottky barrier is formed on the electrode/insulator interface, carriers can be trapped, which in turn change the height of the barrier and affect the transport of the charges. The external voltage applied can modulate the Schottky barrier height and results in the RS behavior. Generally, switching processes occur at the electronic scale are faster, indicating a shorter write time, and small value of resistance. However, good retention cannot be assured meanwhile, as shown in the voltage-time dilemma by Schroeder et al.

- **Migration of point defects**

In fact, migration of point defects can be involved in various mechanisms, including those in the following two sections, while the difference here is the migration of defects playing a dominant role. For the oxides, the formation and migration of anions/cations inevitably cause the valence state change of the cations/anions. Regarding this, point-defects migration based RAM

are also called valence change memory (VCM). Normally, RAM with this mechanism has a bipolar feature as a result of the huge effects of external electric fields on the migration of charged defects. To obtain a big change of the resistance, massive point defects should be formed or clustered, and their clustering usually generates a conduction path called filament. Filamentary conduction mechanism has been confirmed in many RAM. This type of phenomenon is generally observed in transition metal oxides where the transition metal changes its oxidation state. On application of external electric field oxygen anions migrate to one side and a thin metallic filament is formed inside the material which acts as a conduction path for curent resulting in low resistance state (LRS) of the material. When the electric field is applied with a reverse polarity the oxygen ions move to the opposite side resulting in breaking of the metallic filament and hence the conduction path for the curent and the material enters high resistive state (HRS).

- **Metal-insulator-transition (MIT)**

Materials with MIT behavior is naturally a promising RS material, given the distinct conductivity change after the transition. The work left is to figure out whether this MIT is easily controllable. Dioxide of group VB elements $VO_2$and NbO_2, exhibit MIT, as well as Ca_2RuO_4.

VO_2, can exist in three different structures depending on the temperature and strain, including two insulating (M1and M2) and one metallic rutile (R) phases, and the triple point in the phase diagram was measured and confirmed by Park et al. The phase transition can be realized by increasing/decreasing the environmental temperature and/or applied strain. MIT can also be driven by electric field induced Joule heating effect. However, regarding the quiet lower temperature for the MIT, long time stability of different phases is doubtful, i.e., MIT of VO_2, can hardly reach the requirements of non-volatility. Also it has been proved that in the presence of

an external electric field, the formation of oxygen vacancy can suppress the MIT of VO_2, which may further hinder its application. So far, there is no experimental report about the MIT in TaO_2, although its counterparts in group VB (VO_2, and NbO_2) were reported. Recently, using an evolution algorithm in combination with first-principles calculation, an insulating structure of TaO_2, MIT was theoretically predicted. The MIT mentioned above is a typical first-order phase transition, i.e, the microstructure of the phase or at least the atomic structure will be changed. There is also MIT belongs to the electronic scale process, such as a family of compounds AM4X8 Mott insulator (A ¼ Ga. Ge; M ¼ V, Nb; X ¼ S, Se). These compounds exhibit a very small band gap of 0.2 ± 0.1 eV, indicating the high sensitivity to external perturbation, such as the pressure and electric field.

- **Thermochemical reaction**

Electric field can cause Joule heating, which may provide the temperature condition required by any possible chemical reaction in the RAM device. The RS caused by this mechanism is normally unipolar, due to the fact that generation of heat is independent of the polarity of the electric field. Since the oxides formed by one single metallic element are abundant, as indicated by the Ellingham diagram, the different electronic properties of these oxides may induce the RS phenomena. Again, taking RAM based on TiO_2, as the example, the conducting Ti_nO_{2n-1}(n= 3-5 for rutile and 5-7 for anatase) Magnéli phase can be formed after the thermochemical reaction, with contrast resistance compared to insulation rutile TiO_2. In practice, this chemical reaction does not take place in the whole device; instead, a filament-type conductive product is enough to short-circuit the device. Many oxide based RRAM have this mechanism for RS, such as NiO, CoO, Nb_2O_5, etc.

1.10 Material Aspects

Materials	Properties
TiO_2	Enhanced memristive performance with less noise, peak current of 0.04Amp at 5 Volt implying more conductive nature.
SiO_2	Resistive switching in metal free embodiment, switching through voltage-driven modification and formation of silicon nanocrystals, small size ~5nm i.e., scaling to ultra-small domains, healthy non-volatile properties and high ON/OFF ratios $>10^5$, speedy switching to sub 100nm, better endurance with 10^4 read erase cycles, CMOS compatibility to construct memory and or logic devices.
Hcu pc	Fabricated thermally stable nanocomposite having high temperature dielectric and high electric field applications.
SAM	SAM - Self assembled monolayer is a nonconventional technique to avoid high production cost and long processing time. Suitable for controlled adjustment of key parameters in molecular and organic electronic devices. SAM suggests unipolar or bipolar switching, low to high resistance current ratio between 10 to 100, ON/OFF ratio of 100, fabricated RRAM device density of $1 \times 10^{10}/cm^{2.}$
Fe_2O_3	Gradual change in resistance (memristive) and capacitance (mem capacitance) with repeating voltage polarity at the same time owing to nanoparticle assembly. Memristive and memcapacitive characteristics resemble biological synaptic potential and depression motions suggesting potential applications in analog nonvolatile memory and circuits and neuromorphic devices.[11]
NiO	Key phenomenon is resistive switching in RRAM due to binary transition metal oxide (TMO) cells. Phenomenon is rupture and formation

	of conductive filament. The conductive filaments are composed of cation interstitials or oxygen vacancies resulting in change of microscopic oxygen stoichiometry. Cell size is 4 x 4 μm^2, 20 x 20 μm^2 and 88× 88 μm^2 single & two forming and non forming respectively.
PEDOT:SS	A conductive metal filament is formed in the organic layer's middle portion i.e, in Ag/ply(3,4-thylenedioxythiopene):poly(styrenesulfonate)(PEDOT:PSS)/Pt device. A bipolar filamentary resistive switching state results that falls in the category of electrochemical metallization. Potential applications are in the area of artificial synapses since svnaptic plasticity is mainly responsible for filament change in STP,LTP, STD and LTD.
VO_2	VO_2, is a popular material because of the large range of accessible resistance values through metal to insulator (MIT) transition and fast response time. Resistance change is four orders of magnitude.
GO	GO-graphene oxide is a good semiconducting/insulating material suitable for RRAM. Automatically thin and 2D GO allows scaling above present limits of semiconductor technology and high-density fabrication is possible. GO based resistive memory has many benefits like cost effective device fabrication, easy synthesis, compatibility for flexible device applications and scaling down to a few nanometers. Properties also include thermally stable, forming free, multi-bit storage, flexible and high ON/OFF resistive ratios at low voltages.
PZT	PZT is lead zirconate titanate, a piezoelectric material, considered for memristive applications. Use of this material is possible because of heterogeneous integration of technologies by integration of material physicists, computational chemists and bioengineering to explore nonvolatile memory application area.[12]

1.11 Methods of Performance Improvement

To enhance the performance of a RRAM system various methods are used such as doping, electrode engineering, interface engineering, optimization of device structure and measurement circuit, and multilevel storage operation and conductance quantization.

- **Doping**

Doping is a very effective way to modulate the properties of a material such as electrical conductivity and magnetism. This has also been observed in the case of RRAMs where the performance of the RRAMs is enhanced on doping. For example Lei Wu et al. demonstrated a device based on Al doped HfO_2 thin film. The device structure is given as Ti/Al: HfO_2/Pt. The active cell area was defined by the square-shaped Ti top electrode (TE). A 20-nm Ti adhesive layer was deposited by direct current (DC) sputtering on a silicon substrate, then a 100-nm Pt film was deposited as a bottom electrode (BE). The 20 nm Al doped HfO_2 layer was deposited by atomic Layer Deposition technique at 300°C. Another device was fabricated by Chen et al. that successfully showed nonpolar RS behavior in a Cu ion migration-based RRAM device. The thing that is interesting here is that the Pt/AlN: Cu/Pt device shows a nonpolar RS behavior that is remarkably different from the bipolar RS behavior in the Cu/AlN/Pt device. Moreover, the Pt/AlN:Cu/Pt device exhibits good uniformity between different devices, excellent endurance property up to 103 and retention performance up to 10 years, and fast switching speed of 100 ns, thus acting as a strong candidate for high-density memory applications.

- **Electrode Engineering**

It has been demonstrated that the RS behavior of a given storage medium can be significantly affected by the choice of electrode materials. Chen et al. systematically studied the effect of TE materials on the RS behavior of the TE/Ta_2O_5/Pt structure. Six metal electrodes were adopted,

i.e., Ni, Co, Al, Ti, Zr and Hf. During all of the switching cycles, external voltages were applied to the TE with the Pt electrode grounded, and the I comp was set as 1 mA.[13] It can be easily seen that: (i) the Ni/Ta_2O_5/Pt and Co/Ta_2O_5/Pt structures show very scattered distributions of Vset, RLRS, and RHRS: (i) the Zr/ Ta_2O/Pt and Hf/Ta_2O_5/Pt structures have the largest Vset and V reset with a lower scatter in the distribution; and (iii) the Al/Ta_2O_5/Pt and Ti/Ta_2O_5/Pt structures exhibit the best RS property with very concentrated distributions and appropriate amplitudes of all parameters. These results suggest that the choice of the TE has a significant influence on the performance of the TE/Ta_2O_5/Pt RRAM device.

- **Interface Engineering**

Interface engineering mainly means enhancing the performances of RRAM devices by introducing an additional thin layer at either or both of the two electrode/storage medium interfaces. The common additional thin layers are oxides such as AlO_x and SiO_x. The most obvious role played by an additional thin layer is a series resistor. For example, Chen et al. observed a reduction of the operating current in TiN/V:SiO_2(17 nm)/Pt after inserting a 3 nm a-Si layer at the TiN/V:SiO_2 interface. They found that the conduction mechanism of the LRS changed from Ohmic conduction followed by Poole-Frenkel emission in the TiN/V:SiO_2/Pt device to Ohmic conduction followed by Schottky emission in the TiN/a-Si/V:SiO_2/Pt device. The reduction of the operation current is mainly caused by the series resistance of the SiO_2, layer formed by oxidation of the a-Si layer during the set process. Cho et al. observed an enlargement of the memory window in an Al/PI:PCBM (-20 nm)/Al device by carefully controlling the thickness of an additional AlOx layer at the PI:PCBM/Al interface. The additional AlO_x, layer was created by O_2, plasma treatment, and its thickness increases with the total O_2, plasma treatment time. The typical I-V characteristics of the Al/PI:PCBM/Al devices with different lengths of O_2,

plasma treatment time, demonstrate the reduction of operating current with increasing AlO_x layer thickness. The ON and OFF resistances and the ON/OFF ratio as a function of the O_2 plasma treatment time and that both the ON and OFF resistance values gradually increase with the O_2 plasma treatment time. Furthermore, when compared with the ON resistance, a relatively large increase in OFF resistance contributes to a higher ON/OFF ratio in the devices with the O_2 plasma treatment. These results indicate that the additional AIO_x layer serves as a Series resistor and greatly affects the initial OFF resistance. The OFF resistance does not seem to increase further in the device with an O_2, plasma time of 20 min, which is likely to result from the very rough AlO_x layer with a longer O_2 plasma treatment time, resulting in decrease of the ON/OFF ratio.

- **Optimization of Device Structure**

A crossbar array that theoretically results in the smallest cell size is an acknowledged, ideal structure for RRAM integration. However, the ribbed RRAM cell may result in poor performances, such as very limited switching cycles owing to edge effects such as the highest heating effect occurring at the corners of a given device. To enhance the performances of RRAMs integrated in crossbar arrays, several methods have been proposed thus far. Based on a $Al/TiO_x/Al$ structure, Yu et al. have confirmed that the via-hole structure is superior to the ribbed structure in terms of scalability because the via-hole devices have a better uniformity with respect to the size- dependent current, ON/OFF ratio and switching voltages, The second method is to substitute a planar structure for the ribbed structure, Xia et al. have compared planar and ribbed TiO_2-based crossbar devices with 50 nm x 50 nm lateral dimensions and found that planar devices exhibit an improvement by a factor of over four in mean endurance value over ribbed devices

for otherwise identical structures. The last method is a novel structure for filamentary-conduction-type RRAMs, which was proposed by Lee and Wong. In this novel structure, the storage medium is intentionally placed at the sides of the top electrode for the purpose of utilizing the fringing field from the top electrode to effectively confine the position of CFs.

1.12 Application of RRAMs

RRAMs or Memristors can retain memory states, and data, in power-off modes. Non-volatile random access memory, or NVRAM, is pretty much the first to-market memristor application we'll be seeing. There are already 3nm Memristors in fabrication now. Crossbar latch memory developed by Hewlett Packard is reportedly currently about one-tenth the speed of DRAM. The fab prototype's resistance is read with alternating current, so that the stored value remains unaffected. Rosy colored industry analysts state there is industry concurrence that these flash memory or solid state drives (ssd) competitors could start showing up in the consumer market within 2 years. coupled with memcapacitors and meminductors, the complementary circuits to the memristor which allow for the storage of charge, memristors can possibly allow for nanoscale low power memory and distributed state storage, as a further extension of NVRAM capabilities. These are currently all hypothetical in terms of time to market.

- **Analog computation and circuit Applications**

There was a track of electrical/mathematical engineering which was largely abandoned to stasis in the 1960s, as digital mathematics and computers rose to dominance. Analog computations

embodied a whole area of research which, unfortunately, were not as scalable, reproducible, or dependable (or politically expedient in some cases) as digital solutions. However, there still exist some very important areas of engineering and modeling problems which require extremely complex and difficult workarounds to synthesize digitally: in part, because they map economically onto analog models. The early work of Norbert Wiener has already started to be revisited, after the analog/digital split between him and John von Neumann. Analog was great, but required management for scalability beyond what even the extremely complex initial digital vacuum tube computers could provide. RRAM applications will now allow us to revisit a lot of the analog science that was abandoned in the mid 1960's.

- **Circuits which mimic Neuromorphic and biological systems (Learning Circuits)**

  This is a very large area of research, in part because a large part of the analog science detailed above has to do with advances in cognitive psychology, artificial intelligence modeling, machine learning and recent neurology advances. The ability to map people's brain activities under MRI, CAT, and EEG scans is leading to a treasure trove of information about how our brains work. But modeling a brain using ratiocinated mathematics is like using linear algebra to model calculus. Simple electronic circuits based on an LC network and memristors have been built, and used recently to model experiments on adaptive behavior of unicellular organisms. The experiments show that the electronic circuit, subjected to a train of periodic pulses, learns and anticipates the next pulse to come, similar to the behavior of the slime mold Physarum polycephalum periodic timing as it is subjected to periodic changes of environment. These types of learning circuits find applications anywhere from pattern recognition to Neural Networks.[14]

- **Programmable Logic and Signal Processing**

A variety of Control System memristor patents are out there, waiting for the microchips to fall where they may. The memristive applications in these areas will remain relatively the same, because it will only be a change in the underlying physical architecture, allowing their capabilities to design programmable logic circuits[15], however, to the point where their applications will most likely be unrecognizable as related.

1.13 References

1. Poole, C.P. and F.J. Owens, *Introduction to nanotechnology*. 2003.
2. Bhushan, B.J.S.h.o.n., *Introduction to nanotechnology*. 2017: p. 1-19.
3. Tolochko, N.J.E.o.L.S.S., *History of nanotechnology.* 2009.
4. Abid, N., et al., *Synthesis of nanomaterials using various top-down and bottom-up approaches, influencing factors, advantages, and disadvantages: A review.* 2022. **300**: p. 102597.
5. Ramrakhiani, M.J.R.R.i.S. and Technology, *Nanostructures and their applications.* 2012. **4**(8).
6. Cheon, J., W. Chan, and I.J.A.o.c.r. Zuhorn, *The Future of nanotechnology: cross-disciplined progress to improve health and medicine*. 2019, ACS Publications. p. 2405-2405.
7. Javaid, M., et al., *Exploring the potential of nanosensors: A brief overview.* 2021. **2**: p. 100130.
8. Farokhzad, O.C. and R.J.A.n. Langer, *Impact of nanotechnology on drug delivery.* 2009. **3**(1): p. 16-20.
9. Bez, R. and A.J.M.S.i.S.P. Pirovano, *Non-volatile memory technologies: emerging concepts and new materials.* 2004. **7**(4-6): p. 349-355.
10. Kavehei, O., et al., *The fourth element: characteristics, modelling and electromagnetic theory of the memristor.* 2010. **466**(2120): p. 2175-2202.
11. Mikolajick, T., et al., *Nonvolatile memory concepts based on resistive switching in inorganic materials.* 2009. **11**(4): p. 235-240.
12. Espinal, Y., et al., *Dielectric properties and resistive switching characteristics of lead zirconate titanate/hafnia heterostructures.* 2018. **124**(6): p. 064103.

13. Wang, H. and X.J.p.s.s.R.R.L. Yan, *Overview of resistive random access memory (RRAM): Materials, filament mechanisms, performance optimization, and prospects.* 2019. **13**(9): p. 1900073.

14. Wang, Z., et al., *Nanoionics-enabled memristive devices: strategies and materials for neuromorphic applications.* 2017. **3**(7): p. 1600510.

15. Gao, Y., et al., *Efficient erasable PUFs from programmable logic and memristors.* 2018.

Chapter 2

Literature Review

2.1 Review of Past Work : Resistive Switching Memory Device (RRAM)

The idea of Memristor was first described by Leon Chua in 1971, who was then a professor of electrical engineering at the University of California, Berkeley[1]. Based on simple symmetry arguments he proposed a new hypothetical circuit element which will complete the theoretical quartet of four fundamental circuit elements. So, Memristor is the fourth established element along with resistor, capacitor and inductor. In linear circuit theory there is no need for this fourth element, In that context memristor and resistor are equivalent. But in non linear circuit theory memristors are fundamentally different from resistors. It is a resistor with a non volatile memory. By quasi static expansion of Maxwell's equation chua derived the existence of memristor.

However, 40 years later the device was first fabricated in HP labs by a group led by R Stanley Williams. He demonstrated resistive switching behaviour from LRS to HRS by metal oxide thin films which is similar to Chua's prediction of the device[2]. Since then, the field has rapidly grown and there has been a huge amount of work in the area. Very high levels of endurance (120 billion cycles) and retention (10 years or more) have recently been achieved in memristor devices (Nature Nanotechnology, "Memristor crossbar arrays with 6-nm half-pitch and 2-nm critical dimension") and ultrahigh density crossbar arrays, including multiple layer stacking, have been realized with scalability down to 2-10 nanometers[3].

B. Pradhan et al.[4] observed electrical bistability and large resistance switching in functionalized carbon nanotube (CNT)-conjugated polymer composites at room temperature [5]. They functionalized CNTs with butyl groups so that homogeneous films can be formed with P3HT as a matrix material. They observed the electrical bi-stability in P3HT:CNT films which was majorly controlled by the concentration of the CNTs in the polymer matrix[6,7].

The transition to a high-conducting state was explained in terms of charge transfer from the CNTs to conjugated polymer chains [8]. The ratio between the conductances of the high- and low-states increased with an increase in CNT concentration in the polymer matrix. The transitions between the two states were rewritable in nature and associated with memory phenomenon. The active layer retained its high-conducting state until a reverse voltage was applied to erase it. The devices exhibited random-access memory applications under ―write-readerase-read‖ voltage sequence. The conduction mechanisms in the two conducting states were modeled by considering a change in band gap and correspondingly a decrease in barrier height with the electrodes[9].

S. H. Chang et al. fabricated Pt/NiO/Pt capacitor structures by growing polycrystalline NiO films on Pt/TiO_x/SiO_2/Si substrates with various bottom electrode thicknesses tBE and investigated their resistance switching behaviors. Due to its finite size and low thermal convection through air, the top electrode was much less efficient in heat dissipation than the bottom electrode. The capacitors with tBE≥50 nm exhibited typical unipolar resistance memory switching behavior, while those with tBE≤30 nm showed threshold switching clearly showing bottom electrode thickness playing an important role in their resistance switching behaviors. The resistance memory switching phenomena was explained in terms of the temperature-dependent stability of conducting filaments [10]. In particular, the thinner tBE makes dissipation of Joule heat less efficient, so the filaments were at a higher temperature and became less stable [11]. This study demonstrated the importance of heat dissipation in resistance random access memory [12].

W.Y. Chang et al. developed a highly-oriented and columnar-grained ZnO thin film prepared by radio frequency magnetron sputtering and deposited on Pt/Ti/SiO2/Si substrates at room temperature. The Pt/ZnO/Pt devices exhibited reversible and steady bistable resistance switching behaviors with a narrow dispersion of the resistance states and switching voltage

[13]. Only a low forming electric field was required to induce the resistive switching characteristics. The set and reset voltages for the resistance switching were recorded as -2V and -1V respectively with sudden rise and drop in resistance of the device. The resistance ratios of high resistance state to low resistance state were in the range of 3–4 orders of magnitude within 100 cycles of the test. It was also found that the conduction mechanisms dominating the low and high resistance states are Ohmic behavior and Poole-Frenkel emission, respectively [14,15,16].

K. Moshammer et al. developed methods for synthesizing semiconducting SingleWalled Carbon Nanotubes. Two methods density gradient centrifugation and gel electrophoresis have been reported to allow high throughput separation of metallic from semiconducting single walled carbon nanotubes (SWNTs) when using aqueous sodium dodecyl sulfate (SDS) suspensions [17,18]. They showed that both the methods rely on an initial dispersion by sonication step, which is already selective with respect to electronic structure type. The aqueous SDS/ D2O ―starting‖ suspensions were obtained after sonication and purification by simple centrifugation (70,000 g for 1 hour) containing semiconducting SWNTs primarily in the form of small bundles whereas metallic SWNTs are predominantly suspended as individual tubes. Density gradient centrifugation then separated the bundles from the individual tubes on the basis of differences in their overall buoyant densities. Gel electrophoresis method separated the longer bundles from the shorter individual tubes on the basis of their difference in mobilities. It was also demonstrated that such starting suspensions can be fractionated according to electronic structure type by even simpler techniques such as gel filtration or size exclusion chromatography, thus paving the way for simple scale-up techniques [19].

J. Song et al. demonstrated an innovative memory device made of a single crystalline ZnO nanowire/microwire structure that works on a different mechanism from the p-n junction or ferroelectric based memristor. A non-symmetric Schottky–Ohmic contacted ZnO

nano/microwire can serve a memristor if the channel length is short and the applied frequency is high [20,21]. The observed phenomenon could be explained based on a screening model of the polar charges at the two ends of the wire owing to the crystal structure of ZnO. The polar charges are usually fully screened by free electrons coming from the metal sides. When the magnitude of the externally applied field exceeds a threshold value, the free electrons that screen the polar surfaces can be pulled away from the interface region, leading to a transient change in the effective height of the local Schottky barrier height owing to the electrical field formed by the polar surfaces of ZnO nanowires, which acts as a resistor with its magnitude depending on the total transported charges. Such a phenomenon could be used for high density and high speed writing/erasing data storage with frequency possibly up to gigahertz. Also the size of the memory unit can be very small in the range of a few nanometers by using ultra-small single crystalline nanowires [22].

R. Stanley et al. developed a model, to utilize memristors in circuits, it needs high quality predictive models that can be used for simulations to act as a design aid. The model was based on the known physics of the memristors that were being used [23,24]. They also performed a wide range of materials characterizations and electronic measurements on which the model was to be based. However, given the complexity of the physical processes that occur in the devices, such as drift-diffusion-thermophoresis in ion-migration based memristors and Mott transitions in locally active memristors, the corresponding detailed mathematical descriptions were far too complex to solve analytically and numerical solutions were too time consuming to include in a simulation [25,26]. Thus they created a simpler, analytical approximation that can match the measured behavior of the memristors over many orders of magnitude in time and a wide range of applied voltage. Their approach was based on constraining the model by introducing reasonable assumptions about the physics for the electronic conduction and switching dynamics of the device to provide a greater likelihood of predicting the properties of

the memristor for operations outside of the experimental measurement window. They also presented some new models which they have developed and described the derivation in detail [27].

G. A. Salvatore et al. presented a process scheme enabling the fabrication and transfer of few-layers MoS2 thin film transistors from a silicon template to any arbitrary organic or inorganic and flexible or rigid substrate or support. Transition metal dichalcogenides (TMDCs) had attracted interest due to their sizable band gap (around 1–2 eV), large field effective mobility (>100 cm2/V·s) and mechanical properties, which make them suitable for high performance and flexible electronics [28,29]. The two-dimensional semiconductor was mechanically exfoliated from a bulk crystal on a silicon/polyvinyl alcohol (PVA)/polymethyl methacrylate (PMMA) stack optimized to ensure high contrast for the identification of sub-nanometer thick flakes [30]. Thin film transistors (TFTs) with structured source/drain and gate electrodes were fabricated following a designed procedure including steps of UV lithography, wet etching, and atomic layer deposited (ALD) dielectric. Successively, after the dissolution of the PVA sacrificial layer in water, the PMMA film, with the devices on top, can be transferred to another substrate of choice. Here, they transferred the devices on a polyimide plastic foil and studied the performance when tensile strain was applied parallel to the TFT channel. The device exhibited current Ion/Ioff ratio greater than 106 , electron field effective mobility of 19 cm2 /(V s), threshold voltage of about -2V, subthreshold swing of about 250 mV/dec and gate leakage current as low as 0.3 pA/μm. The devices continued to work properly even when bent to a radius of 5 mm and after 10 consecutive bending cycles. The proposed fabrication strategy could be extended to any kind of 2D materials and enabled the realization of electronic circuits and optical devices easily transferable to any other support [31]

P K. Sarkar et al. fabricated a hybrid polymer/inorganic nanocomposite device consisting of SnO2 nanoparticles (NPs) embedded in an insulating polymethylmethacrylate (PMMA) layer

sandwiched between aluminium (Al) and conductive indium tin oxide (ITO) electrodes using a spin-coating technique. X-ray diffraction measurements were performed for assessment of the crystallographic nature of SnO2 nanoparticles while the microstructural nature of SnO2 nanoparticles embedded in the PMMA matrix was confirmed using transmission electron microscopy. Detailed electrical characterizations suggested bistable characteristics and an influence of the NP concentration on the switching characteristics of the Al/SnO2- PMMA/ITO memory devices. The maximum resistance ratio (Roff/Ron) > 103 was observed in a device with 2% weight of SnO2 NPs. The retention tests on the fabricated device demonstrated the consistency in current of the ON/OFF state even after 10^4 s. The conduction mechanisms of the fabricated nanocomposite based memory cell were discussed on the basis of experimental data using a charge trapping–detrapping mechanism in the NPs [32,33]. This work offered a feasible and low cost chemical approach to fabricate transparent and high density RS memory devices [34].

Y. Lin et al. demonstrated non-volatile, transferable and flexible resistive switching (RS) memory devices using a simple, efficient and nondestructive water-dissolution method. For satisfying future demands, the free-standing Al/Fe3O4-PMMA/Al devices with Fe3O4 nanoparticles embedded into PMMA films as the switching layer were transferred onto various nonconventional substrates to demonstrate various features, such as 3-D conformality, flexibility and biocompatibility. Due to the strong Van der Waals interaction, the devices can easily be conformed to different substrates and displayed resistive switching behavior even after undergoing rigorous bending tests [35]. Particularly, the memory devices with the PET substrate presented excellent memory performance as well as high flexibility and transparency, including large ROFF/RON ratio of ∼4 × 105 , fast switching speed (<50 ns) and long retention time (>104 s). No degradation of performance was observed even after bending the device to different angles and up to 104 times. The RS mechanism can be attributed to the trapping/de-

trapping of electrons at the sites of Fe3O4 nanoparticles [37]. This result provided a feasible approach to achieve transferable RS memory devices for future conformal and flexible electronics [38].

Kumar et al. and his colleagues worked on a memristor model based on conduction channel formation due to Oxygen diffusion in Hafnium Oxide. This device consist of stacking of layers of (top to bottom) Pt (15 nm)/ Hf(15 nm) /HfO2 (5 nm)/Pt (15 nm), with HfO_2 acting as the switching layer, Hf as a reactive electrode, and the Pt layers as the contact electrodes[39]. The application of bipolar sweep voltage to this system resulted in switching from native high resistance state to a low-resistance state which was observed under scanning transmission synchrotron X-ray spectromicroscopy to study in situ switching of hafnium oxide memristors, several X-ray energies in the STXM revealed a region of localized non uniformity.

Y. Sun et al. developed a bi-stable electrical switching and nonvolatile memory devices with the configuration of indium tin oxide (ITO)/ active layer /aluminum (Al). The active layer was prepared from mixed compositions of 2-(4-tert-butylphenyl)-5-(4-biphenylyl)-1,3,4-oxadiazole, (PBD) and poly(N-vinylcarbazole) (PVK) coated on the substrate by spin coating process. The as-fabricated ITO/PBD: PVK/Al sandwiched devices exhibited electrically bistable switching mode and rewritable flash memory property [40]. Due to the strong interaction between carbazole donor and oxadiazole acceptor, the devices demonstrated excellent performance [41]. The memory devices could operate over a small range of voltage, with the switching-on (write) threshold voltage of less than |-1 |V and the switching-off (erase) threshold voltage of less than 3.5 V. The ON/OFF current switching ratio was in the range of 102 –104 during the variation of applied voltage and retention time of more than 4 h and good cycling endurance. The conductance switching effects of the composite can be attributed to the electric field-induced charge transfer between PVK and PBD and follow the SCLC conduction process [42,43].

X. Zhang et al. fabricated non-volatile memory devices based on topological insulator Bi2Se3/Pt fibers. Pt fibers (15 μm) were coated with topological insulator Bi2Se3 nanoplates via a single mode microwave-assisted synthesis technique [44]. With the Bi2Se3/Pt fibers, flexible memory devices were easily assembled on polyethylene terephthalate (PET) substrates. Two parallel Bi2Se3/Pt fibers and one more across them were fixed onto a PET substrate using conductive Ag paste to form a memory device. They also exhibited typical bipolar resistive rewritable nonvolatile switching characteristics at low switching voltages (-1.2 V and +0.7 V) which are desirable for the low-power digital storage application. A very huge ON/OFF current ratio of 106 was obtained with a good retention time of 4500 s showing the potential application in data storage. The resistive switching mechanism was analyzed by TE and SCLC models on the bases of formation and rupture of conductive filaments [45,46].

Xiao-Yong Xu et al.developed a new resistive switching memory device consisting of reduced graphene oxide and indium tin oxide as top/bottom two electrodes, separated by dielectric MoS2. nanosphere assemblies as the active interlayer, was fabricated by a simple hydrothermal method. It was found that the MoS2 nanospheres channel conductivity depended directly on the bias voltage, resulting significantly in the bipolar RS effect with low switching voltage. The device exhibited the rewritable nonvolatile resistive switching with low SET/RESET voltage (2 V), high ON/OFF resistance ratio of 104 and a superior electrical bistability, introducing a potential application in data storage field. The resistance switching mechanism of MoS2 nanosphere assemblies was analyzed in the assumptive model of electron tunneling across the polarization potential barriers modulated by the external electric field as one possible interpretation[47]. The observed RS behavior, indicating the unusual electrical properties in the nanosphere or nanoparticle assemblies, can further expand the application of relevant nanodevices [48]. This work was devoted to deepen the understanding of RS mechanism and to expand nonvolatile memory devices based on the MoS2 nanosphere assemblies [49].

Y.C. Lai et al. fabricated a re-writable, flexible, and transferable sticker-type organic memory on universal substrates is demonstrated through a simple, low-temperature and cost-effective one-step methodology [50]. Fabrication of functional devices on arbitrary nonconventional substrates has significant advantages for broadening device applications and the development of soft electronic systems such as flexible, stretchable, wearable, and epidermal electronic modules [51]. Information storage devices are one of crucial elements of electronics in modern digital circuitries. Herein, The organic memory sticker based on the graphene electrode grown by chemical vapor deposition (CVD) consisted of a blending composite of polymer (poly methyl methacrylate) (PMMA):poly (3-hexylthiophene) (P3HT) in chlorobenzene (CB) fabricated by mature solution processes and facilities. The blending polymer layer can serve as the memory active layer as well as the protective layer during the transferring processes. Due to the mechanical elasticity of organic materials and graphene electrodes, the sticker-type organic memory can be easily tagged on flexible substrates after etching away the supporting metal [52]. The universal substrate selectivity of the sticker-type organic memory with re-writable characteristics revealed here may greatly broaden the application of information storage devices in immense areas and hence advance the future functional soft circuitries [53].

Deok H. Kwon et al. developed a metal oxide based resistive switching memory device and observed it under high-resolution transmission electron microscopy to get a better understanding of its switching mechanism. The sample consisted of a metal-insulator-metal structure with metals being Platinum and the insulator layer being the TiO2. The working of this system is based on change in resistance in TiO2 due to the electromigration of the oxygen vacancies inducing the redistribution of carrier density which resulted in formation of a filament like structure which connected the top and the bottom electrodes through metallic paths creating a conduction path for the current [54,55]. When an electric field was applied across the material to SET state a blown of region was observed, the high-resolution image of

the HRTEM and the FFT images confirmed the formation of a new phase of the material in the filament like structure called the Magne´li phase which is Ti4O7 this phase of the material is devoid of oxygen due to the migration of the oxygen ions to the nearby region. These filaments were grown from the cathode and conical in shape with wider diameter towards the cathode side [56].

C. Chen et al. fabricated an Al/ZnO/Si memory device at room-temperature by depositing ZnO films on n+ Si substrate by Magnetron sputtering method. Electrical characteristics revealed stable and reproducible clockwise bipolar resistive switching phenomena with self-rectifying effects in the low resistance state in this complementary metal oxide semiconductor compatible memory structure. The current-voltage curve at different temperatures and the corresponding Arrhenius plot confirmed the semiconducting conduction behavior of both the high resistance state (HRS) and the low resistance state (LRS) [57]. The conduction mechanisms were explained by the Poole-Frenkel emission and space-charge-limited conduction mechanisms for the high resistance state and the low resistance state, respectively [58]. It is proposed that the resistive switching originated from the formation and dissolution of the AlOx barrier layer which were induced by the migration of the oxygen ions at the Al/ZnO interface [59].

O.A. Ageev et al. reported the results of experimental study of an array of vertically aligned carbon nanotubes (VA CNTs) by using a scanning tunnel microscopy (STM). It is also shown that upon the application of an external electric field to the STM probe/VA CNT system, individual VA CNTs are combined into bundles whose diameter depends on the radius of the tip of the STM probe and independent of the polarity of the applied voltage. The memristor effect in VA CNTs was detected [60,61,62]. Depending on the applied voltage The VA CNT bundles can be in the low resistance or high resistance state which can be associated with polarization of carbon nanotubes and the formation of a space charge at the tip of the STM probe. The resistivity ratio in the high and low resistance states was measured to be 28 at a

voltage of 180 mV. These results can be used in the development of structures and technological processes for designing nanoelectronics devices based on VA CNT arrays, including elements of energy effective and ultra-high access memory cells for vacuum microelectronics devices [63].

2.2 References

[1] Leon O. Chua, Memristor-The Missing Circuit Element, IEEE Transactions on Circuit Theory, Vol. CT-18, No. 5, September 1971.

[2] D. B. Strukov, G. S. Snider, D. R. Stewart & R. S. Williams, The missing memristor found, Nature 453, 80–83 (2008).

[3] S. Pi, C. Li, H. Jiang, W. Xia, H. Xin, J. J. Yang & Q. Xia, Memristor crossbar arrays with 6-nm half-pitch and 2-nm critical dimension, Nature Nanotechnology volume 14, pages 35-39(2019).

[4] B. Pradhan, S. K. Batabyal, and A.J. Pal, Electrical Bistability and Memory Phenomenon in Carbon Nanotube-Conjugated Polymer Matrices, J. Phys. Chem. B 2006, 110, 8274-8277.

[5] J. B. Cui, R. Sordan, M. Burghard, K. Kern, Carbon nanotube memory devices of high charge storage stability, Appl. Phys. Lett. 2002, 81, 3260-3262.

[6] S. Wang, P. Sellin, Pronounced hysteresis and high charge storage stability of single walled carbon nanotube-based field-effect transistors, Appl. Phys. Lett. 2005, 87, 133117.

[7] A. Bandhopadhyay, A. J. Pal, Large conductance switching and binary operation in organic devices: Role of functional groups, Journal of Phys. Chem. B, 2003, 107, 2531- 2536.

[8] J. Chen, M.A. Hamon, H. Hu, Y. Chen, A. M. Rao, P. C. Eklund, and R.C. Haddon ,Solution Properties of Single-Walled Carbon Nanotubes, Science 1998, 282, 95-98.

[9] B. Pradhan, S. K. Batabyal, and A.J. Pal, Electrical Bistability and Memory Phenomenon in Carbon Nanotube-Conjugated Polymer Matrices, J. Phys. Chem. B 2006, 110, 8274-8277.

[10] B. J. Choi, S. Choi, K. M. Kim, Y. C. Shin, C. S. Hwang, S.-Y. Hwang, S. Cho, S. Park, and S.-K. Hong, Study on the resistive switching time of TiO2 thin films, Appl. Phys. Lett. 89, 012906 (2006).

[11] I. H. Inoue, S. Yasuda, H. Akinaga, and H. Takagi, Nonpolar resistance switching of metal/binary-transition-metal oxides/metal sandwiches: Homogeneous/inhomogeneous transition of current distribution, Phys. Rev. B 77, 035105 (2008).

[12] S. H. Chang, S. C. Chae, S. B. Lee, C. Liu, T. W. Noh, J. S. Lee, B. Kahng, J. H. Jang, M. Y. Kim, D.W. Kim, and C. U. Jung, Effects of heat dissipation on unipolar resistance switching in Pt/NiO/Pt capacitors Appl. Phys. Lett. 92, 183507 (2008).

[13] X. Wu, P. Zhou, J. Li, L. Y. Chen, H. B. Lv, Y. Y. Lin, and T. A. Tang, Reproducible unipolar resistance switching in stoichiometric ZrO2 films, Appl. Phys. Lett. 90, 183507 (2007).

[14] P. Yeh, Optical Waves in Layered Media (Wiley, New York, 1988).

[15] D. C. Kim, S. Seo, S. E. Ahn, D.-S. Suh, M. J. Lee, B.H. Park, I. K. Yoo, I. G. Baek, H.J. Kim, E. K. Yim, J. E. Lee, S. O. Park, H. S. Kim, U.I. Chung, J. T. Moon, and B. I. Ryu, Electrical observations of filamentary conductions for the resistive memory switching in NiO films, Appl. Phys. Lett. 88, 202102 (2006).

[16] W.Y. Chang, Y.C. Lai, T.B. Wu,1, S.F. Wang, F. Chen and M.J. Tsai, Unipolar resistive switching characteristics of ZnO thin films for nonvolatile memory applications, Appl. Phys. Lett. 92, 022110 (2008).

[17] K. Moshammer, F. Hennrich and M. M. Kappes, Selective Suspension in Aqueous Sodium Dodecyl Sulfate According to Electronic Structure Type Allows Simple Separation of Metallic from Semiconducting Single-Walled Carbon Nanotubes, Nano Res., 2009, 2, 599–606.

[18] C.S. Lao, J. Liu, P.X. Gao, L.Y. Zhang, D. Davidovic, R. Tummala, Z.L. Wang, ZnO Nanobelt/Nanowire Schottky Diodes Formed by Dielectrophoresis Alignment across Au Electrodes, Z. L. Nano Lett. 2006, 6 (2), 263–266.

[19] J. H. Song, J. Zhou, Z. L. Wang, Piezoelectric and Semiconducting Coupled Power Generating Process of a Single ZnO Belt/Wire. A Technology for Harvesting Electricity from the Environment, Nano Lett. 2006, 6 (8), 1656–1662.

[20] J. Song, Y. Zhang, C. Xu, W. Wu, and Z. L. Wang, Polar Charges Induced Electric Hysteresis of ZnO Nano/Microwire for Fast Data Storage, Nano Lett. 2011, 11, 2829– 2834.

[23] D. B. Strukov, J. L. Borghetti and R. S. Williams, "Coupled Ionic and Electronic Transport Model of Thin-Film Semiconductor Memristive Behavior," Small, vol. 5, pp. 1058-1063,2009.

[24] D.B. Strukov, F. Alibart and R.S. Williams, Thermophoresis /diffusion as a mechanism for unipolar resistive switching in metal oxide-metal memristors, Appl. Phys. A, vol. 107, pp. 509-518, 2012.

[25] R. Stanley Williams, Matthew D. Pickett and John Paul Strachan, Physics-based memristor models, 2013 IEEE International Symposium on Circuits and Systems (ISCAS),(2013).

[26] J.A. Wilson, A.D. Yoffe, The Transition Metal Dichalcogenides Discussion and Interpretation of the Observed Optical, Electrical and Structural Properties Adv. Phys. 1969, 18, 193-335.

[27] B. Radisavljevic, A. Radenovic, J. Brivio, V. Giacometti, A. Kis, Single-Layer MoS2 Transistors Nature Nanotech. 2011, 6, 147-150.

[28] C. Dean, A. Young, I. Meric, C. Lee, L. Wang, S. Sorgenfrei, K. Watanabe, T. Taniguchi, P. Kim, K. Shepard, Boron Nitride Substrates for High-Quality Graphene Electronics Nature Nanotech. 2010, 5, 722-726.

[29] G. A. Salvatore, N. Munzenrieder, C. Barraud, L. Petti, C. Zysset, L. Buthe, K. Ensslin, and G. Troster, Fabrication and transfer of flexible few-layers MoS2 thin film transistors to any arbitrary substrate ,ACS Nano 7(10), 8809 (2013).

[30] Y. Zhou, S.T. Han, Y. Yan, L. Zhou, L.B. Huang, J. Zhuang, P. Sonar and V. A. L. Roy, Ultra-flexible nonvolatile memory based on donor-acceptor diketopyrrolopyrrole polymer blends, Sci. Rep., 2015, 5, 10683.

[31] Y. Sun, L. Li, D. Wen and X. Bai, Bistable electrical switching and nonvolatile memory effect in mixed composite of oxadiazole acceptor and carbazole donor, Org. Electron., 2015, 25, 283– 288.

[32] P. K. Sarkar, S. Bhattacharjee, M. Prajapat and A. Roy, Incorporation of SnO2 nanoparticles in PMMA for performance enhancement of a transparent organic resistive memory device, : RSC Adv., 2015, 5, 105661.

[33] Y. Z. Lv, Q. Wang, Y. Zhou, C. R. Li, Y. Ge, and B. Qi, Effects of nanoparticle charging on streamer development in transformer oil-based nanofluids, AIP Adv. 6(3), 035110 (2016).

[34] Y. Lin, H. Y. Xu, Z. Q. Wang, T. Cong, W. Z. Liu, H. L. Ma, and Y. C. Liu, Transferable and flexible resistive switching memory devices based on PMMA films with embedded Fe3O4 nanoparticles, Applied Physics Letters 110, 193503 (2017)

[35] S. Kumar, Z. Wang, X. Huang, N. Kumari, N. Davila, J. P. Strachan, D. Vine, A. L. David Kilcoyne, Y. Nishi and R. S. Williams, Conduction Channel Formation and Dissolution Due to Oxygen Thermophoresis/ Diffusion in Hafnium Oxide Memristors, ACS Nano 2016, 10, 11205−11210.

[36] Y. Sun, L. Li, D. Wen, X. Bai, Bistable electrical switching and nonvolatile memory effect in mixed composite of oxadiazole acceptor and carbazole donor, Organic Electronics 25(2015) 283-288.

[37] A. Kalantarian, G. Bersuker, B. Butcher, D.C. Gilmer, S. Privitera, S. Lombardo, R. Geer, Y. Nishi, P. Kirsch, R. Jammy, In Microscopic Model for the Kinetics of the Reset Process in HfO2 RRAM, IEEE VLSI-TSA International Symposium VLSI Technology,2013, pp 1−2.

[38] M.W. Ruckman, J. Chen, S.L. Qiu, P. Kuiper, M. Strongin and B.I. Dunlap, Interpreting the Near Edges of O2 and O2- in Alkali Metal Superoxides, Phys. Rev. Lett. 1991, 67, 2533.

[39] Y. He, Y. L. Zhong, Y. Y. Su, Y. M. Lu, Z. Y. Jiang, F. Peng, T. T. Xu, S. Su, Q. Huang, C. H. Fan, and S. T. Lee, Water-Dispersed Near-Infrared-Emitting Quantum Dots of Ultrasmall Sizes for In Vitro and In Vivo Imaging, Angew. Chem. Int. Ed. 50, 5695 (2011).

[40] N. A. Tulina, I.Yu. Borisenko, I. M. Shmytko, A. M. Ionov, N. N. Kolesnikov, and D. N. Borisenko, Induced non-metallicity during resistive switching in structures based on a topological insulator Bi2Se3 ,Phys. Lett. A 376, 3398 (2012).

[41] X. Zhang, F. Wen, J. Xiang, X. Wang, L. Wang, W. Hu, and Z. Liu, Wearable nonvolatile memory devices based on topological insulator Bi2Se3/Pt fibers, Appl. Phys. Lett., 107, 103109 (2015)

[42] X. T. Li, D. J. Bergman and D. Stroud, Electric forces among nanospheres in a dielectric host, Europhys. Lett., 69, 1010 (2005).

[43] T. H. Kim, E. Y. Jang, D. J. Lee, K. J. Lee, J. T. Jang, J. S. Choi, S. H. Moon, and J. Cheon, Nanoparticle Assemblies as Memristors, Nano Lett. 9, 2229 (2009).

[44] X.Y. Xu, Z.Y. Yin, C.X. Xu, J. Dai, and J.G. Hu, Resistive switching memories in MoS2 nanosphere assemblies, Applied Physics Letters 104, 033504 (2014)

[45] B. Cho, S. Song, Y. Ji, T. W. Kim, T. Lee, Organic Resistive Memory Devices: Performance Enhancement, Integration, and Advanced Architectures, Adv. Funct. Mater., 2011, 21 , 2806 – 2829.

[46] S. H. Chae , W. J. Yu , J. J. Bae , D. L. Duong , D. Perello , H. Y. Jeong , Q. H. Ta , T. H. Ly , Q. A. Vu , M. Yun , Transferred wrinkled Al2O3 for highly stretchable and transparent graphene–carbon nanotube transistors, Nat. Mater. 2013, 12, 403 – 409.

[47] Y. Ji, S. Lee, B. Cho, S. Song, and T. Lee, Flexible Organic Memory Devices with Multilayer Graphene Electrodes, ACS Nano 2011, 5, 7, 5995–6000.

[48] Y. C. Lai , Y. X. Wang , Y. C. Huang , T. Y. Lin , Y. P. Hsieh , Y. J. Yang , and Y. F. Chen, Rewritable, Moldable, and Flexible Sticker-Type Organic Memory on Arbitrary Substrates, Adv. Funct. Mater., 2014, 24, 1430–1438.

[49] K.M. Kim, B.J. Choi, Y.C. Shin, S. Choi & C.S. Hwang, Anode-interface localized filamentary mechanism in resistive switching of TiO2 thin films. Appl. Phys. Lett. 91, 012907 (2007).

[50] K.M. Kim, & C.S. Hwang, The conical shape filament growth model in unipolar resistance switching of TiO2 thin film. Appl. Phys. Lett. 94, 122109 (2009).

[51] D.H. Kwon, K.M. Kim, J.H. Jang, J.M. Jeon, M.H. Lee, G.H. Kim, X.S. Li, G.S. Park, B. Lee, S. Han, M. Kim & C.S. Hwang, Atomic structure of conducting nanofilaments in TiO2 resistive switching memory, Nature Nanotechnology volume 5, pages 148– 153(2010).

[52] Y. C. Yang, F. Pan, Q. Liu, M. Liu, and F. Zeng, Fully room-temperature-fabricated nonvolatile resistive memory for ultrafast and high-density memory application, Nano Lett. 9, 1636 (2009).

[53] S. L. Li, D. S. Shang, J. Li, J. L. Gang, and D. N. Zheng, Resistive switching properties in oxygen-deficient Pr0.7Ca0.3MnO3 junctions with active Al top electrodes, J. Appl. Phys. 105, 033710 (2009).

[54] C. Chen, F. Pan, Z. S. Wang, J. Yang and F. Zeng, Bipolar resistive switching with self-rectifying effects in Al/ZnO/Si structure, Journal Of Applied Physics 111, 013702 (2012).

[55] J. B. Cui, R. Sordan, M. Burghard, K. Kern, Carbon nanotube memory devices of high charge storage stability, Appl. Phys. Lett. 2002, 81, 3260-3262.

[56] S. Wang, P. Sellin, Pronounced hysteresis and high charge storage stability of single walled carbon nanotube-based field-effect transistors, Appl. Phys. Lett. 2005, 87, 133117.

[57] A. Bandhopadhyay, A. J. Pal, Large conductance switching and binary operation in organic devices: Role of functional groups, Journal of Phys. Chem. B, 2003, 107, 2531- 2536.

[58] J. Song, Y. Zhang, C. Xu, W. Wu, and Z. L. Wang, Polar Charges Induced Electric Hysteresis of ZnO Nano/Microwire for Fast Data Storage, Nano Lett. 11, 2829–2834 (2011).

[59] G. Zhou, B. Sun, Y. Yao, H. Zhang, A. Zhou, K. Alameh, B. Ding, and Q. Song, Investigation of the behaviour of electronic resistive switching memory based on MoSe2-doped ultralong Se microwires, Appl. Phys. Lett. 109, 143904 (2016).

[60] Y. Z. Lv, Q. Wang, Y. Zhou, C. R. Li, Y. Ge, and B. Qi, Effects of nanoparticle charging on streamer development in transformer oil-based nanofluids, AIP Adv. 6(3), 035110 (2016).

[61] Y. Lin, H. Y. Xu, Z. Q. Wang, T. Cong, W. Z. Liu, H. L. Ma, and Y. C. Liu, Transferable and flexible resistive switching memory devices based on PMMA films with embedded Fe3O4 nanoparticles, Applied Physics Letters 110, 193503 (2017).

[62] Y. C. Lai, Y. X. Wang, Y. C. Huang, T. Y. Lin, Y. P. Hsieh, Y. J. Yang, and Y. F. Chen, Rewritable, Moldable, and Flexible Sticker-Type Organic Memory on Arbitrary Substrates, Adv. Funct. Mater., 24, 1430 (2014).

[63] C. Scott and L.D. Bozano, Nonvolatile Memory Elements Based on Organic Materials, Adv. Mater., 19, 1452 (2007).

Chapter 3

Instruments and Apparatus

3.1 Synthesis and Device Fabrication

3.1.1 Hydrothermal Synthesis

Hydrothermal synthesis can be defined as a method of synthesis of single crystals that depends on the solubility of minerals in hot water under high pressure. The crystal growth is performed in an apparatus consisting of a steel pressure vessel called an autoclave, in which a nutrient is supplied along with water. A temperature gradient is maintained between the opposite ends of the growth chamber. At the hotter end the nutrient solute dissolves, while at the cooler end it is deposited on a seed crystal, growing the desired crystal. Advantages of the hydrothermal method over other types of crystal growth include the ability to create crystalline phases which are not stable at the melting point. Also, materials which have a high vapour pressure near their melting points can be grown by the hydrothermal method[1]. The method is also particularly suitable for the growth of large good-quality crystals while maintaining control over their composition. Disadvantages of the method include the need of expensive autoclaves, and the impossibility of observing the crystal as it grows if a steel tube is used. There are autoclaves made out of thick walled glass, which can be used up to 300 ˚C and 10 bar.

(a) **(b)**

Fig 3.1 (a) Photograph of an Oven for Hydrothermal Synthesis, (b) Autoclave with Teflon container

The hydrothermal autoclave is primarily used for the crystallization process, which involves the process of treating hydrothermal solvent under high temperature and pressure conditions. There are two types of reactor depending on the inner vessel type, One made of Teflon/PTFE lined hydrothermal autoclave, the other one is a Teflon lined autoclave particularly used for the high-temperature method, i.e., above 250° C. Prime users of the two reactor varieties are Research labs, academic institutes as well as industries. Many types have been designed & developed after factoring the Teflon liner capacity starting from 10ml, to 3000 ml. The other industry term for hydrothermal autoclave is also known as hydrothermal synthesis reactor used to carry out the hydrothermal reaction. One interesting development when it comes to the hydrothermal reaction is to sustain high peak pressure at peak temperature for a prolonged period. The gold lining was put to use during the early days while designing steel autoclaves by researchers. Thus along with new designs more & better new lining materials were used to design reliable autoclaves which would perform under peak pressure & peak temperature and therefore such specially designed hydrothermal autoclave came to termed as "hydrothermal bomb" that helped to induce the desired ideal conditions for the synthesis of several high-temperature oxide minerals.

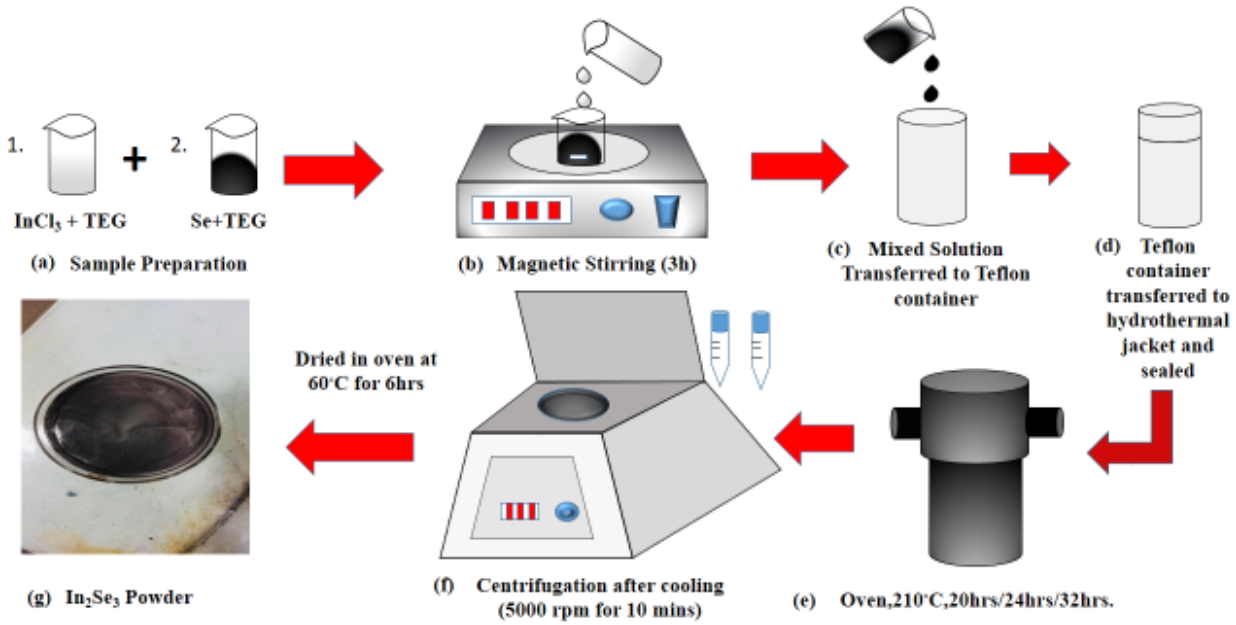

Fig 3.2 Hydrothermal Synthesis of In_2Se_3

3.1.2 Spin Coating

Spin coating is a procedure used to apply uniform thin films to flat substrates. A typical process involves depositing a small puddle of a fluid resin onto the center of a substrate and then spinning the substrate at high speed (typically around 3000 rpm). Centrifugal force will cause the resin to spread to, and eventually off, the edge of the substrate leaving a thin film of resin on the surface. Final film thickness and other properties will depend on the nature of the resin (viscosity, drying rate, percent solids, surface tension, etc.) and the parameters chosen for the spin process. Factors such as final rotational speed, acceleration, and fume exhaust contribute to how the properties of coated films are defined. A machine used for spin coating is called a spin coater, or simply spinner.[2] Rotation is continued while the fluid spins off the edges of the substrate, until the desired thickness of the film is achieved. The applied solvent is usually volatile, and simultaneously evaporates. So, the higher the angular speed of spinning, the thinner the film. The thickness of the film also depends on the concentration of the solution and the solvent.

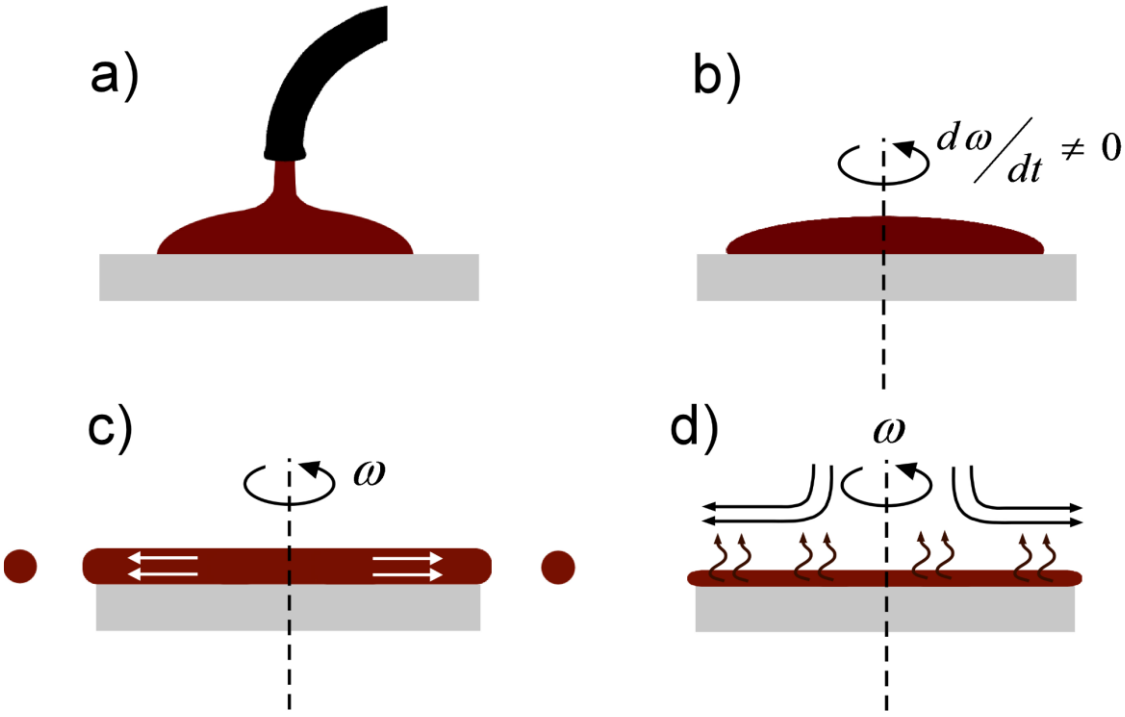

3.3 Four Fig distinct stages of Spin Coating

Spin coating is widely used in micro-fabrication, where it can be used to create thin films with thicknesses below 10 nm. It is used intensively in photolithography, to deposit layers of photoresist about 1 micrometre thick. Photoresist is typically spun at 20 to 80 revolutions per second for 30 to 60 seconds. Owing to the low values of thickness which can be achieved using spin coating methods, this method is often employed in the fabrication of transparent titanium dioxide thin films on quartz or glass substrates, such thin film coatings may exhibit self-cleaning and self-sterilizing properties.

One of the most important factors in spin coating is repeatability. Subtle variations in the parameters that define the spin process can result in drastic variations in the coated film. In spite of few studies regarding the spin coating method, it has substantial merits, such as the easy control and handling of chemicals and substrates, and fabrication of thin film at faster rates.

3.1.3 Thermal Evaporation

One of the most popular physical deposition techniques is this one. It is simple method and one can evaporate a large variety of materials on various substrates. In this method, deposition material is created in a vapor form by heating bulk material in vacuum using resistive heater. The vapor atoms are transported through vacuum to get deposited on the desired substrate. Almost all materials are vaporizing from a solid or liquid phase as neutral atoms or molecules. This vapour deposition is done only at pressure less than 5- 10 torr. By the help of this instrument, we mainly deposit low melting point materials like Silver, Aluminium and Gold (schematic diagram shown in Fig 3.4). The evaporation of the desired material is done in vacuum system, which consists of a diffusion pump backed by a rotary pump. The desired evaporate material is supplied by a continuous source which is then heated to a sufficiently high temperature to produce desired vapour pressure. The vacuum system employed to deposit

and characterize thin films in the present work contain a variety of pumps, tubing, valves and gauges to establish and measure the required pressure. The "Hind Hivac" coating unit's vacuum system (Model No. 12 A4) essentially comprises of a 0.4 m diffusion pump working in tandem with an oil-sealed rotary pump. Optical image of the device shown in figure 3.5. The ultimate pressure achieved in a 30 cm diameter stainless steel bell jar is of the order of 6 x 10^{-6} Torr. Substrates can be cleaned by ion bombardment. [3]

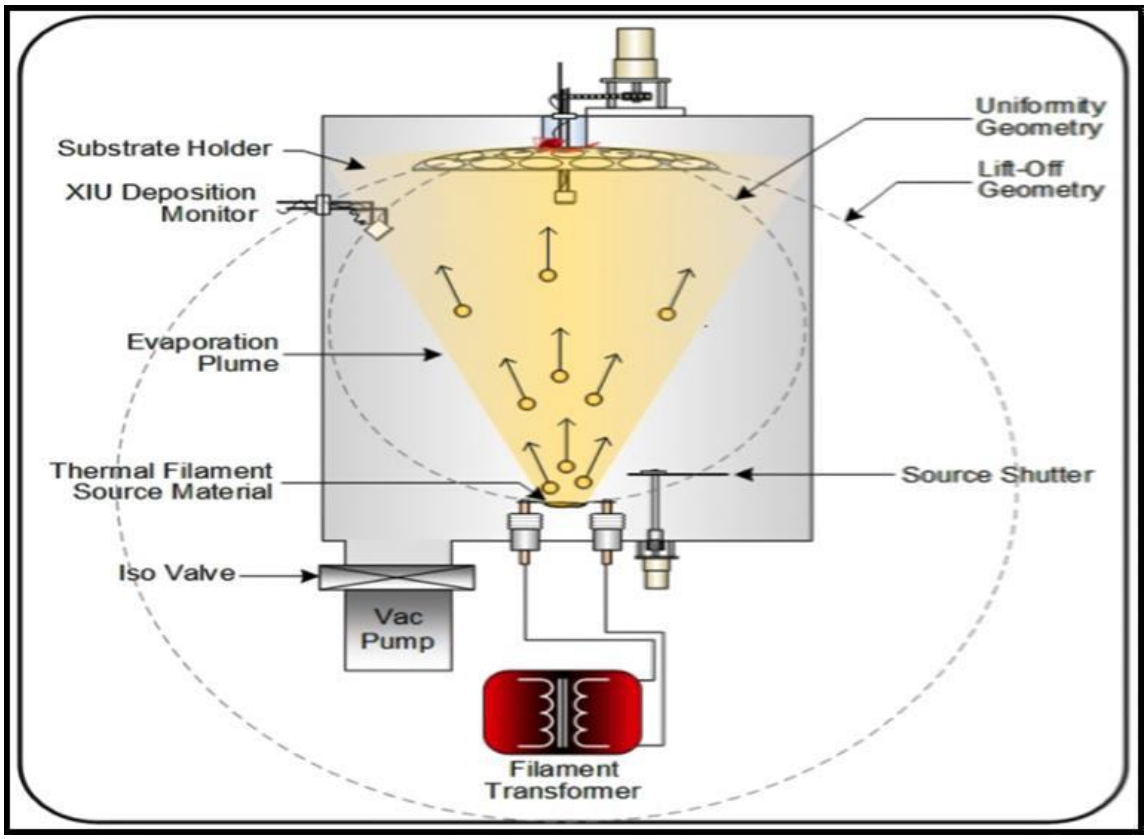

Fig 3.4 Schematic diagram of experimental setup for Thermal Evaporator

A low-tension transformer of 10V-100 A is used for filament heating. Most of the evaporations are carried out at pressures of (1-8) x 10^{-4} Torr. The pressure obtained by the rotary pump is measured by means of a Pirani gauge and a Penning gauge measures the diffusion vacuum. This machine was used to deposited Al (Aluminium) electrode in our experiment.

Fig 3.5 Thermal Evaporator unit with accesssories

3.2 Characterization

3.2.1 X-Ray Diffractometer (XRD)

X-Ray diffractometer analysis (XRD), in which X-Ray diffraction patterns are recorded using Cu (Kα) radiation source (λ=1.5406), is the primary characterization technique used to determine the structural phase and crystallinity of a certain material.

- X-Ray diffraction principle and Bragg's Law:

Considering a crystal to be regular arrays of atoms and X-rays to be the electromagnetic waves then electrons inside the atoms gets scattered through impinging X-ray waves. This is an example of elastic scattering. So, for a regular array of atoms, regular array of spherical waves is generated. These emanating waves of electrons from inside the crystal cancel out each other in most cases through destructive interference barring a few exceptions in which they lead to constructive interference according to Bragg's law:

$$2d\sin\theta = n\lambda \text{ .....(i)}$$

Here, d is the distance between diffracting planes, θ is the incident angle of the X-rays, n is any integer and λ is the wavelength of the incoming X-ray beam.

Usually when an XRD pattern for a material is obtained it is then compared with standard diffraction database files published by the Inorganic Crystal Structure Database (ICSD) for the material with specific crystal symmetry to match and confirm the phase purity. Other than crystallinity and phase information of a material, information of strain can also be obtained using XRD analysis.[4]

Calculation of strain can be done by observing the shift in diffraction peak positions due to presence of defects or doping as it gives the change in d-spacing and signifies change in lattice constant under homogeneous strain. Information about inhomogeneous strain can also be obtained using XRD analysis in some cases. However, the most accepted way to calculate crystallite size in absence of inhomogeneous strain is given by the Scherrer's formula:

$$D = (k\lambda / \beta \cos\theta) \text{……..(ii)}$$

Here, D is the crystal size, β is full width and half maxima of diffraction peak, θ is diffraction angle, k is Scherrer constant generally 0.9, λ is the wavelength of x-ray.

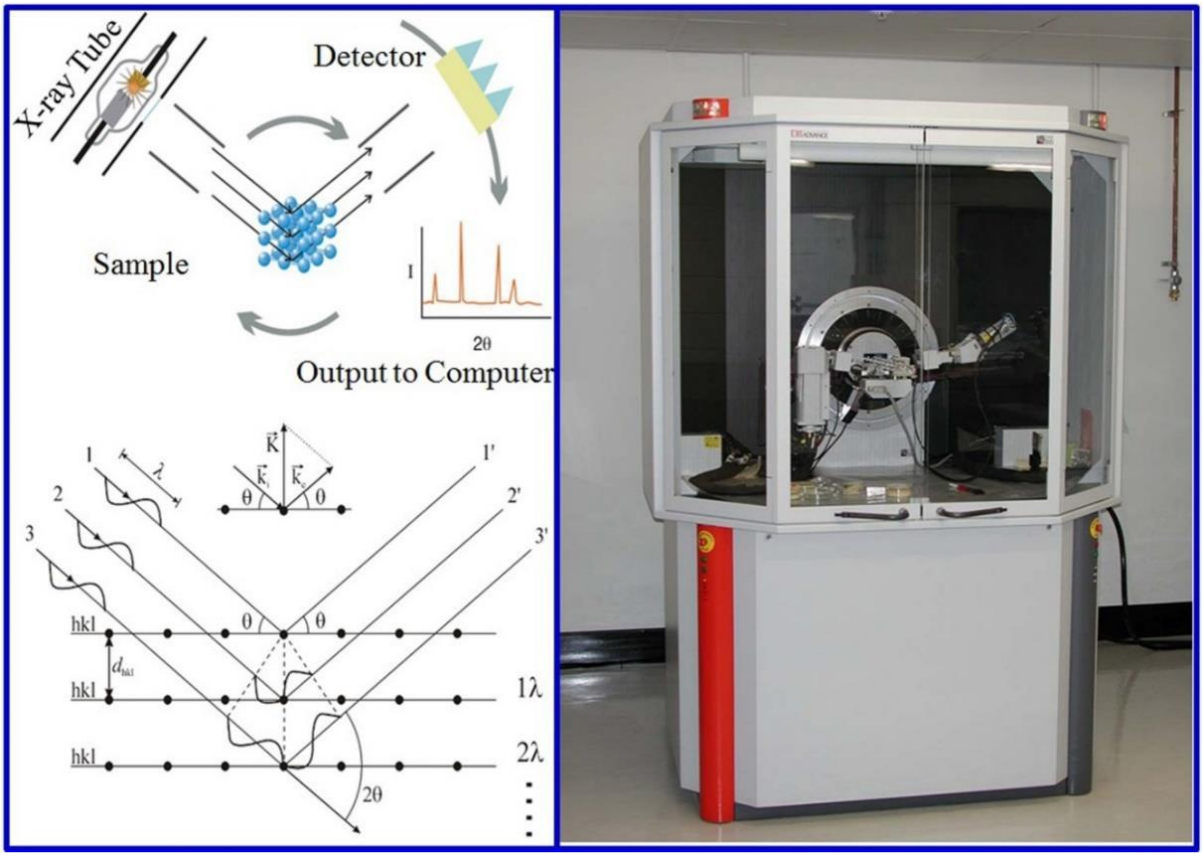

Fig 3.6 Schematic of working principle behind X-Ray diffraction according to Bragg's law with XRD machine in left side

After getting the XRD data, I plot that data with the help of Origin software to get the XRD pattern. With the help of X-part High Score software and Origin I derived the crystallites sizes and Miller indices for my samples. Here XRD unit and schematic representation of mechanism involved in XRD technique also Bragg's law shown in figure 3.6.

3.2.2 Field Emission Scanning Electron Microscopy (FESEM)

The most effective and widely used method for characterising materials at the nanoscale is electron microscopy. Ernst Ruska invented the TEM in 1939 as a result of the constrained imaging resolution of the time's optical microscopes. The discrepancy is due to the wavelength

of the sources that are being utilized, in this case light and electrons. Two research teams, Davisson & Germer and Thomson & Reid, independently conducted their classic electron diffraction experiment in 1927, barely two years after de Broglie's theoretical prediction of the wave qualities of electrons. This experiment verified the wave nature of electrons. The use of electron microscopes over optical microscopes is preferred for two main reasons (OM). The electromagnetic lenses inside the microscope column can readily and effectively manipulate the electrons, which is the first justification. The second factor is the electron's extremely narrow wavelengths, which provide better resolution than the OM. The wavelength of the source has a significant impact on the resolution of microscopes.

High resolution imaging is achieved using the field emission scanning electron microscope (FESEM),[5] which accelerates electrons from a field emission source in a field gradient under high vacuum. These so-called primary electrons are focused and refracted by electronic lenses within the high vacuum column to create a narrow scan beam that bombards the target. In most cases, incident electrons interact with a specimen and six different types of electrons are produced: transmission, backscattered, reflected, secondary, Auger, and trapped electrons (Figure 3.7 c). As a result, each area on the item emits secondary electrons. The surface structure of the item is related to the angle and speed of these secondary electrons. The secondary electrons are captured by a detector, and a picture of the sample surface is created by contrasting their intensity with that of the primary electron beam that is scanning. Different signals (secondary electrons, backscattered electrons, etc.) are released from each point that is exposed to an electron beam when it is scanned across a specimen surface.

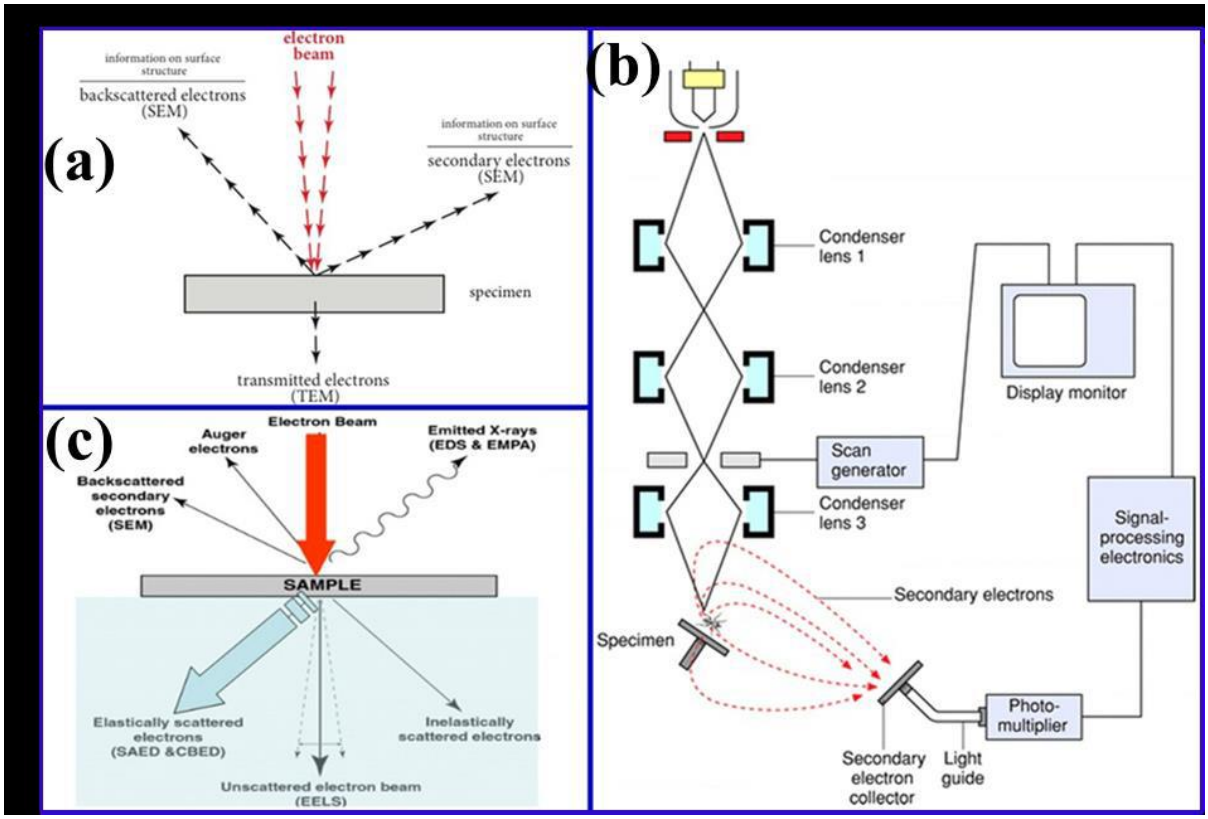

Fig 3.7 Schematic line diagram of FESEM machine. Also, electron paths and different types of secondary beams shown in left side of the image

These signals are recognized, translated into electric signals, amplified, and either converted into a digital image that can be saved and processed further or into a video scan-image that can be displayed on an LCD monitor. A field emission scanning electron microscope is depicted simply schematically in figure 3.7 (b).

The In_2Se_3 nanostructures were subjected to detailed morphological investigations with a FESEM (FEI - INSPECT F50) instrument. Coating the sample with a thin layer of conductive material, such gold or platinum, applied using a sputtering machine, is a popular preparation technique. The instrument's resolution was 2 nm (1 kV of accelerating voltage) and 1 nm (Accelerating voltage 15 kV). Between 0.5 and 30 kV is the range of the accelerating voltage (in 100 V steps). It was possible to alter the magnification between 30 X and 3,000 X (low magnification mode) and 100 X and 800,000 X. Figure 3.8 depicts a shot of the FESEM device.

With narrower probing beams available at both low and high electron energies thanks to a scanning electron microscope's field-emission cathode, spatial resolution is increased while sample charging and damage are reduced. Original optical image of FEI INSPECT F50 FESEM machine shown in figure 3.8.

Fig 3.8 Image of FEI INSPECT F50 FESEM machine

3.2.3 High Resolution Transmission Electron Microscopy (HRTEM)

Transmission electron microscope (TEM) is an analytical tool allowing visualisation and analysis (1 micron = 10^{-6}m) to nanospace (1 nanometer/nm = 10^{-9}m). A beam of electrons is transmitted through an ultrathin specimen, interacting with the specimen as it passes through. An image is formed from the interaction of the electrons transmitted through the specimen; the image is magnified and focused onto an imaging device, such as a fluorescent screen, on a layer

of photographic film, or to be detected by a sensor such as a CCD camera. TEMs are capable of imaging at a significantly higher resolution than light microscopes, owing to the small de Broglie wavelength of electrons.

- **Working Principle**

The “Virtual Source” at the top represents the electron gun, producing a stream of monochromatic electrons. This stream is focused to a small, thin, coherent beam by the use of condenser lenses 1 and 2. The first lens (usually controlled by the “spot size knob”) largely determines the "spot size"; the general size range of the final spot that strikes the sample. The second lens (usually controlled by the "intensity or brightness knob" actually changes the size of the spot on the sample; changing it from a wide dispersed spot to a pinpoint beam. The beam is restricted by the condenser aperture (usually user selectable), knocking out high angle electrons (those far from the optic axis, the dotted line down the centre). The beam strikes the specimen and parts of it are transmitted. This transmitted portion is focused by the objective lens into an image. Optional Objective and Selected Area metal apertures can restrict the beam; the Objective aperture enhancing contrast by blocking out high-angle diffracted electrons, the Selected Area aperture enabling the user to examine the periodic diffraction of electrons by ordered arrangements of atoms in the sample. The image is passed down the column through the intermediate and projector lenses, being enlarged all the way. The image strikes the phosphor image screen and light is generated, allowing the user to see the image.[6]

- **Sample Preparation**

Sample preparation for TEM generally requires more time and experience than for most other characterization techniques. A TEM specimen must be approximately 1000 Ao or less in thickness in the area of interest. The entire specimen must fit into a 3 mm diameter up and be

less than about 100 microns in thickness. A thin, disc shaped sample with a hole in the middle, the edges of the hole being thin enough for TEM viewing, is typical. The initial disk is usually formed by cutting and grinding from bulk or thin film/substrate material, and the final thinning done by ion milling. Other specimen preparation possibilities include direct deposition onto a TEM-thin substrate (Cu, carbon grid); direct dispersion of powders on such a substrate; grinding and polishing using special devices like tripod; chemical etching and electro-polishing; and lithographic patterning of walls and pillars for cross-section viewing.

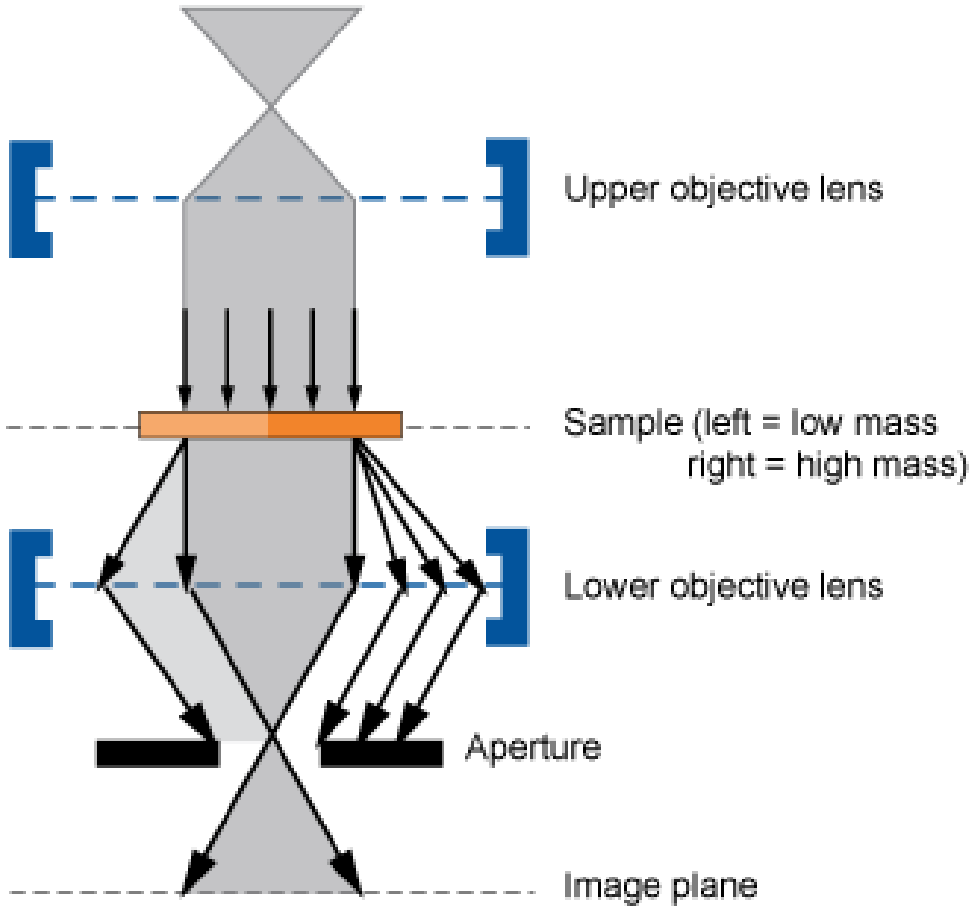

Fig 3.9 Schematic of TEM

3.2.4 UV-Vis Spectroscopy

UV-Vis-NIR spectrophotometer is used to study the optical properties of nano samples. Optical transmittance, absorbance and reflectance can be measured using this spectrometer. The Bouguer-Lambert-Beer law forms the mathematical physical basis for the light absorption measurements on gas and in solution. According to this law, absorbance is directly proportional to the path length, l and the concentration of the absorbing substance, c, and can be expressed as $A = \alpha lc$, where α is a constant of proportionality, called the absorptivity. An important technique for measuring the band gap of the semiconductor material is to study its absorption or transmission of incident photon by the material. Since the photon with energies greater than band gap are absorbed while photon with energy less than the band gap is transmitted. Hence the experiment gives the accurate measure of the material's band gap. A Shimadzu UV-Vis-NIR (UV-3101-PC) spectrophotometer was used to measure absorbance spectra [7]of the In_2Se_3 solution.

A beam of light of selected wavelength is passed through the sample. Visible, near-infrared or ultraviolet light from the lamp enters the monochromators, which disperse the light (spread it into a spectrum) and select the particular wavelength chosen by the operator for the measurement.

Shimadzu UV-Vis-NIR (UV-3101-PC) spectrophotometers were used to measure the extent to which the samples under consideration absorbance light of different wavelengths. A photograph of the instrument is shown in the Fig. 3.10. The instrument automatically records a graph of absorbance vs. wavelength. From that graph the bandgap of In_2Se_3 measured using some mathematical process.

Fig 3.10 Photograph of Shimadzu UV-Vis-NIR (UV-3101-PC) spectrophotometer.

3.2.5 Raman Spectroscopy

Raman scattering was first observed by Dr. C. V. Raman in 1928 and was used to investigate the vibrational states of many molecules. Raman Spectroscopy technique is based on the principle of inelastic scattering of monochromatic light on the sample. A laser beam is used as the monochromatic light to irradiate a spot on the sample under investigation. Inelastic scattering deals with the phenomenon in which frequency of photons in monochromatic light changes upon interaction with a sample. Frequency of the reemitted photons is shifted up or down in comparison with original monochromatic frequency, which is called the Raman Effect. The scattered radiation produced by the Raman Effect contains information about the energies of molecular vibrations and rotations, and these depend on the particular atoms or ions that

comprise the molecule, the chemical bonds connect them, the symmetry of their molecule structure, and the physico-chemical environment where they reside. Raman spectroscopy can be used to study solid, liquid and gaseous samples.

- **Working Principle**

When a sample is irradiated with an intense monochromatic light source (usually a laser), most of the radiation is scattered by the sample and the same wavelength as that of the incoming laser radiation in a process known as Rayleigh scattering. However, a small proportion of the incoming light, approximately one photon out of a million, is scattered at a wavelength that is shifted from the original laser wavelength.

The Raman effect is based on molecular deformations in electric field E determined by molecular polarizability α. The laser beam can be considered as an oscillating electromagnetic wave with electrical vector E. Upon interaction with the sample it induces electric dipole moment $P = \alpha E$ which deforms molecules. Because of periodical deformation, molecules start vibrating with characteristic frequency υm amplitude of vibration is called a nuclear displacement. In other words, monochromatic laser light with frequency υ_0 excites molecules and transforms them into oscillating dipoles. Depending upon the change of frequency of the scattered light Raman Scattering[8] phenomenon can be classified as:

1. Rayleigh scattering - A molecule with no Raman-active modes absorbs a photon with the frequency υ_0. The excited molecule returns back to the same basic vibrational state and emits light with the same frequency υ_0 as an excitation source. This type of interaction is called an elastic Rayleigh scattering.

2. Stokes - A photon with frequency υ_0 is absorbed by a Raman-active molecule which at the time of interaction is in the basic vibrational state. Part of the photon's energy is transferred to

the Raman-active mode with frequency υm and the resulting frequency of scattered light is reduced to υ_0 - υm. This Raman frequency is called Stokes frequency, or just “Stokes”.

3. Anti-Stokes - A photon with frequency υ0 is absorbed by a Raman-active molecule, which, at the time of interaction, is already in the excited vibrational state. Excessive energy of excited Raman active mode is released, the molecule returns to the basic vibrational state and the resulting frequency of scattered light goes up to υ_0 + υm. This Raman frequency is called Anti-Stokes frequency, or just “Anti-Stokes”.

- **Components of Raman Spectroscopy**

Raman Spectrometer consists of the following components :

1. Monochromatic source - A sample is normally illuminated with a laser beam in the ultraviolet (UV), visible (Vis) or near infrared (NIR) range. Scattered light is collected with a lens and is sent through an interference filter or spectrophotometer to obtain Raman spectrum of a sample. Sample illumination and light collection (probe). The probe is a collection device that collects the scattered photons, filters out the Rayleigh scatter and any background signal from the fibre optic cables, and sends the scattered light to the spectrograph. Many probes also focus and deliver the incident laser beam.

2. Wavelength selector (Filter or Spectrophotometer) - When Raman-scattered photons enter the spectrograph, they are passed through a transmission grating to separate them by wavelength and are passed to a detector. The same transitions between molecular vibrational states (M) and (M*) in the infrared absorption can also result in Raman scattering. A key difference between the Raman and infrared processes is that, in the former process, the photons involved are not absorbed or emitted but rather shifted in frequency by an amount corresponding to the energy of the particular vibrational transition.

3. Detector (Photodiode array, CCD or PMT) - Optical multichannel analyzer, PMT, intensified photo array, a charged coupled device (CCD) records the intensity of the Raman signal at each wavelength. This data is represented as a Raman spectrum. The monochromatic light from a laser passes through focusing optics and a beam splitter to the sample. The scattered light passes through the beam splitter to a detector. The laser light illuminates the sample through a microscope objective (magnification from 100x to 1000x, typically), which is used both for the illumination (laser beam coming from the laser through mirrors and/or optical fibre) and collection of the scattered light. The scattered light goes to the CCD detector via two steps, the first one to suppress the Rayleigh scattering and the second one to split the selected spectral window on the CCD array in order to be able to see all the spectral components. A computer is used to scan, collect, and process the data creating a graph showing the intensity of light at each wavelength. The change in energy is observed as a change in frequency of the incident beam upon scattering.

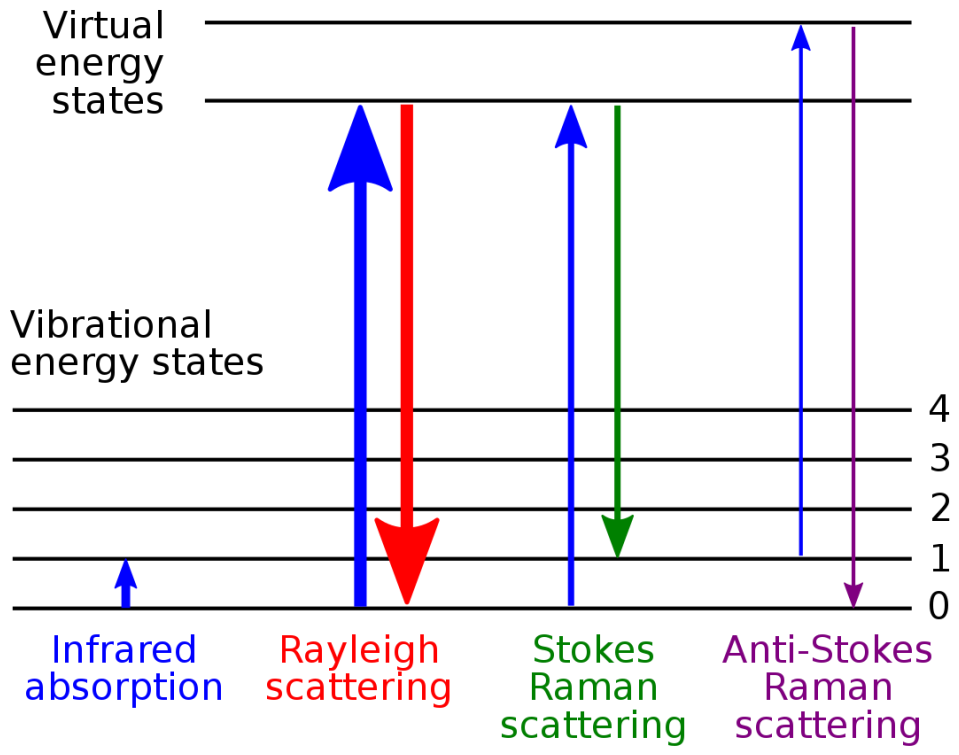

Fig 3.11 Different Scatterings of Raman Spectra

for our sample In_2Se_3 the experiment is done by Horiba Xplora Plus Raman Spectrometer with a laser of wavelength 532 nm.

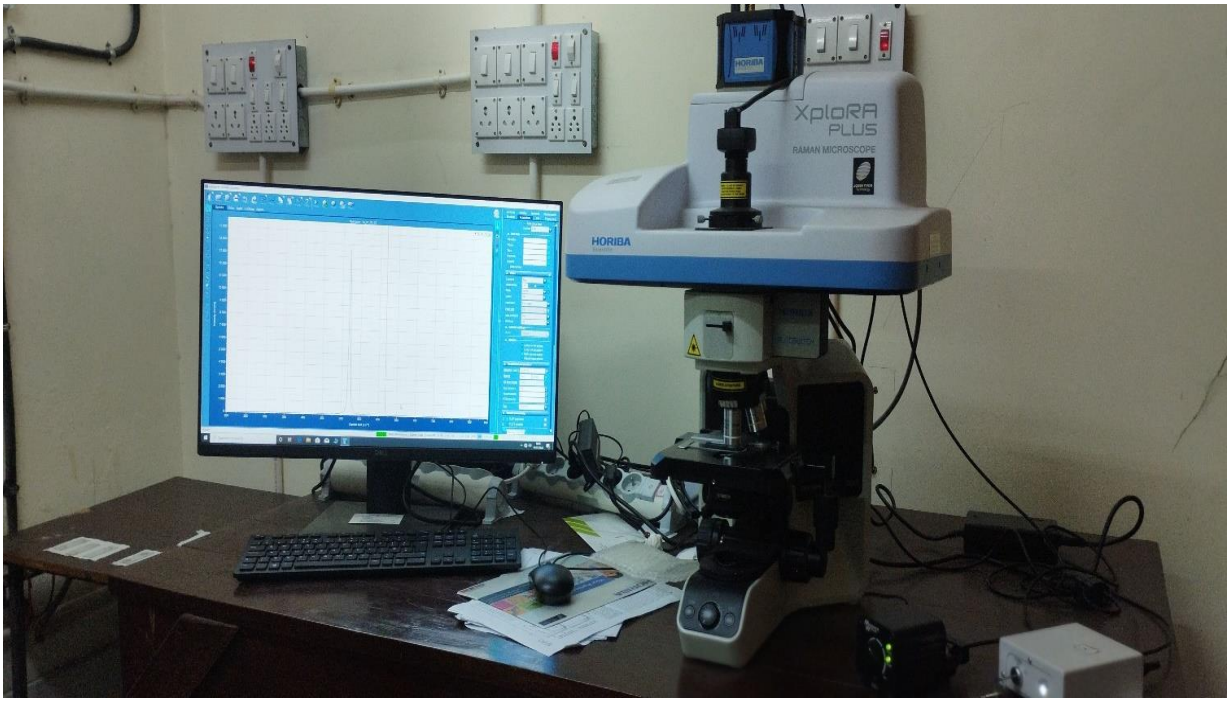

Fig 3.12 The Raman Spectrometer Set Up

3.2.6 X-Ray Photoelectron Spectroscopy (XPS)

X-Ray Photoelectron Spectroscopy is one of the most powerful surface analytical techniques capable to provide accurate qualitative elemental analysis (for all elements except hydrogen and helium), quantitative composition and determination of chemical states such as binding and oxidation can also be done. The information should be originated within ~10 nm from the outer surface.

3.2.6.1 Principles of XPS

XPS is based on the photoelectric effect which is discovered by Hertz in 1887. In this case, electron emission from the surface is resulted due to the interaction of an x-ray photon of sufficient energy with the solid surface. The applied x-ray of 1-15 KeV energy is capable to induce electrons not only from the outer shells but also from the core levels of all elements of periodic table. The governing equation of this phenomenon is as follows:[9]

$$h\boldsymbol{\nu} = E_b + E_{kin} + W_f$$

Where E_b is binding energy, E_{kin} is the kinetic energy of the photoelectron, W_f is the work function of the instrument.

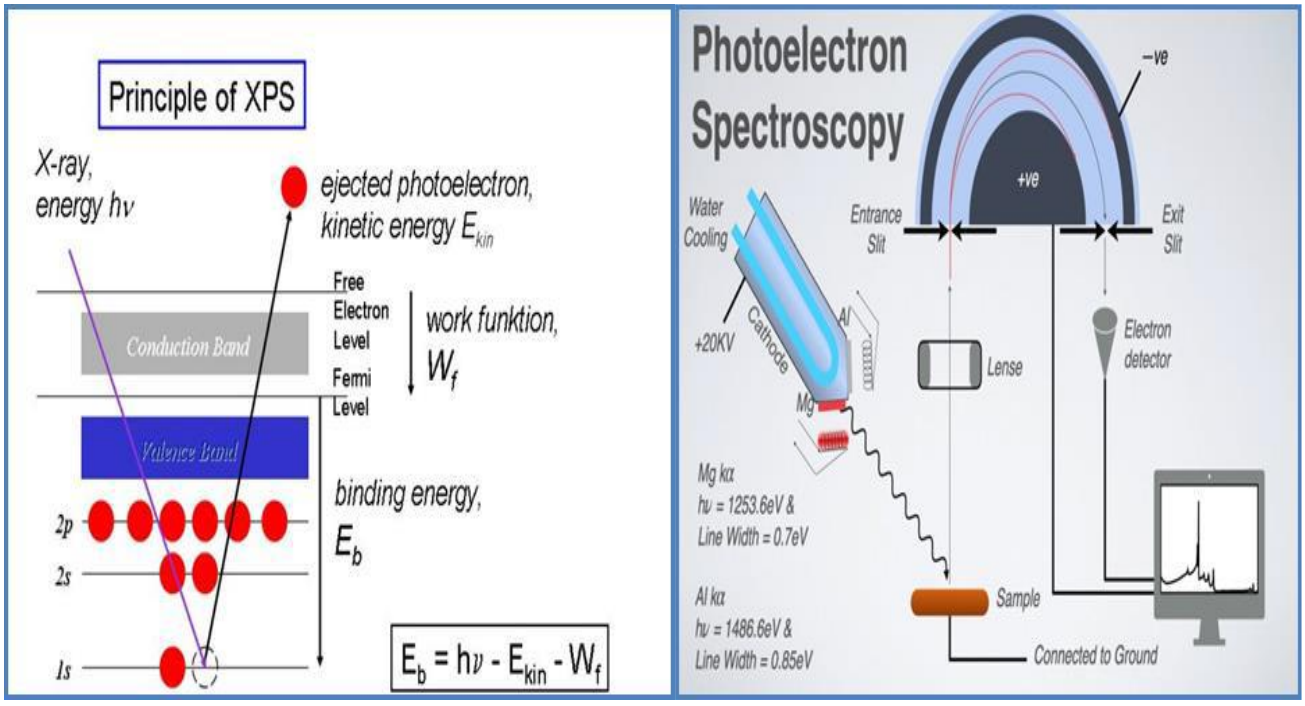

Fig 3.13 Basic principle and construction of XPS

3.2.6.2 Configuration of XPS instrument

The experimental set-up contains mainly the following parts: (i) an X-ray source for XPS, (ii) an electron energy analyzer, combined with a detection system, and (iii) a sample stage, all contained within a vacuum chamber. As for most techniques, the system is operated and controlled by a computer, usually provided a software allowing mathematical treatment.

• X-ray source

Since XPS is concerned with the analysis of core electrons from a solid surface, sources used in XPS must be able to produce photons of sufficient energy to access a suitable number of core electron levels. Photons of this energy lie within the X-ray region of the electromagnetic spectrum. As a result, these are otherwise referred to as X-rays. X-ray tubes produce X-rays by directing a sufficiently energetic electron beam at some metallic solid. This metallic object is referred to as the X-ray anode, with the electron source being the cathode. Although any solid can in principle is used as an X-ray anode, Al has become the most commonly used in XPS due to the relatively high energy and intensity of Al-Kα X-rays, the minimal energy spread of Al-Kα X-rays and the fact that Al is an effective heat conductor.

• Electron energy analyzer

Since the information in XPS is derived from the Ekin of the electron emissions, effective analysis requires an energy filter that exhibits both a high-energy resolution and a high transmission. The former allows for the separation of closely spaced peaks, thereby optimizing speciation identification capabilities, while the latter allows for sensitivity to be maximized. The two primary energy filter configurations used in XPS named Cylindrical Mirror Analyzer (CMA), and Concentric Hemispherical Analyzer (CHA).

• Detector

In XPS, it is not only important to measure the energy of the electron emissions but also the number of electrons produced. XPS spectra are plotted in units of energy versus intensity, with the energy defined by the energy analyzer used and the intensity defined by the number of electrons recorded by the detector. To obtain the best possible sensitivity, the detector must be capable of recording individual electrons, that is, operating in pulse counting mode. This signal is recorded in units of current (A), which are then represented in units of counts per second.

• Sample stage

The mounting of the samples on the sample holder should be done in such a way that electrical conduction is guaranteed. This is achieved by using metallic clips or bolt-down assemblies. Alternatively, metal-loaded tape may also be used. In the case of powders, the particles can be pressed into an indium foil or carbon tape.

• Vacuum requirement

As XPS is a surface-sensitive method, impurities can play a major role in the observed spectra. The criterion is that a good vacuum is needed to maintain the integrity of the surface. In general, 10-5Torr is sufficient to allow the Photoelectron to reach the detector without suffering collisions with other gas molecules. On the other hand, 10-9Torr or lower is required to keep an active surface clean for more than several minutes. So, 10-8 - 10-9Torr provides a reasonable pressure range for XPS measurement. Sample analysis was performed on the SPECS with a hemispherical energy analyzer (HAS 3500). Photoelectrons were excited using the monochromatic Mg Kα X-ray (1253.6eV) or Al Kα X-ray (1486.6eV) was used as the excitation source operated at 10 kV and with an anode current 17 mA.

3.2.7 I–V Measurements Keysight Source Meter (B2902A):

Keysight B2902A source meter used to measure all current-voltage measurements including resistive switching and synaptic properties during my project work. This SMU is very much portable and advanced, cost effective, easy to use compare to other competitors in market. A 2-channel, small, and reasonably priced bench-top SMU, the Keysight B2902A Precision Source / Measure Unit (SMU) has the ability to source and measure both voltage and current. [10].It can easily and accurately monitor current vs. voltage because to its versatility. I-V measurement is made simple and straightforward without the need to configure different instruments thanks to the integration of 4 quadrant source and measurement capabilities. The minimal expenditure is made possible by the single instrument's extensive coverage of 210 V, 3 A DC, and 10.5 A pulse. Accurate characterization of the DUT is supported by a minimum measurement resolution of 100 fA/100 nV. The Keysight B2902A Precision Source / Measure Unit (SMU) is a benchtop SMU with two channels that can used as source and measure current as well as voltage.

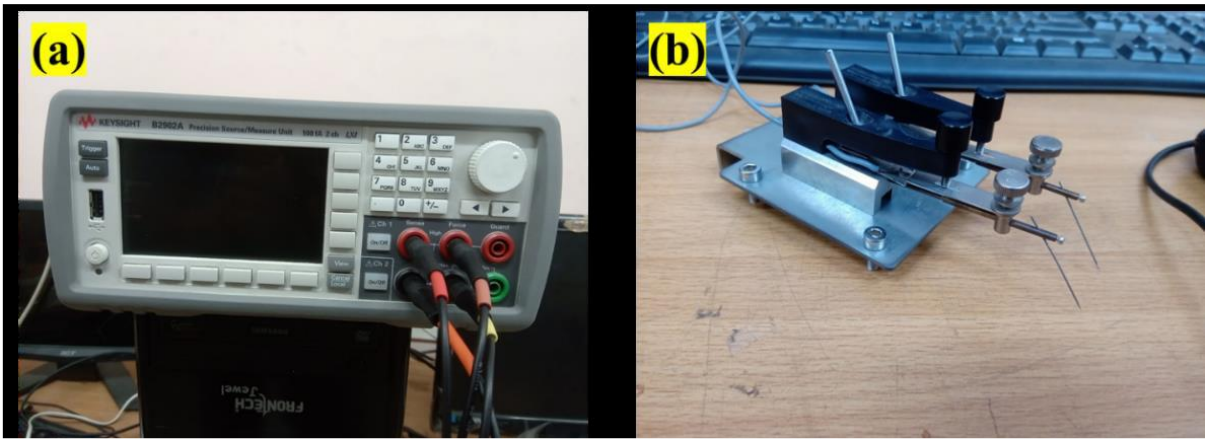

Fig 3.14 (a) Keysight SMU B2902A, (b) Tungsten Probs

I also use tungsten(W) probs for connecting top and bottom electrodes with this system. Keysight B2902A SMU and tungsten probs are shown in figure 3.14.

3.3 References

1. *Morey, G.W.J.J.o.t.A.C.S., Hydrothermal synthesis. 1953.* ***36****(9): p. 279-285.*
2. *Sahu, N., B. Parija, and S.J.I.J.o.P. Panigrahi, Fundamental understanding and modeling of spin coating process: A review. 2009.* ***83****(4): p. 493-502.*
3. *Heinemeyer, F., et al. Inline high-rate thermal evaporation of Aluminum as a novel industrial solar cell metallization scheme. in 2nd Workshop on Metallization for Crystalline Silicon Solar Cells. 2010.*
4. *Chauhan, A. and P.J.J.A.B.T. Chauhan, Powder XRD technique and its applications in science and technology. 2014.* ***5****(5): p. 1-5.*
5. *Shi, X., et al., A FESEM/EDX investigation into how continuous deicer exposure affects the chemistry of Portland cement concrete. 2011.* ***25****(2): p. 957-966.*
6. *Toth, P.J.C., Nanostructure quantification of turbostratic carbon by HRTEM image analysis: State of the art, biases, sensitivity and best practices. 2021.* ***178****: p. 688-707.*
7. *Beard, E.J., et al., Comparative dataset of experimental and computational attributes of UV/vis absorption spectra. 2019.* ***6****(1): p. 307.*
8. *Lyon, L.A., et al., Raman spectroscopy. 1998.* ***70****(12): p. 341-362.*
9. *Seah, M.J.S. and I. Analysis, The quantitative analysis of surfaces by XPS: A review. 1980.* ***2****(6): p. 222-239.*

10. *Cai, C., et al., A flexible and highly sensitive pressure sensor based on three-dimensional electrospun carbon nanofibers. 2021.* ***11****(23): p. 13898-13905.*

Chapter 4
Synthesis and Characterization

4.1 Introduction

In this chapter, the synthesis of Indium Selenide (In_2Se_3) homojunction is described by a simple solvothermal method and several characterizations are performed for its structural, morphological and band gap analysis. As an important III-VI group inorganic semiconductor, diindium triselenide (In_2Se_3) recently attracts much attention due to its unique electrical, optical and mechanical properties and low toxicity and eco-friendly, which is widely employed to phototransistors, phase-change memories, visible-light sensor, photodetectors and photovoltaic solar cells. However, using In_2Se_3 as a dielectric for RRAM device has rarely been studied.

To date, various strategies have been used to fabricate In_2Se_3 nanomaterial, such as two-step hydrothermal-calcining process, hot-injection method, molecular beam epitaxy technique, and chemical vapor deposition techniques. However, high cost, high-energy consumption and high-level instruments requirements are needed in the above methods. Besides, different stoichiometric ratios exist in In-Se system including InSe, In_2Se_3, In_3Se_4 and In_6Se_7. Hence, there still exists a huge challenge in fabricating the stoichiometric In_2Se_3 RRAM using an easy and eco-friendly synthetic method. Moreover, the same stoichiometric In_2Se_3 has at least five crystalline phases of α (two-layer hexagonal), β (three-layer rhombohedral), γ (defect wurtzite in hexagonal), δ and κ at different temperatures. Among them, α and γ phases are two most stable phases of In_2Se_3 at room temperature. The diversified crystal phases give In_2Se_3 unique phase-change property, state transition and memorized effect. Several studies have explored the phase transition about $\alpha \longrightarrow \beta$, $\alpha \longrightarrow \gamma$ and $\gamma \longrightarrow \alpha$ and the structure transition between amorphous and crystalline states. However, as far as we Know, there is no report about the effects of phases change of In_2Se_3 material on its memory application.

4.2 Synthesis

The In_2Se_3 nanoparticle/In_2Se_3 nanosheet homojunctions were synthesized via a facile solvothermal method. In detail, 0.8 mmol $InCl_3$ was dissolved into 10 mL of triethylene glycol ($C_6H_{14}O_4$, TEG) and stoichiometric amount of Se according to indium was well dispersed in 50 mL of TEG, respectively. Then, the former was added to the latter, stirring for 3 h to get the mixed solution. After that, the mixed solution was transferred into a 100 mL Teflon-lined autoclave, which was sealed and maintained at 210 °C for several hours. Finally, the autoclave was gradually cooled to room temperature, and the resultant was centrifuged at 5000 pm for 10 mins and washed with absolute ethanol at least 4 times and dried at 60 °C for 6 h. The products are collected at 20 h, 24 h, and 32 h.[1]

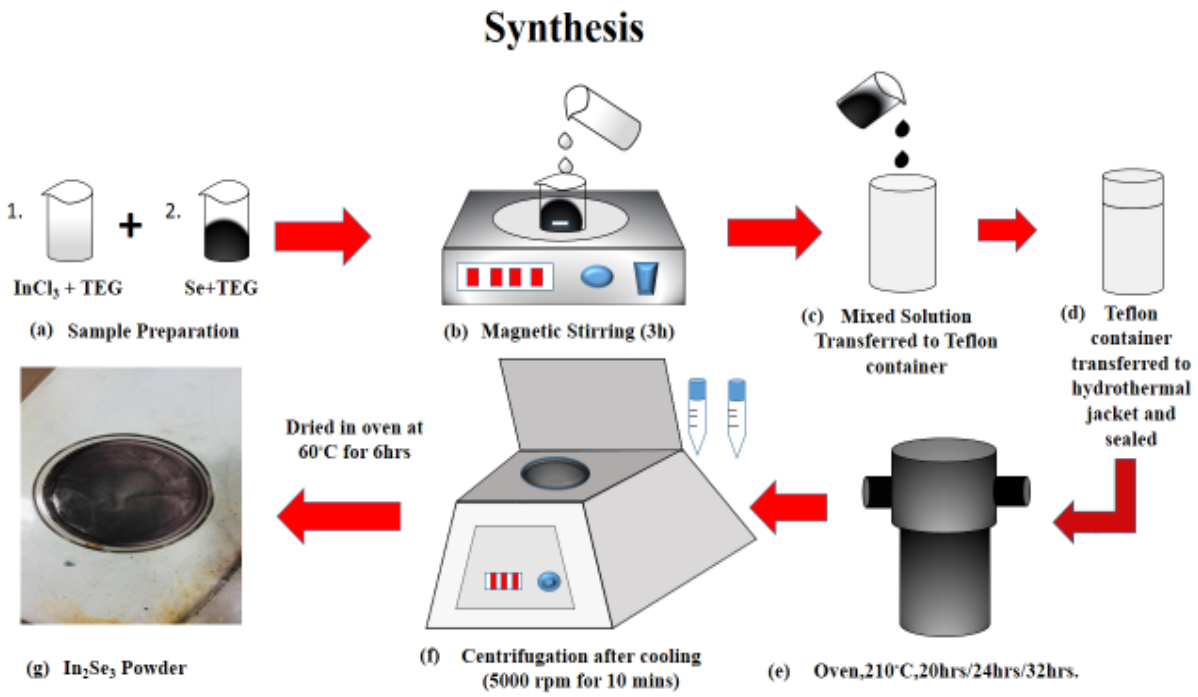

Fig 4.1 Schematic Illustration of the synthesis of In_2Se_3

4.3 Results and Discussion

The synthesized samples were characterized further structurally, morphologically and compositionally using several characterization techniques, such as, X-ray diffraction (XRD), Field emission scanning electron microscopy (FESEM), High-resolution transmission electron microscopy (HRTEM), X-Ray Photoelectron spectroscopy (XPS), UV-Visible spectroscopy (UV-Vis), Raman spectroscopy.

4.3.1 Crystal structure Analysis

X-ray diffraction (XRD) patterns were recorded to identify the phase and crystallinity of the synthesized samples with the help of powder X-ray diffractometer operating with Cu Kα radiation (λ= 1.5406) in a 2θ range from 10° to 70°. As shown in below figures,both α-phase In_2Se_3 (JCPDS no. 40-1408, a=b=4.02 Å, c=19.23 Å) and γ-phase In_2Se_3 (JCPDS no. 40-1407, a=b=7.14 Å, c=19.36 Å) are observed in the samples of In_2Se_3 collected at 20hr, 24hr, 32hr. Besides that peak of α-phase gradually decreases from 20hr sample to 32hr sample and peak of γ-phase gradually increases, indicating a phase transition behavior occurred in this process. For α-In_2Se_3 diffraction peaks observed at 2θ= 18.72°, 27.55°, 29.5°, 32.03°, 35.02°, 38.48°, 42.18°, 45.33°, 46.196°, 49.5°, 55°, 56.5°,57.85° that corresponds to the lattice plane 104 and For γ-In_2Se_3 diffraction peaks observed at 2θ= 14.95°, 16.92°, 24.87°, 27.46°, 30.3°, 37.45°, 38.72°, 43.9°, 45.25°, 47.6°, 49.42°, 51.23°,52.57°, 54.45° that corresponds to the lattice plane 111.[2]

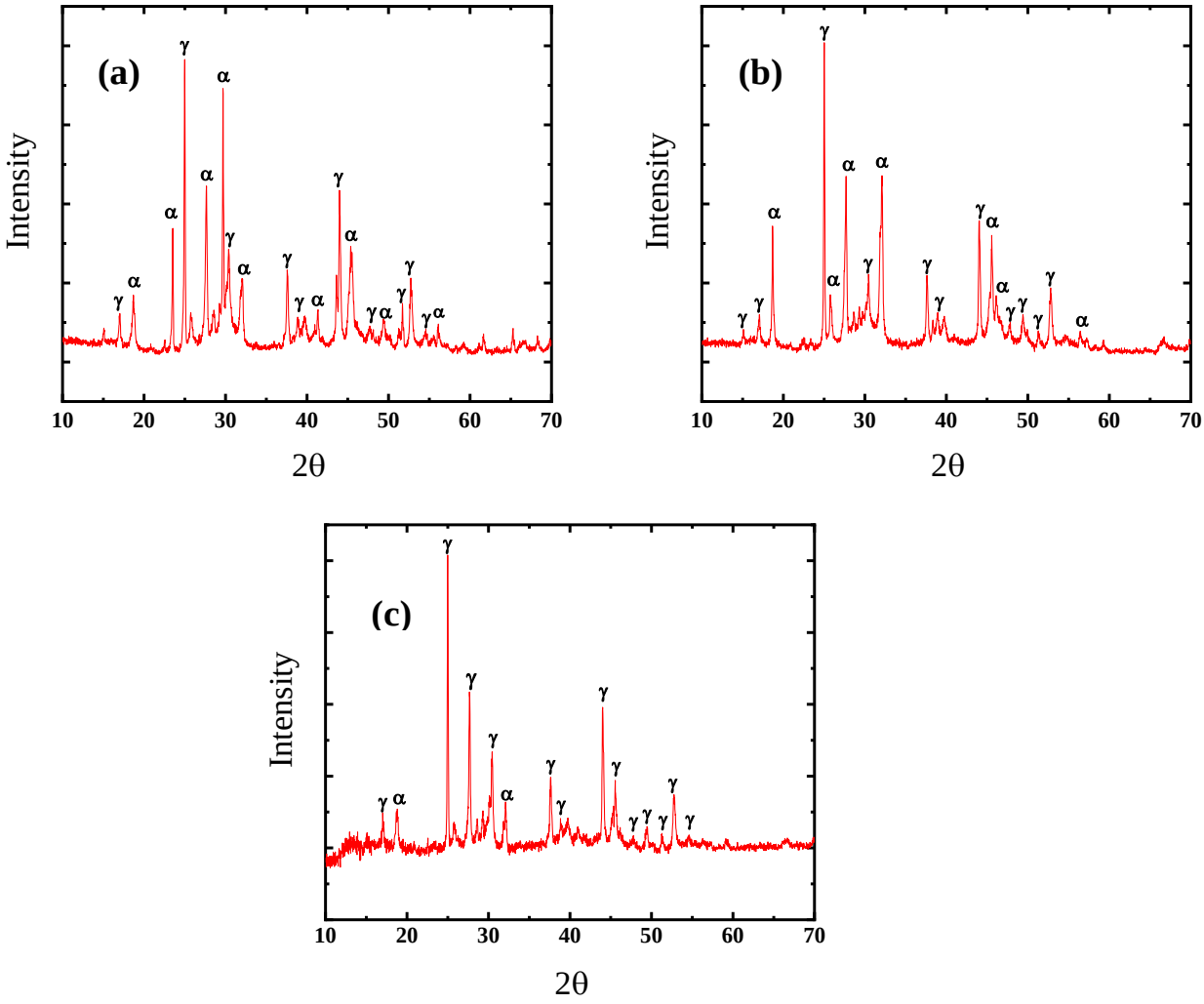

Fig 4.2 XRD patterns of In_2Se_3 (a) growth time 20hr, (b) growth time 24hr, (c) growth time 32hr

4.3.2 Morphological Analysis

I. FESEM Analysis

The morphologies and microstructures of the synthesized In_2Se_3 samples were examined by FESEM. As depicted in Fig 4.5 the 20hr prepared sample is mainly composed of flexural nanosheets with several micron diameters, coexisting with a few hexagonal nanoparticles, indicating that two types of In_2Se_3 are formed during the growth process. As the reaction time increases the size of nanoparticles is also increased. The nanoparticle and nanosheets display a uniform distribution and intimate contact with each other.[3]

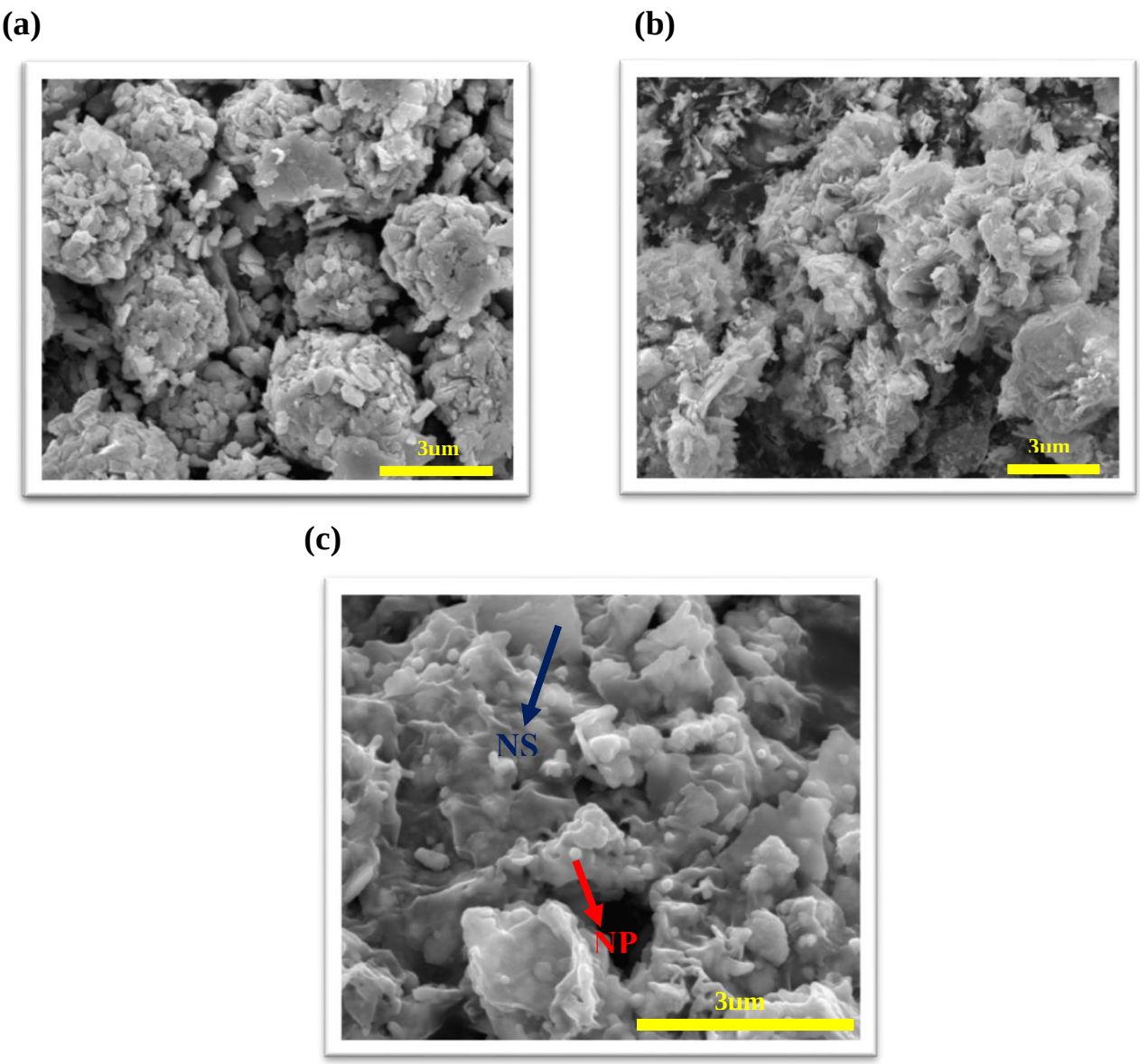

Fig 4.3 FESEM image of In_2Se_3 (a) growth time 20hr, (b) growth time 24hr, (c) growth time 32hr

(a) **(b)**

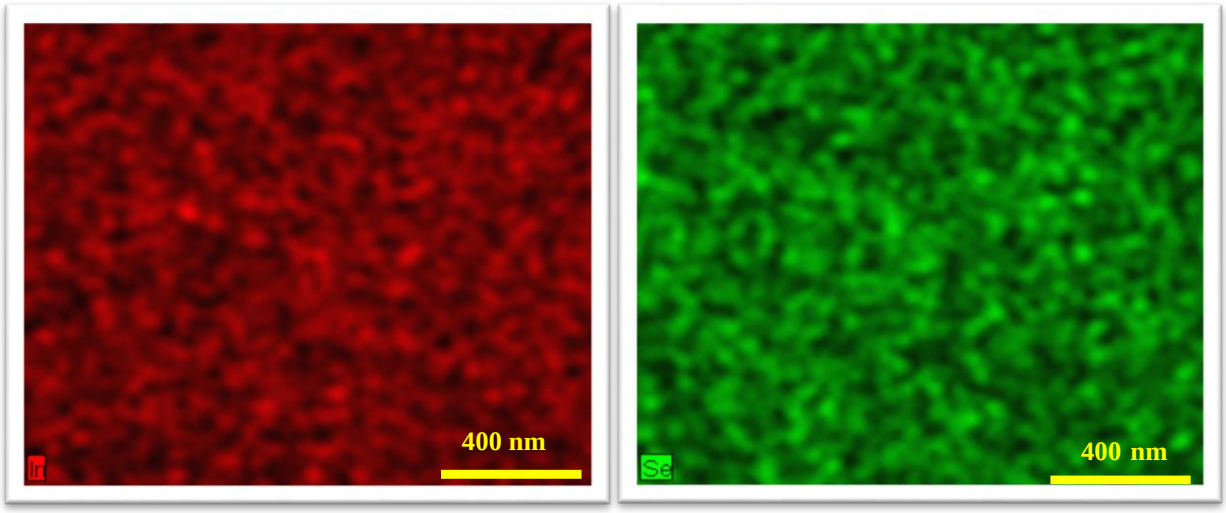

(c)

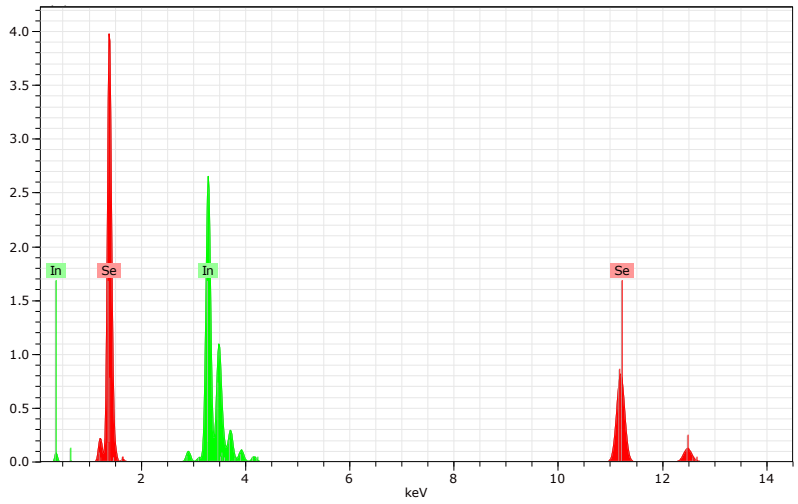

Fig 4.4 Elemental mapping of (a) Indium (In), (b) Selenium (Se), (c) Energy dispersive X-ray spectrometry (EDX) results of the sample

EDX Result

Time	In (%)	Se (%)
20hr	39.88	60.12
24hr	39.80	60.20
32hr	38.61	61.39

From the Energy dispersive X-ray spectrometry (EDX) it is found that the atomic ratio of Indium (In) and Selenium (Se) in the prepared sample is 2:3 and from the above table it can be concluded that as the growth time increases the percentage of Indium (In) decreases and the percentage of Selenium (Se) increases.

II. HRTEM Analysis

High Resolution Transmission electron microscopy (HRTEM) was also employed to further characterize the morphology and structural phase of In_2Se_3 homojunction. As depicted in Fig 4.5 it can be observed that the γ-In_2Se_3 nanoparticles are well dispersed on the surface of α-In_2Se_3 nanosheets, and γ-In_2Se_3 nanoparticles show a distorted hexagonal structure and display a compactly contact with α-In_2Se_3 nanosheets. [4]SAED (Selected area diffraction) pattern is taken and Energy dispersive spectroscopy (EDS) is also performed for elemental composition analysis of the sample.

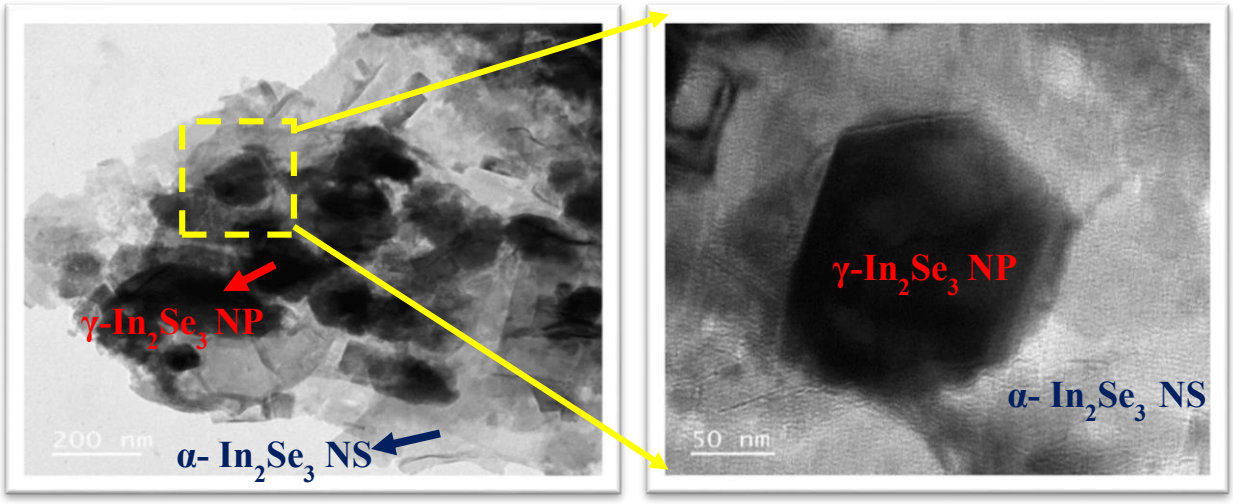

Fig 4.5 HRTEM Image of In_2Se_3 homojunction (growth time 20hr)

(a) **(b)**

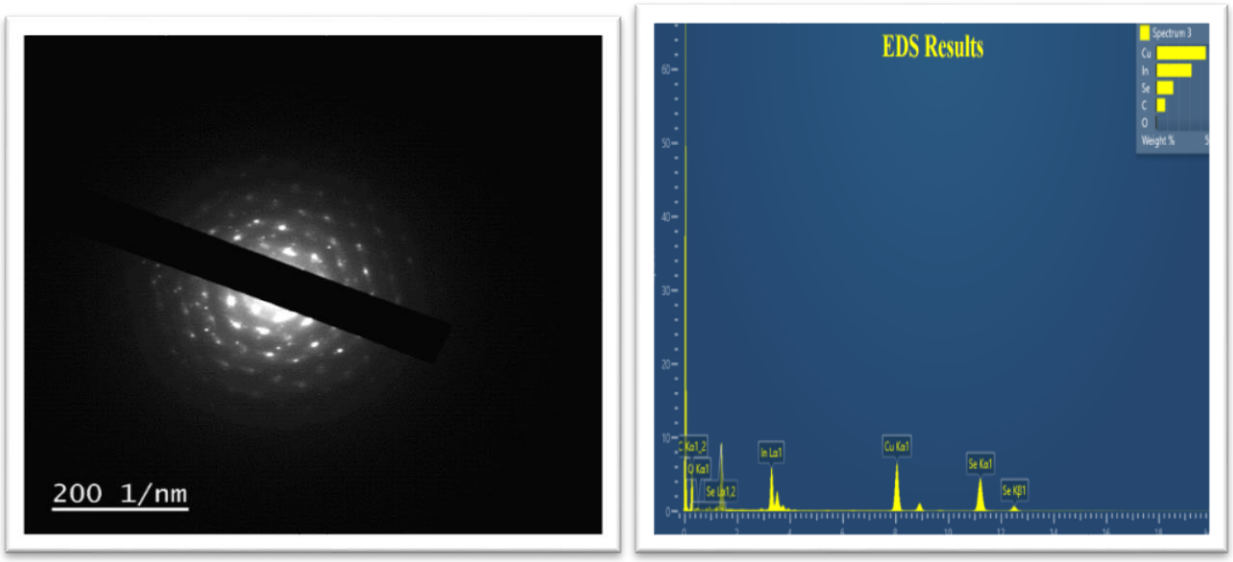

Fig 4.6 (a) SAED (Selected area diffraction) pattern, (b) Energy dispersive spectroscopy (EDS) for elemental composition analysis of In_2Se_3 homojunction (growth time 20hr)

4.3.3 Surface Analysis

X-ray photoelectron spectroscopy (XPS) was employed to investigate the surface elemental composition and chemical state of the synthesized sample and the results are shown in below figure 4.7. The XPS survey spectrum confirm that In and Se elements are detected on prepared sample. Three obvious peaks at 444.7 eV, 452.2 eV and 54.3 eV are ascribed to the binding states of In $3d_{5/2}$, In $3d_{3/2}$ and Se 3d of In_2Se_3.

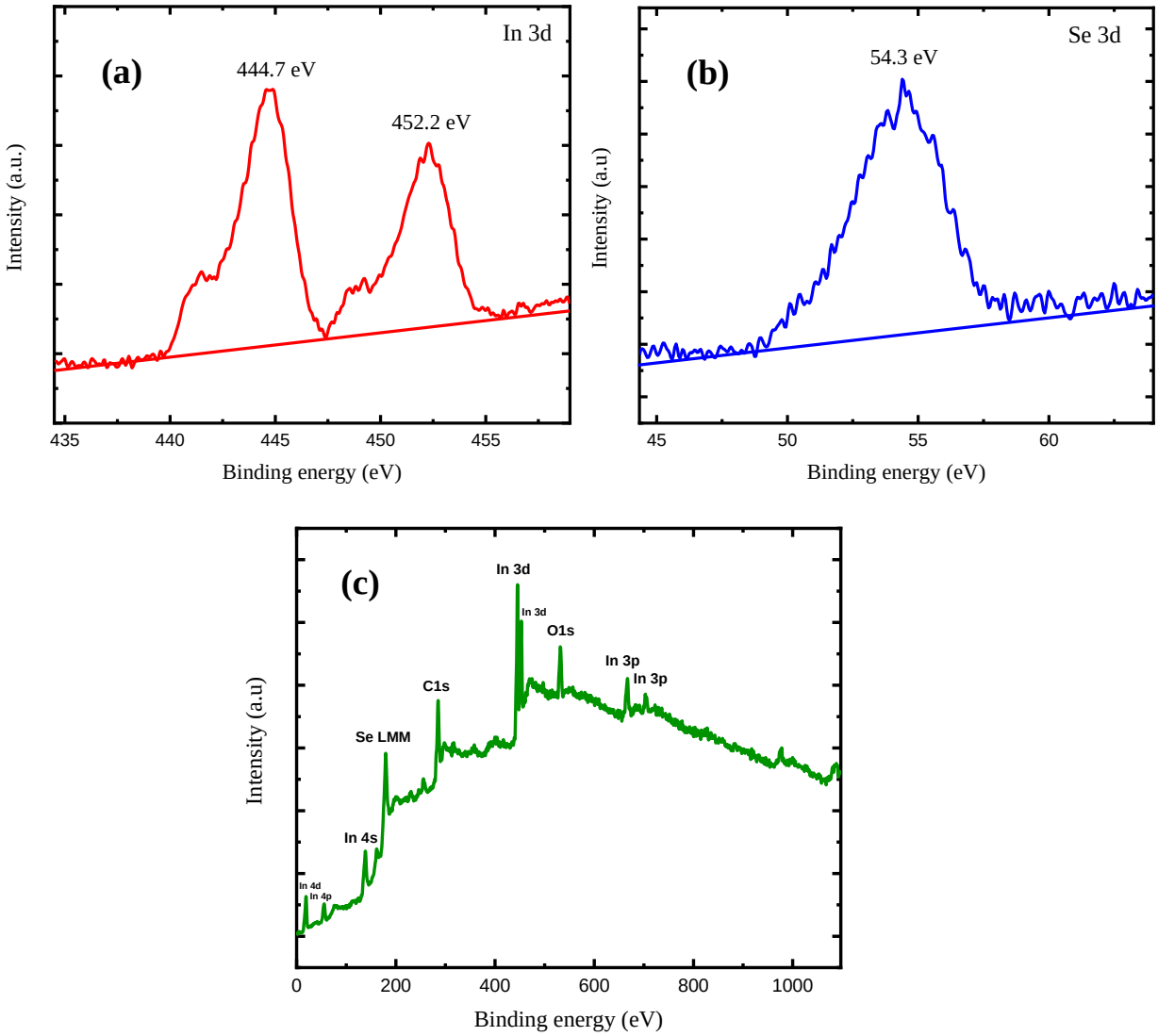

Fig 4.7 XPS high resolution spectra of (a) In 3d,(b) Se 3d, (c) survey spectra of In_2Se_3 growth time 20hr

4.3.4 Optical Property Analysis

I. UV-Vis Absorbance

UV-Visible absorbance spectroscopy is one of the important methods to reveal the energy structures and optical properties of the semiconductor nanocrystals. The absorbance spectra of In_2Se_3 are shown in below figure 4.8 and the energy band gap of the material is calculated using Tauc equation, $\alpha h\nu = A(h\nu - E_g)^n$, where α is absorption coefficient, $h\nu$ is the photon energy, E_g is the band gap, n=2 for direct transition and n=1/2 for indirect transition. The band gap of

In_2Se_3 found to be 1.42 eV, 1.87 eV, 1.9 eV for 20hr, 24hr, 32hr samples respectively. Thus it can be concluded that as the growth time is increased band gap of the material also increases.

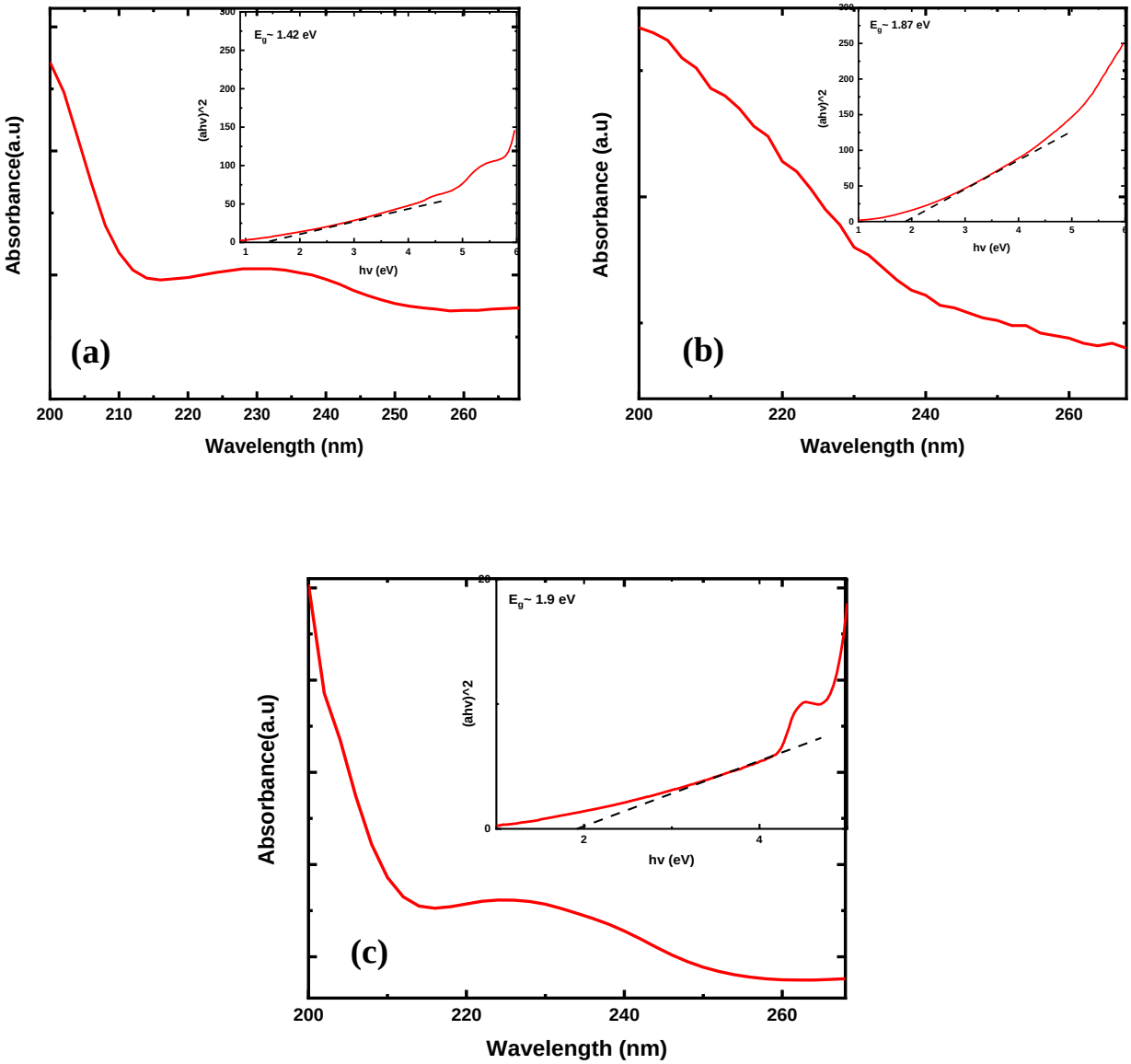

Fig 4.8 UV-Vis Absorbance spectra and $(\alpha hv)^2$ vs hv plot for band gap calculation of the sample In_2Se_3 of (a) growth time 20hr, (b) growth time 24hr, (c) growth time 32hr

II. Raman Analysis

Raman spectroscopy is a widely used tool that provides identification fingerprints to classify the individual structure of the In_2Se_3 among various phases. Here for our sample In_2Se_3 the experiment is done by Horiba xplora plus Raman Spectrometer with a laser of wavelength 532 nm. From the analysis of the spectra major Raman peak comes at 128 cm^{-1}.[5]

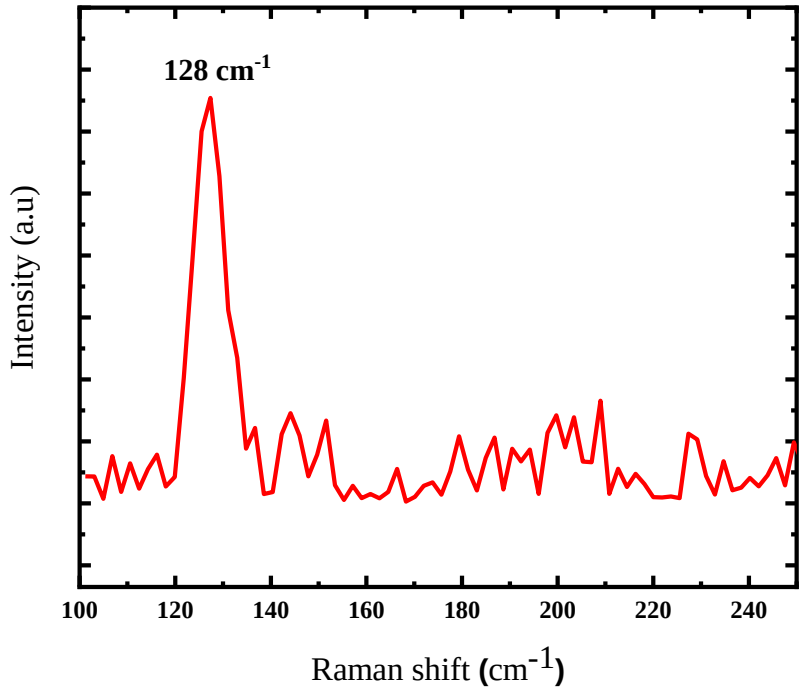

Fig 4.9 Raman Spectra of In_2Se_3 (growth time 20hr)

4.4 Conclusion

In summary indium selenide (In_2Se_3) homojunction had been synthesized by a simple solvothermal method. Confirmation of the crystallinity and phase has been done using X-Ray diffraction (XRD). It reveals that the synthesized material comprises of two phase α and γ. Morphology and structure were analysed by FESEM and HRTEM analysis revealing that the material is formed of hexagonal type of nanoparticle and sheet like nanoplates. Optical properties were investigated by UV-Vis measurement revealing a band gap varying from 1.42 to 1.9 eV and Raman analysis gives a band at 128 cm^{-1}. Further the material will be used as the active layer of the memory devices.

4.5 References

1. *Wang, R., et al., Synthesis of In2Se3 homojunction photocatalyst with α and γ phases for efficient photocatalytic performance. 2018.* ***151****: p. 74-82.*
2. *Popovic, S., B. Celustka, and D. Bidjin, X-ray diffraction measurement of lattice parameters of In2Se3, in Volume 6, Number 1 July 16. 2022, De Gruyter. p. 301-304.*
3. *Yan, Y., et al., Fabrication of high-quality γ-In2Se3 nanostructures using magnetron sputtering. 2013.* ***109****: p. 291-294.*
4. *Yang, M., et al., Structural and optical characteristics of γ-In2Se3 nanorods grown on Si substrates. 2011.* ***2011****: p. 7-7.*
5. *Mukherjee, S. and E.J.I.J.o.C. Koren, Indium Selenide (In2Se3)–An Emerging Van-der-Waals Material for Photodetection and Non-Volatile Memory Applications. 2022.* ***62****(3-4): p. e202100112.*

Chapter 5

Device fabrication and I-V Measurement

5.1 Introduction

Moore's law of transistor scaling is approaching its ultimate limit mainly due to the excessive power consumption caused by both static and dynamic leakage processes. The power consumption issue may in principle be attenuated by novel devices with lower voltage supply and steep subthreshold slope, including finFET, trigate FET, tunnel FET, negative capacitance FET, and alternative non-charge based switch concepts. On the other hand, novel computing architectures are proposed to solve the von Neumann bottleneck, where the physical separation between the data processing and the memory units in conventional computers pose increasing limitations of latency and power consumption, especially for data centric computation .The von Neumann bottleneck can be solved either by creating a 3D structure for co-integration of computing and memory elements, or by introducing whole new architecture concepts of in-memory computing, such as in-memory logic, and neuromorphic computing. These research efforts generally require novel switches, such as resistive switching memory (RRAM) or phase change memory (PCM), which can serve as memory and computing element at the same time. In my work, α-In_2Se_3 nanosheet/ γ-In_2Se_3 nanoparticle homojunction embedded in Organic Polymer (PMMA) is employed for the first time for the RRAM application. The material is synthesized by simple solvothermal method as described in previous chapter and the composite sample is deposited on FTO coated glass substrate to form Al/ In_2Se_3@PMMA/FTO. The metallization is done by thermal evaporation. I-V characterization of the cell reveal a formation free, bipolar, non volatile and multilevel RS effect. The device shows a significantly large resistance ON/OFF ratio of 10^4, low operating voltage (< 2V) and long retention time (10^4 s) at room temperature. Based on data analysis the conduction mechanism of the device is

explained by trap-assisted space charge limited conduction (SCLC) for high resistive state and ohmic conduction for low resistive state (LRS).

5.2 Device Fabrication

At first the FTO coated glass substrates are cleaned by acetone, 2-propanol, DI in the ratio of 1:1:2 and sonicate for 10mins and then rinsed with 10ml ethanol and sonicate for 10 mins. Then different weight concentrations (1mg, 3mg, 5mg) of the synthesized sample of In_2Se_3 is dispersed in 30mg PMMA (Polymethyl-methacrylate) solution. The composite sample is then deposited on FTO coated glass substrate by spin coating at 1500 rmp. Then aluminium (Al) electrodes are deposited on the samples by thermal evaporation technique.[1]

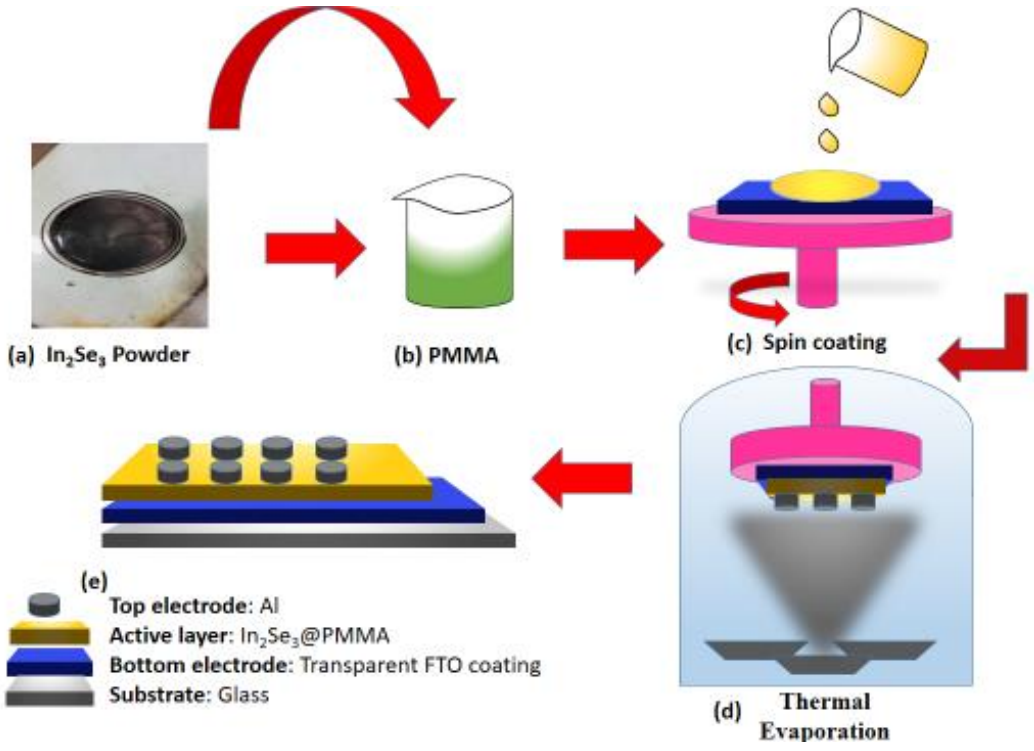

Fig 5.1 Process flow of Device Fabrication

5.3 I-V Measurements

The memory storage behaviour was investigated by analysis of current-voltage (I-V) curves of devices using a semiconductor characterization system (Keysight B2902A) at room temperature. The top electrode (TE) was positively biased and the bottom electrode (BE) was grounded throughout the entire electrical study.

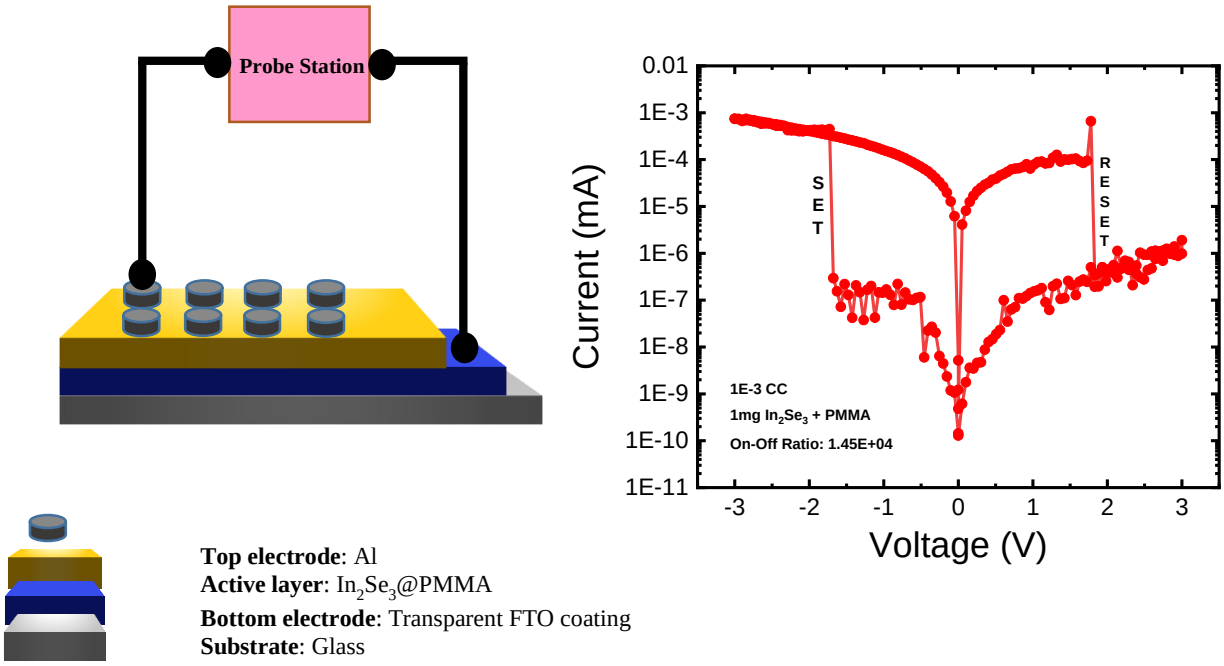

Fig 5.2 I-V Measurements: Resistive Switching

To analyse the switching performance, the I-V characteristics of In_2Se_3 @PMMA composite memory devices have been studied with different concentrations of In_2Se_3. Fig 5.3 distinctively displays bipolar resistive switching (BRS) characteristics in Al/In_2Se_3@ PMMA/FTO memory devices[2] with concentration of In_2Se_3 1mg, 3mg, 5mg under a dc mode at Room temperature.

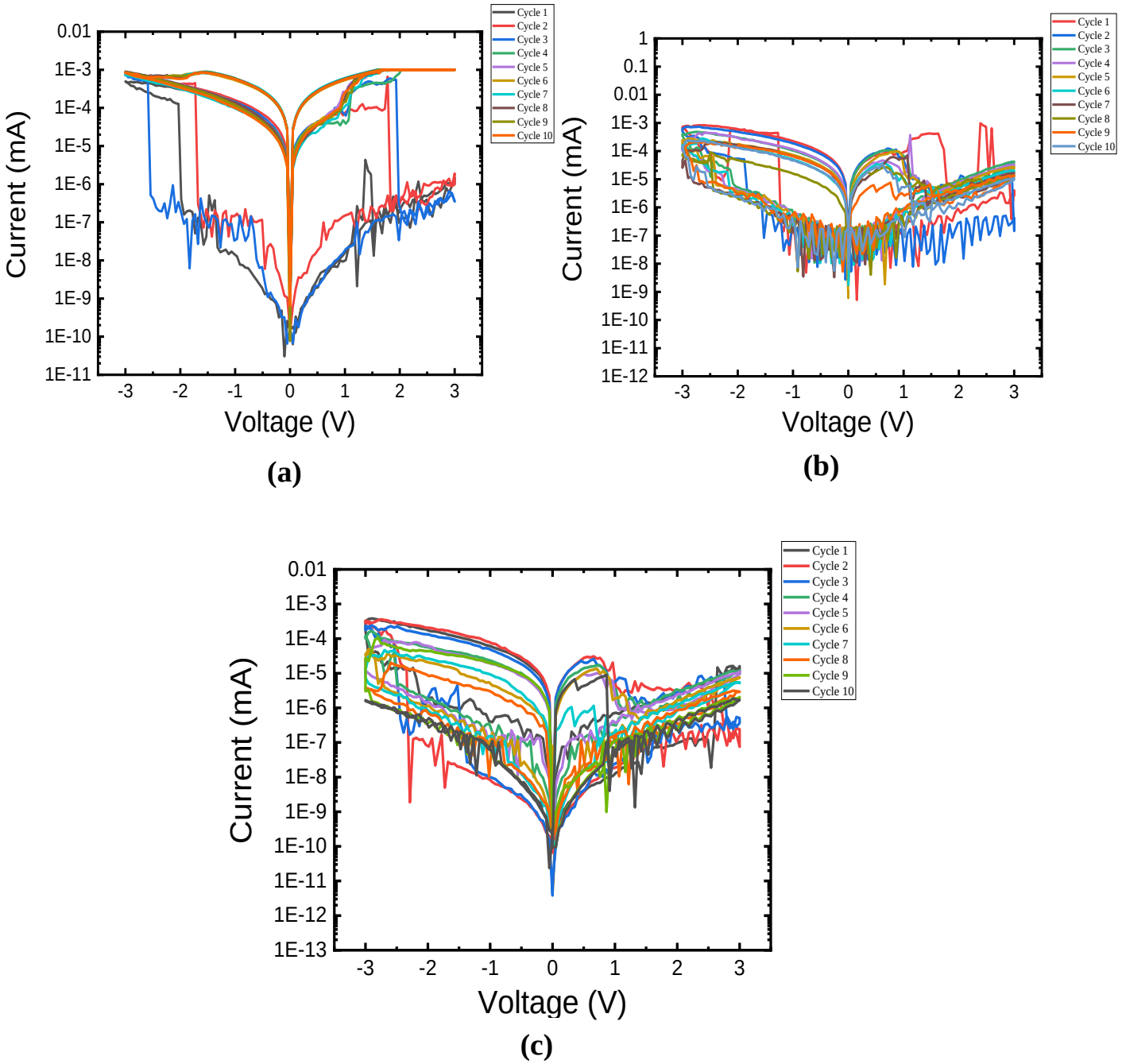

Fig 5.3 I-V curves of Al/ In_2Se_3@ PMMA/ FTO Memory Device; a) 1mg In_2Se_3, b) 3mg In_2Se_3, c) 5mg In_2Se_3

Since PMMA is an insulating material with the lowest unoccupied molecular orbital (LUMO) and highest occupied molecular orbital (HOMO) levels 1.8 eV and 7.3 eV respectively, the I-V characteristics of Al/In_2Se_3@ PMMA/FTO memory device would be dominated by the presence of In_2Se_3 in PMMA. Fig 5.3 represented that increasing voltage from 0 to -3V

increased the current gradually. However, an abrupt increase in current occurred between -3V to -2V, which indicated the transition of the device from OFF (HRS) to ON (LRS)state. This is called SET process. The maximum current in this process is called compliance current (CC). The device remained stable in the ON state during the subsequent voltage sweep (-3V to 0V and 0V to 3V). After some positive voltage the device goes from ON (LRS) to OFF (HRS) state. This called RESET process.[3] It should be noted here that for the real time application it is necessary to test the reproducibility of the resistive switching behaviour of the device. Therefore 10 repeated cycles were performed to check the uniformity in the performance for all the device. During these measurements as depicted in Fig 5.4 the device containing 1mg In_2Se_3 sample shows highest switching cycles approx. 50 and a ON/OFF ratio ~ 10^4 containing both analog and abrupt switching. This device is taken for further measurements of resistive switching.

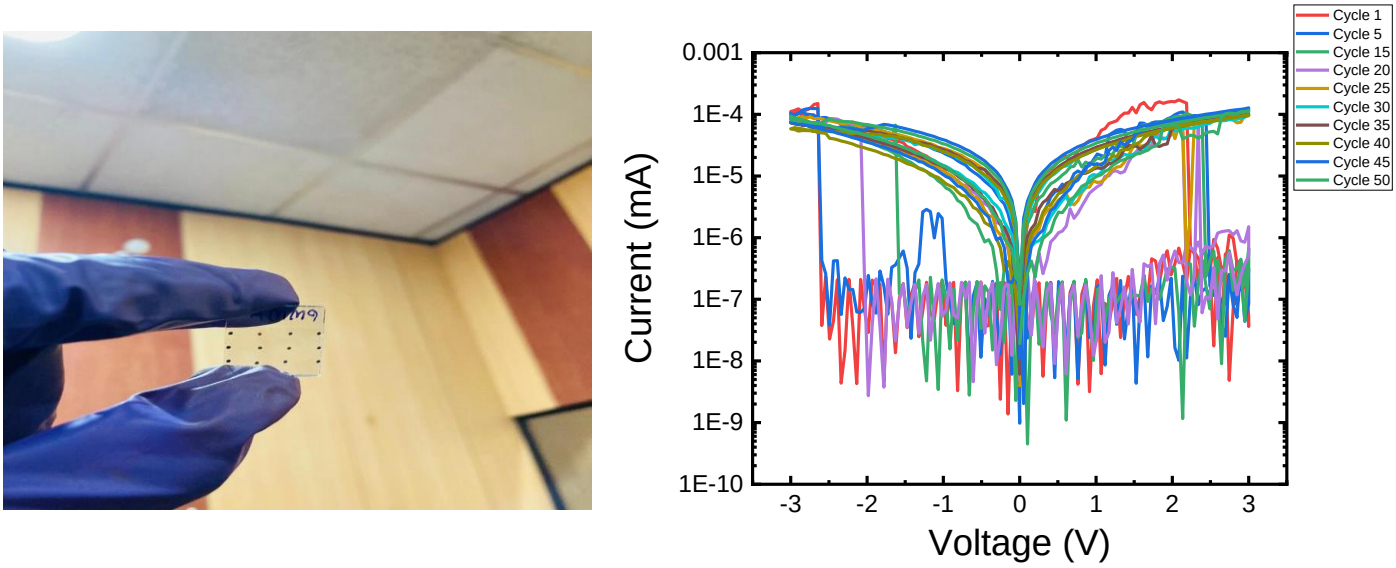

(a) **(b)**

Fig 5.4 (a) Real image of the fabricated device of size 2×2 cm, (b) I-V curves of the device containing 1mg sample with 50 repeatitive cycle

5.4 Statistical distribution

Statistical distribution of switching parameters, retention properties, the memory performance of the Al/In_2Se_3@ PMMA/FTO cell was studied elaborately. A SET and RESET voltage distribution plot and a cumulative plot of resistance states i.e, HRS(High resistance state) and LRS (Low resistance state) were also performed to check the performance of the device.[4]

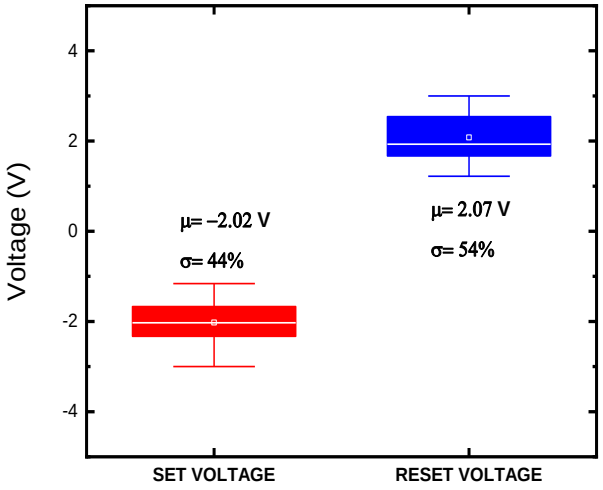

(a)

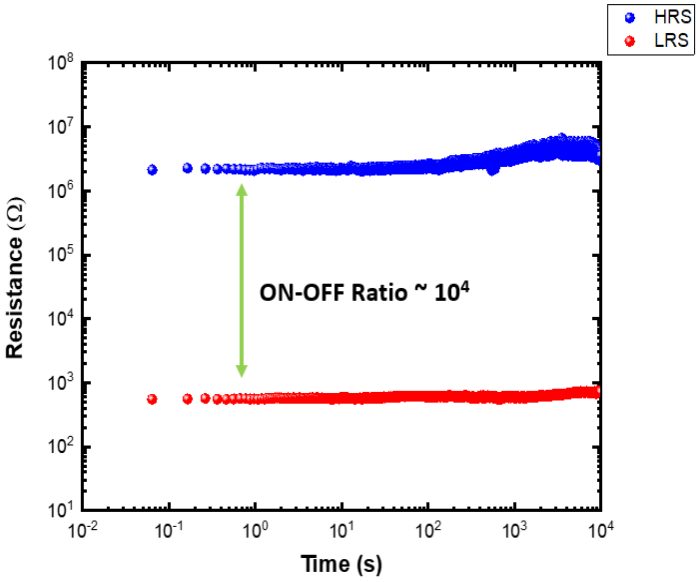

(b)

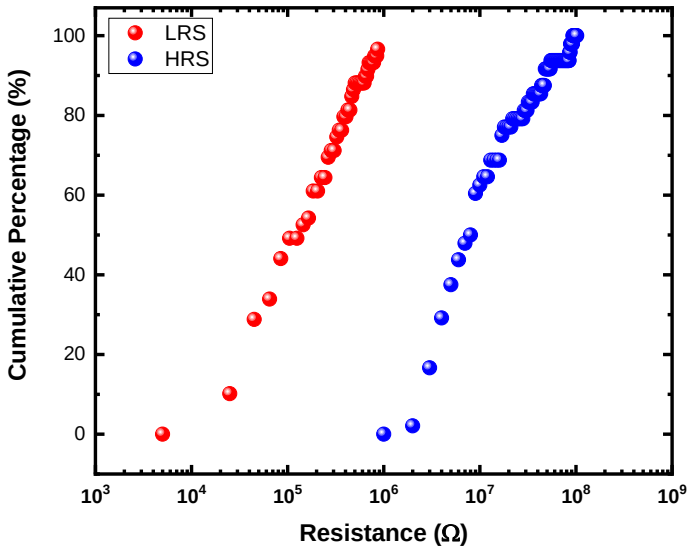

(c)

Fig 5.5 (a) SET & RESET Voltage distribution, (b) Retention Analysis, (c) Cumulative Probablity of LRS & HRS

Fig 5.5 (a) shows the mean values (μ) and standard deviations (σ) of V_{SET} and V_{RESET} are -2.02 V, 44% and 2.07 V,54% respectively. Fig 5.5 (b) shows the retention time behaviour of the device, it shows long retention time upto 10000s with a ON/OFF ratio~ 10^4 at room temperature. Fig 5.5 (c) indicates uniform cumulative distribution of R_{LRS}/R_{HRS} of the composite devices during the cycle-to-cycle (C/C) operations.

5.5 Conduction mechanism

To figure out the charge conduction mechanism which dominates the observed performance of bipolar resistive switching (BRS) RRAM device, the I-V characteristics of Al/In_2Se_3@ PMMA/FTO device in the positive and negative bias regions are plotted in Fig 5.6. in the logarithmic scale. There are various suggested theoretical models such as filament formation, Poole- Frenkel (PF) conduction, ohmic conduction, Schottky emission, thermionic model etc. to describe the conduction mechanism of resistive switching devices. However in this device the LRS (Low resistive state) regime consists of one segment and HRS (High resistive state) regime consists of another segment. From the linear fitting of those segments, it concludes that the slope of the LRS region is ~ 1, that represents ohmic conduction and the slope of the HRS region is ~ 2, that represents space-charge limited conduction (SCLC).

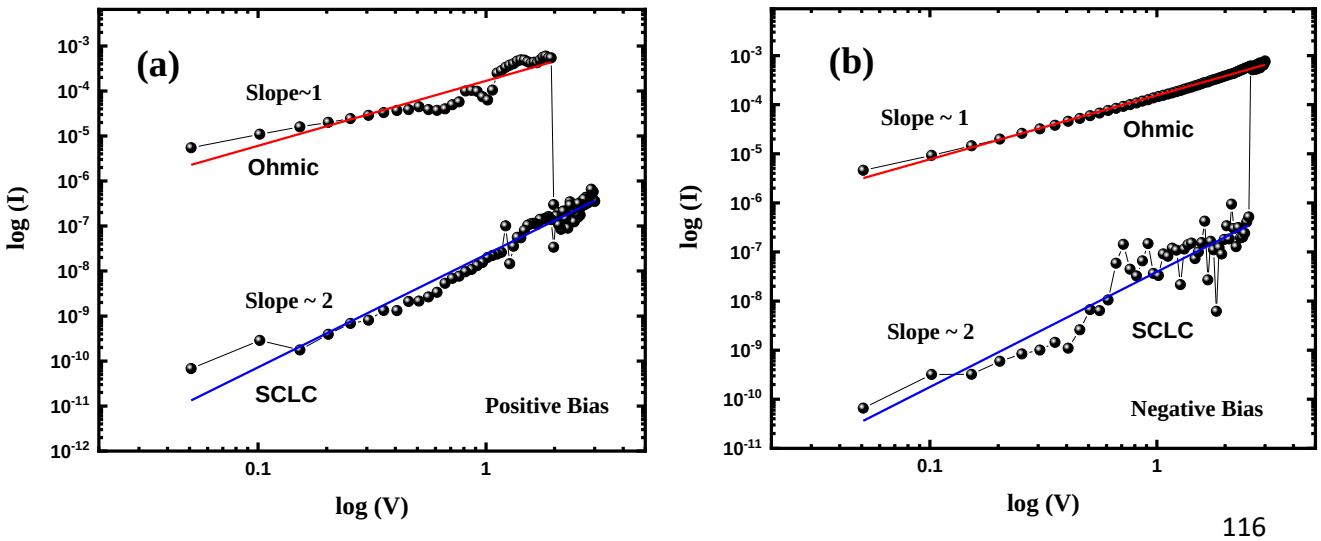

Fig 5.6 log I-Iog V characteristics for (a) positive bias (b) negative bias

Detail charge transfer has been described in Fig 5.7, that represents the energy level diagrams corresponding to different states to explain the physical mechanisms of the RS behaviour of Al/In_2Se_3@ PMMA/FTO device. The energy levels of In_2Se_3 are known to be within the lowest unoccupied and highest occupied molecular orbitals (LUMO and HOMO) of PMMA, serving as electron blocking layers due to wide energy gap. The In_2Se_3 nanoparticles surrounded in PMMA can create a large number of sites for charge carriers, trapping-detrapping sites and quantum tunnelling centres. When the traps are fully occupied by charge carriers, the device goes into LRS and in order to bring it back to HRS, all the filled traps must be emptied by applying opposite polarity voltage. After a negative voltage is applied to the TE (Al), energy band bending occurs. A subsequent increase in current is followed due to few electrons emitted or tunneled through the FTO/ PMMA barrier. However, those electrons are only trapped in In_2Se_3 due to the high energy barriers offered by PMMA species. Those electrons lack sufficient energy to overcome the interface barrier. As a result, when the applied voltage is greater than the SET voltage, all trap states are completely occupied and free electron density increases. So, the Fermi level of In_2Se_3 reaches the LUMO level of PMMA. As the barrier is reduced, it favours free electrons to make conduction through metal causing the switching of the device from OFF to ON state resulting in ohmic conduction. After turning the power off, the In_2Se_3@PMMA network still retains the trapped electrons. By the application of reverse electric field, the built in electric field prevents electrons being trapped. Moreover, under a sufficient reverse bias, the trapped electrons are extracted from active layer to FTO, as shown in Fig. 5.7.The career transport path is fully disconnected due to the unoccupied trapped sites turning the device from ON to OFF state. Moreover, The above mentioned trapping/detrapping mechanism[5] is further justified with the high ON/OFF ratio of ~10^4 obtained experimentally in an optimum concentration of 1 wt. % In_2Se_3.

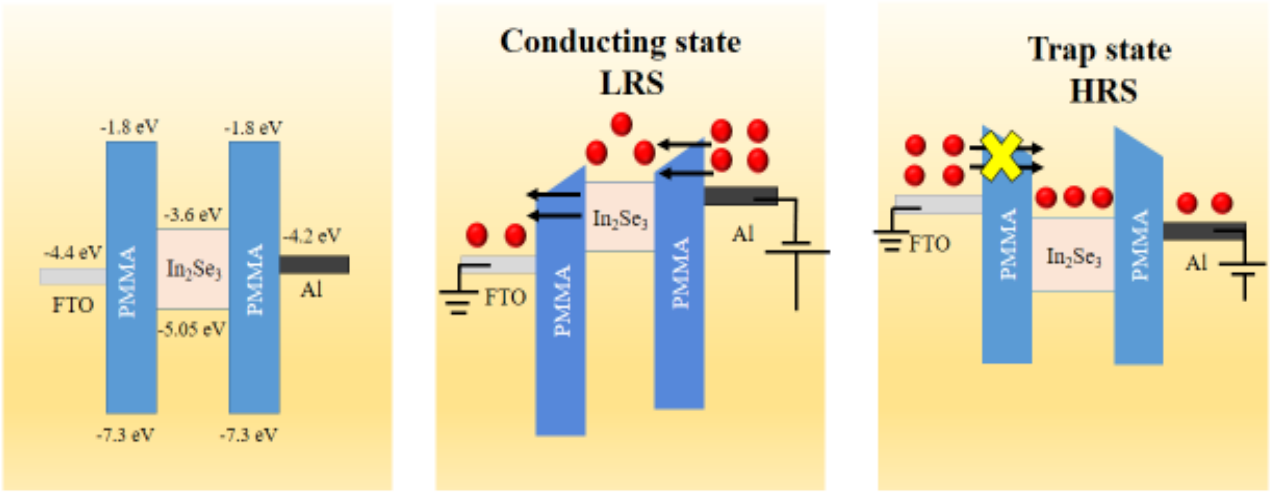

(a) **(b)** **(c)**

Fig 5.7 Energy band diagram of Al/In_2Se_3@ PMMA/FTO memory device (a) Unbiased condition, (b) Negative region, (c) Positive region

5.6 Conclusion

Al/In_2Se_3@ PMMA/FTO based RRAM device was fabricated by varying the concentration of In_2Se_3 in PMMA solution. The fabricated memory device exhibits bipolar resistive switching behaviour with non-volatile memory effect. The device shows a significantly large resistance ON/OFF ratio of 10^4, low operating voltage (< 2V) and long retention time (more than 9000 s) at room temperature. After the analysis of experimental data, the conduction mechanism for our In_2Se_3-PMMA based RRAM device is explained by trap-assisted space-charge limited conduction (SCLC) for high resistive state (HRS) and ohmic conduction for low resistive sate (LRS). The proposed RS active material is a promising candidate for future artificial neural systems for mimicking the characteristics of human memory.

5.7 References

1. *Das, B., et al., Flexible, transparent resistive switching device based on topological insulator Bi2Se3-organic composite. 2018.* ***124****(12): p. 124503.*
2. *Wu, Z., et al., Bipolar resistive switching in the Ag/Sb2Te3/Pt heterojunction. 2021.* ***3****(6): p. 2766-2773.*
3. *Kwon, D.-H., et al., Atomic structure of conducting nanofilaments in TiO2 resistive switching memory. 2010.* ***5****(2): p. 148-153.*
4. *Das, B., et al., Copper (II) Phthalocyanine (CuPc) Based Optoelectronic Memory Device with Multilevel Resistive Switching for Neuromorphic Application. 2021.* ***7****(4): p. 2001079.*
5. *Lim, E.W. and R.J.E. Ismail, Conduction mechanism of valence change resistive switching memory: a survey. 2015.* ***4****(3): p. 586-613.*

Chapter 6

Conclusion and Future Scope

6.1 Conclusion

My entire thesis work can be summarized into three different parts, 1) Synthesis and characterization of In_2Se_3 homojunction, 2) Device fabrication of Al/In_2Se_3@PMMA/FTO Memory Device, 3) Electrical characterizations of the fabricated RRAM device to check resistive switching performance.

At first α-In_2Se_3 nanosheet/ γ-In_2Se_3 nanoparticle homojunction is synthesized by a simple solvothermal method. Then the synthesized sample is embedded with PMMA solution with different weight concentrations 1mg, 3mg, 5mg of the sample. Then for device fabrication the composite sample is deposited on FTO coated glass substrate and then aluminium (Al) electrodes are deposited onto the sample by thermal evaporation to form Al/In_2Se_3@PMMA/FTO RRAM device. I-V characterization of the memory cell is performed by keysight that reveals a formation free, bipolar, non-volatile and multilevel resistive switching (RS) properties. The reproducibility of the best device was tested for 50 voltage sweeps and the device shows both analog and abrupt switching. The device shows a significantly large resistance ON/OFF ratio of 10^4, low operating voltage (<2V) and long retention time at room temperature. SET and RESET voltage distribution and a cumulative probability of resistance states i.e, HRS(High resistance state) and LRS (Low resistance state) were also performed to check the performance of the device. The device shows the mean values (μ) and standard deviations (σ) of V_{SET} and V_{RESET} are -2.02 V, 44% and 2.07 V,54% respectively. The experimental datas are analysed to find the conduction mechanism of the RRAM device. The conduction mechanism for my fabricated In_2Se_3-PMMA based RRAM device is explained by trap-assisted space charge limited conduction (SCLC) for high resistive state (HRS) and ohmic conduction for low resistive state (LRS). My work offers a strategy enabling RRAM with inorganic-organic polymer based composite for the integration of information storage and data processing with transparent nonvoaltile electronics in the future.

6.2 Future Scope

The proposed RS active material is a promising candidate for future artificial neural network that mimic the characteristics of human memory. As the fabricated Al/In_2Se_3@PMMA/FTO based RRAM device shows both analog and abrupt switching and for neuromorphic computing/in-memomry computing requires analog conductance, so the devices show analog switching can be implemented for neuromorphic application. Pulse measurements can be done to simulate the characteristics of neural networks such as STP (short term plasticity), LTP(long term potentiation), STM (short term memory), LTM(long term memory),STDP(spike timing dependent plasticity). Besides the RRAM devices can be implemented for various other application, such as non-volatile logic, hardware security primitives (TRNG-True random number generator,PUF-Physical unclonable functions), non volatile SRAM, Biosensors for ultrasensitive diagnostics and therapeutics etc. Although, significant success has been achieved in RRAM technology; however, more work is needed as RRAM still suffers from various challenges in terms of high operation current, lower resistance ratios, and reliability issues. More efforts in research should aim to develop methods to achieve faster programming/erasing, lower power consumption, enhancing the storage density by implementing multilevel storage capability and improvement in the fabrication process for enhanced uniformity. In addition, renewed focus should be towards use of RRAM in embedded memory and non-volatile logic applications as breakthroughs in these fields are much more exciting and significant. With continued work and improvements, it is imperative that RRAM devices will be a standout technology for future non-volatile memory applications.